

Influence of Strong Donors on Industrial Platinum Catalysts in the Hydrosilylation Reaction

Michael Johannes Sauer

Vollständiger Abdruck der von der TUM School of Natural Sciences der Technischen
Universität München zur Erlangung eines
Doktors der Naturwissenschaften (Dr. rer. nat.)
genehmigten Dissertation.

Vorsitz: Prof. Dr. Lukas Hintermann

Prüfer der Dissertation:

1. Prof. Dr. Fritz E. Kühn
2. Prof. Dr. Klaus Köhler

Die Dissertation wurde am 18.03.2024 bei der Technischen Universität München eingereicht
und durch die TUM School of Natural Sciences am 10.04.2024 angenommen.

“Through endurance we conquer.”

— Ernest H. Shackleton

Die vorliegende Arbeit wurde im Zeitraum von Mai 2020 bis März 2024 im Fachbereich Professur für Molekulare Katalyse der Technischen Universität München angefertigt.

Mein ganz besonderer Dank gilt meinem Doktorvater,

Herrn Prof. Dr. Fritz E. Kühn

für die freundliche Aufnahme in seine Arbeitsgruppe, das mir entgegengebrachte Vertrauen im Rahmen einer Kooperation mit der Wacker Chemie AG ein spannendes Forschungsthema zu bearbeiten und die Freiheit bei dessen Umsetzung. Ihre Expertise und Rat waren eine großartige Unterstützung, und ich schätze die Diskussionen, die wir gemeinsam geführt haben und die mir neue Perspektiven in der Wissenschaft und darüber hinaus eröffnet haben.

Diese Arbeit ist im Rahmen einer Kooperation der TU München mit der Wacker Chemie AG entstanden.

Danksagung

Diese Arbeit wäre ohne den Beitrag und die Unterstützung – fachlich oder persönlich – vieler Menschen in dieser Form nicht möglich gewesen. Unzählbare Gespräche haben mir erst geholfen, Lösungen zu finden oder den Rückhalt und die nötige Zuversicht, einen weiteren Versuch in Angriff zu nehmen. Deshalb möchte ich mich an dieser Stelle bei allen Unterstützern und Weggefährten bedanken und einige namentlich erwähnen.

Mein großer Dank gilt **Herrn Dr. Richard Weidner**, stellvertretend für die Firma **Wacker Chemie AG**, für die spannende Aufgabenstellung, fachliche Unterstützung und Resonanz, insbesondere im Rahmen der halbjährlichen Symposien.

Bei meiner Mentorin **Frau Dr. Theresa Dellermann** möchte ich mich herzlich für die außerordentliche Unterstützung bedanken. Deine freundliche Art und fachliche Kompetenz habe ich sehr zu schätzen gelernt und konnte sogar noch einige Tricks für den Laboralltag von dir lernen. Vielen Dank und alles Gute für deine berufliche und private Zukunft!

Der unermüdliche Einsatz, die Bürokratie von uns Doktoranden fernzuhalten und reibungslose Abläufe in der Arbeitsgruppe zu ermöglichen, ist der Verdienst von **Frau Ulla Hifinger**. Vielen Dank für die freundliche Zusammenarbeit und Ihre unerschöpfliche Geduld.

Für seinen organisatorischen Einsatz im Arbeitskreis bin ich **Robert Reich** äußerst dankbar. Du hast dich immer um eine möglichst faire Verteilung von Aufgaben gekümmert, wobei ich auch vermehrt die Ehre hatte, was aber schließlich zu einem positiven Arbeitsklima beigetragen hat. Deine konstruktiven wissenschaftlichen Beiträge und Erfahrung, insbesondere bei den Diskussionen im wöchentlichen Seminar, haben den Diskurs immer aufgewertet. Durch deine kollegiale und unkomplizierte Art habe ich immer gerne mit dir zusammengearbeitet und deine Flachwitze suchen auch abseits der Arbeit ihresgleichen. Dein Ausscheiden aus dem Arbeitskreis ist ein großer Verlust für die Gruppe, nichtsdestotrotz wünsche ich dir weiterhin alles Gute!

Für die fortwährenden Unterweisungen zu den Feinheiten der Gaschromatographie, der Hilfe bei Kalibrierung und Methodenentwicklung möchte ich mich bei **Jürgen Kudermann** bedanken. Es hat mir sehr geholfen, aus deinem Wissen schöpfen zu können und dass du auch beim fünften Spritzenwechsel noch die Ruhe bewahrt hast. Von **Dr. Alexander Pöthig** und **Dr. Christian Jandl** die Messung von Einkristallstrukturen zu lernen, war aufschlussreich und hat enorm Spaß gemacht. Danke für Eure Zeit und dass man bei Verfeinerungsproblemen immer auf Euch zählen konnte. In diesem Zusammenhang möchte ich auch **Thomas Pickl** erwähnen – mit dir waren die Messungen auch spätabends immer lustig

und lehrreich. Außerdem auch den **SC-XRD Raum**, der in heißen Sommern immer für wohltuende Abkühlung gesorgt hat bis hin zur Erkältung. Die Elementaranalysen wurden von **Ulrike Ammari, Petra Ankenbauer, Bircan Dilki** und **Manuel Seiler** aus der Zentralanalytik im CRC stets zeitnah, zuverlässig und auch mit Sonderwünschen gemessen – danke! Für die Praktikumsorganisation bin ich **Dr. Gabriele Raudaschl-Sieber, Dr. Markus Drees, Tobias Kubo** und **Thomas Miller** verbunden, die sich immer zuverlässig und freundlich um auftretende Probleme gekümmert haben.

Die Promotionszeit habe ich insbesondere wegen erstklassiger Kollegen genossen, die die Arbeit äußerst lustig gestaltet haben und wegen derer ich immer gerne in das Labor gekommen bin. Die „alte Garde“ aus **Florian Dyckhoff, Daniela Hey, Jens Oberkofler, Marco Bernd, Benjamin Hofmann, Christian Jacob** und **Jonas Schlagintweit** hat mich freundlich in den Arbeitskreis aufgenommen und mit Hintergrundwissen zur Arbeitskreischemie und –geschichte versorgt. Besonderen Dank schulde ich Dani, die meine Masterarbeit mit viel Geduld und Einsatz betreut hat und Ben, der als Bindeglied zur Promotion gewirkt hat und mir viel über die Hydrosilylierung, Platin und Rhenium beigebracht hat. Von Marcos synthetischen Fähigkeiten und Musikgeschmack konnte ich viel lernen und auch wegen seinem direkten und unkonventionellen Charakter war er eine Bereicherung für das untere Labor. Mit Dycki, Chris und Jonas hat sich noch immer ein Schafkopftisch gebildet – in Kombination mit Bierkrug oder auch Paulaner Spezi – wobei es sicherlich nicht an fachlichen Diskussionen gefehlt hat. Der teils grenzenlose Konsum von Chris und Jonas an Kaffee, Leberkäse und anderem Essen verstört mich bis heute. Als Stimmungsmacherin der Gruppe warst du, **Eva-Maria Esslinger**, ungeschlagen und hast ein ums andere Mal überrascht. Danke auch für deinen Einsatz mir bei meinen ersten Kristallstrukturen zur Seite zu stehen. Ein ganz besonderes Dankeschön gilt **Alexander Böth**, der mich, wenn auch unwissend, von **Lorenz Pardatscher** direkt zu Promotionsbeginn als Forschungspraktikanten zugewiesen bekommen hat und dadurch meinen Einstieg in den Arbeitskreis ermöglicht hat. Die Zusammenarbeit mit dir an diversen Publikationen war immer angenehm und geprägt durch deine vorbildliche Arbeitsmoral. Die diversen Diskussionen mit dir im Labor oder Seminarraum waren immer lustig, wenn auch, je nach Tageszeit, nicht immer sonderlich sinnvoll. Danke auch, dass dir deine Zeit nicht zu schade war und du mit mir zusammen die Glovebox zerlegt hast bis wir den/die Fehler gefunden hatten. Wenn alle Stricke reißen, treffen wir uns bei einem namhaften Gloveboxhersteller in Garching und heuern als Techniker an! **Alexander Imhof**, das gemeinsame Fachsimpeln über das Fahrradfahren war immer eine nette Abwechslung in den Pausen, bei denen du nie vergessen hast andere mit Kaffee zu versorgen. Als weiterer Brotzeitfan warst du mir von Anfang an sympathisch und deine ehrliche offene Art hat diesen ersten Eindruck nur noch vertieft. Deine handwerkliche Begabung hast du auf den 3D-Druck ausgeweitet und hast immer nach Möglichkeiten gesucht, durch gezielte Drucke den Laboralltag effizienter zu gestalten. Zusätzlich wünsche ich dir, dass dich die Chemie beim Brauen nie im Stich lässt und natürlich auch abseits davon alles Gute!

Unter den aktuellen Kollegen bedanke ich mich bei **Nicole Dietl**, mit der das gemeinsame Leiden schon in der Masterarbeit begonnen hat, wo wir häufig von den gleichen Problemen geplagt wurden. In der Promotion hat sich dieser Umstand leider auf die Katalyse ausgeweitet, aber unser Austausch dazu hat immer für Entwirrung gesorgt und häufig habe ich auf diese Weise gleich noch den neuesten Tratsch erfahren. Du hast eine zentrale Rolle in der Gruppe eingenommen und für den nötigen Zusammenhalt, Spaß und Organisation gesorgt – danke dafür! Beim Thema Katalyse möchte ich mich auch bei **Greta Zámbo** bedanken, ohne die meine Methodenentwicklung sicherlich noch länger gedauert hätte. Deine fachliche Kompetenz kann dir sicherlich niemand absprechen, aber spätestens nach der Apferteilung war auch der Respekt da. Auch wenn ich es nicht geschafft habe, die Kristallstruktur von deinem Goldkomplex zu bestimmen, wünsche ich dir das Beste für deine letzte Publikation. Solltest du eine Arbeit außerhalb der Wissenschaft suchen, bin ich mir sicher, dass du als Pokémon-Verkäuferin ein Auskommen hast. Die effiziente und zielgerichtete Zusammenarbeit mit **Schlachta Tim** hat mir immer gefallen. Obwohl ich Mitleid mit dem ESI habe, ist die Produktivität nicht von der Hand zu weisen. Abschließend hoffe ich, dass der Cyanidkomplex zur publiziert wird und wünsche dir alles Gute für deine Karriere. Für die Schnappsynthese bin ich **Leon Richter** äußerst dankbar, auch wenn ich leider in der Glovebox arbeiten musste. Dein Einsatz beim 3D-Druck ist bemerkenswert, gerade um Metallkomplexe haptisch greifbar zu machen. Als Mario Kart Experte musste man dir ungünstigerweise zu oft den ersten Platz überlassen, während man von hinten zuschauen durfte – hier ist Hopfen und Malz verloren. Auch an **Wolfgang Büchele alias Yogi** vielen Dank für die Zusammenarbeit und alles Gute für die Veröffentlichung deiner Publikation. Beim Mittagessen war dein Referieren über den Nachtsch fester Bestandteil (oh Mann, nach was schmeckt das denn?!) und allen war schnell klar, dass dich nur eine Buttercremetorte glücklich stimmen kann. Ich kann mich noch an den ersten Tag von **Mayr Johannes** erinnern, als er zusammen mit Yogis Synthesepraktikanten im unteren Labor für Chaos gesorgt hat. Dein erfolgreiches Forschungspraktikum bei Greta hat uns gezeigt, dass man dich nur schwer von der Forschung abhalten kann. Umso besser, dass du für Masterarbeit und Promotion dem unteren Labor treu geblieben bist. Auch wenn deine Rutheniumkristalle nicht zu meinen Favoriten zählen, hat die Zusammenarbeit im Labor, auch wegen guter Musik, immer Spaß gemacht. Ich wünsche dir viel Erfolg im Labor, auch weil sonst die Glatze durch Haare raufen droht. **Hoefler Carla**, du musstest zwar in das obere Labor wechseln, aber so hat man immer noch mehr Kontakt, als wenn du – verständlicherweise – nach Kanada zu den Ottern flüchtest. Zusammen mit deiner Stefan-Belegschaft habe ich keinen Zweifel, dass du eine erfolgreiche Promotionszeit haben wirst, drücke aber natürlich trotzdem die Daumen. Gleiches gilt für das Tanzen, wo wir auf der Hütte leider meinen Mangel an Talent akzeptieren mussten. **Hoffmann Melanie**, unsere aktive Laborzeit am AK Kühn hat sich nur minimal überschritten, trotzdem ist dein Einsatz für die Gruppe und gemeinsame Unternehmungen

offenkundig. Ich hatte die zweifelhafte Ehre dir meine Gruppenaufgaben zu übergeben, aber bin mir absolut sicher, dass du auch wissenschaftlich ein Zugewinn für die Gruppe bist.

Ich bin dankbar, **Kaikhosravi Mohammad** aus dem Iran als Gastdoktorand in unserem Arbeitskreis kennengelernt zu haben. Mo, deine Offenheit und Einsatz, Deutsch zu lernen, haben mich beeindruckt. Von deiner Arbeitsmethodik und auch kulinarisch habe ich hoffentlich einiges von dir lernen können. Du hast dich ab dem ersten Tag in den Arbeitskreis integriert und hast nie bei einer sozialen Unternehmung gefehlt. Für die Veröffentlichung der ausstehenden Publikation drücke ich dir die Daumen. **Campagnolo Filippo** und **Alberto Piccoli** aus Italien haben unsere Arbeitsgruppe als Gastdoktorand, beziehungsweise Masterand bereichert. Eure witzige Art und das Philosophieren über Italienische Küche vermisse ich jetzt schon. Filippo, von deinem Wissen über Mechanismen und NMR haben wir enorm profitiert, auch wenn du an unseren Geräten verzweifelt bist. Für deine Bergtouren wünsche ich dir bestes Wetter, sicheren Fels und Berg heil!

Dem **unteren Labor** und allen, die dort gearbeitet haben, möchte ich für das angenehme Arbeitsklima danken und den Spaß, den wir hatten. Bei dem gemeinsam genutzten Arbeitsplatz und Geräten kann schnell die Harmonie leiden, aber wir haben es immer geschafft, miteinander zu reden, und auch deshalb habe ich die Arbeit jederzeit genossen. Deswegen hoffe ich, dass auch nach meinem Ausscheiden das untere Labor dem Arbeitskreis immer erhalten bleibt.

Zusätzlich zu meinen Kollegen möchte ich mich auch bei meinen Praktikanten und Auszubildenden, **Maximilian Auer, Victor König, Adile Parlak, Carolin Lauerburg** und **Jeff Offorjindu**, für die harte Arbeit bedanken. Es war mir eine große Freude, euer Betreuer gewesen zu sein, und ich wünsche euch alles Gute fürs weitere Studium oder Ausbildung. Für deinen vollen Einsatz bei den zahlreichen Katalysen bin ich dir sehr verbunden, Jeff. Ohne deine selbstständige Arbeit hätten die Projekte bedeutend länger gedauert.

Von Herzen danke ich meiner **Familie** und insbesondere meinen **Eltern** und **Großeltern**, die mich immer unterstützt haben und das Studium ermöglicht haben. Eure aufmunternden Worte und Rückhalt sind eine Stütze, auf die ich immer bauen kann. Gleichermäßen bin ich dankbar für meine **Geschwister**, die immer für mich da sind und mit denen ich besonders verbunden bin.

Zuletzt möchte ich mich bei meiner Frau **Franziska** bedanken. Du gibst mir Kraft, bereicherst mein Leben und bist mein Ausgleich zum Labor. Du zeigst immer Verständnis und baust mich nach Rückschlägen wieder auf. Ich freue mich auf die gemeinsame Zukunft und alles, was sie bringt.

Abstract

Silicones possess a multitude of remarkable properties, rendering them indispensable for everyday life. For their industrial-scale manufacturing, platinum-catalyzed hydrosilylation is essential, which leads to the regrettable depletion of platinum resources due to catalyst encapsulation in cured silicones, calling for efforts to reduce the amount of spent precious metal. To be mentioned in this context is the innovative development of excellent (NHC)Pt(dvtms) catalysts by Markó that is only accompanied by one adverse effect – the excessive induction period.

Two distinct strategies aimed at surpassing the constraints of Markó-type catalysts are elucidated in this thesis, commencing with the investigation of selected alkyl and aromatic NHC wingtips with the aim to deduce direct structure-reactivity relationships, with focus on the influence of *N*-donors. These compounds are conveniently stable and easily accessible using the industrially highly important Karstedt's catalyst [Pt₂(dvtms)₃] as platinum source. Evaluation of the catalytic properties in well-established model reactions revealed unfavorable stabilization of the Pt(II) oxidation state by *N*-donors, while phenyl wingtips more than double the activity with regards to a reference catalyst in combination with improved yield and selectivity.

Adding to this, bimetallic platinum complexes were designed, which demonstrate superior catalytic activity and shorter induction periods despite structural and electronic similarities with the parent monometallic complexes, unveiling synergistic interactions between platinum centers. Experiments with varying catalyst loading and temperature demonstrate fundamentally different reactivity of the mono- and bimetallic catalyst classes, which is also reflected by the activation behavior in the presence of silane, where intermediate stabilization of the bimetallic complex as di- μ -hydrido complex is postulated. Additional insight into the stability and reactivity of bimetallic systems is gained by stoichiometric reactions and mercury poisoning studies, suggesting promising avenues for future application in hydrosilylation catalysis.

Zusammenfassung

Silikone verfügen über eine Vielzahl bemerkenswerter Eigenschaften, die sie für das tägliche Leben unverzichtbar machen. Für ihre Herstellung im industriellen Maßstab ist die platinkatalysierte Hydrosilylierung unerlässlich, was langfristig zu einer bedauerlichen Erschöpfung der Platinressourcen führt, da der Katalysator in ausgehärteten Silikonen eingeschlossen wird, sodass Anstrengungen unternommen werden müssen, um die Menge des verbrauchten Edelmetalls zu verringern. Die innovative Entwicklung herausragender (NHC)Pt(dvtms)-Katalysatoren durch Markó wird nur von einem negativen Effekt begleitet - der exzessiven Aktivierungsdauer.

Zwei unterschiedliche Strategien, die darauf abzielen, die Beschränkungen von Markó-Katalysatoren zu überwinden, werden in dieser Arbeit erläutert. Zu Beginn werden ausgewählte alkyl- und aromatische NHC-Flügelspitzen mit dem Ziel untersucht, direkte Struktur-Reaktivitäts-Beziehungen abzuleiten, wobei der Schwerpunkt auf dem Einfluss von *N*-Donatoren liegt. Diese Verbindungen sind stabil und unter Verwendung des industriell äußerst wichtigen Karstedt-Katalysators $[\text{Pt}_2(\text{dvtms})_3]$ als Platinquelle leicht zugänglich. Die Evaluierung der katalytischen Eigenschaften in etablierten Modellreaktionen ergab eine ungünstige Stabilisierung der Pt(II)-Oxidationsstufe durch *N*-Donatoren, während die Phenyl-Flügelspitzen die Aktivität im Vergleich zu einem Referenzkatalysator mehr als verdoppeln, bei gleichzeitig verbesserter Ausbeute und Selektivität.

Darüber hinaus wurden bimetallische Platinkomplexe entwickelt, die trotz struktureller und elektronischer Ähnlichkeiten mit den monometallischen Ausgangskomplexen eine überlegende katalytische Aktivität und kürzere Induktionszeiten aufweisen, was synergistische Wechselwirkungen zwischen den Platin-Zentren offenbart. Experimente mit variierender Katalysatorbeladung und Temperatur zeigen eine grundlegend unterschiedliche Reaktivität der mono- und bimetallischen Katalysatorklassen, was sich auch im Aktivierungsverhalten in Gegenwart von Silan widerspiegelt, wo eine Zwischenstabilisierung des bimetallischen Komplexes als di- μ -hydrido-Komplex postuliert wird. Weitere Einblicke in die Stabilität und Reaktivität bimetallischer Systeme werden durch stöchiometrische Reaktionen und Quecksilbervergiftungsstudien gewonnen, die eine vielversprechende Zukunft für Anwendungen in der Hydrosilylierungskatalyse aufzeigen.

List of Abbreviations

Asp	Aspartic acid
[BAR ₄]	B[3,5-(CF ₃) ₂ C ₆ H ₃] ₄ ⁻
CAAC	Cyclic(alkyl)(amino)carbene
COD	Cycloocta-1,5-diene
Cp	η ⁵ -C ₅ H ₅
Cp*	η ⁵ -C ₅ Me ₅
Cy	Cyclohexyl
Cys	Cysteine
d	Doublet
Dipp	2,6-Diisopropylphenyl
dvtms	1,1,3,3-Tetramethyl-1,3-divinylsiloxane
eq.	Equivalents
<i>et al.</i>	<i>Et alia</i>
EXAFS	Extended X-ray absorption fine structure
FID	Flame ionization detector
FTIR	Fourier-transform infrared spectroscopy
GC	Gas chromatography
Glu	Glutamic acid
hept	Heptet
His	Histidine
HREM	High-resolution electron microscopy
INEPT	Insensitive nuclei enhancement by polarization transfer
ⁱ Pr	<i>iso</i> -Propyl
J	Coupling constant
KIE	Kinetic isotope effect
Lys	Lysine
m	Multiplet
MD ^h M	1,1,3,5,5-Heptamethyltrisiloxane
Me	Methyl
Mes	2,4,6-Trimethylphenyl
MM ^{vi}	1,1,1,3,3-Pentamethyl-3-vinylsiloxane
MS	Mass spectrometry
NHC	<i>N</i> -heterocyclic carbene
NMR	Nuclear magnetic resonance
OMCVD	Organometallic chemical vapor deposition
ppm	Parts per million
Py	Pyridine
Rds	Rate-determining step
RT	Room temperature
s	Singlet
SAXS	Small-angle X-ray scattering
SC-XRD	Single Crystal X-ray Diffraction
t	Triplet
TEM	Transmission electron microscopy
TOF	Turnover frequency
TON	Turnover number
UV-vis	Ultraviolet–visible
XPS	X-ray photoelectron spectroscopy
δ	Chemical shift [ppm]

Table of Contents

1	Introduction.....	1
1.1	Fundamentals of Catalysis.....	1
1.2	The Chemistry of Silicones	5
1.3	Hydrosilylation Catalysts	7
1.3.1	Synopsis of the Periodic Table of Elements.....	7
1.3.2	Supremacy of Platinum Catalysts	12
1.3.3	Markó-type Complexes	14
1.3.4	Bimetallic Hydrosilylation – An Emerging Prospect	19
1.4	Mechanistic considerations of Platinum-Catalyzed Alkene Hydrosilylation	22
1.4.1	The (Modified) Chalk-Harrord Mechanism	22
1.4.2	Activation and Decomposition of Karstedt’s catalyst – An In-Depth Study	23
1.4.3	State of the Art Kinetic and Mechanistic Considerations.....	26
1.4.4	Mechanistic Aspects and Reactivity of Markó-type Complexes	26
2	Objective.....	28
3	Results and Discussion	29
3.1	Synthesis and Characterization of Markó-type (NHC)Pt(dvtms) Complexes and their Evaluation in the Hydrosilylation Reaction of Alkenes.....	29
3.1.1	Publication Summary.....	29
3.1.2	Publication Reprint.....	31
3.2	Homobimetallic <i>bis</i> -NHC(Ptdvtms) ₂ Complexes for the Hydrosilylation of Alkenes.....	42
3.2.1	Publication Summary.....	42
3.2.2	Publication Reprint.....	44
4	Conclusion and Outlook	59
5	Reprint Permissions.....	61
6	Complete List of Publications	62
7	References.....	64

1 Introduction

1.1 Fundamentals of Catalysis

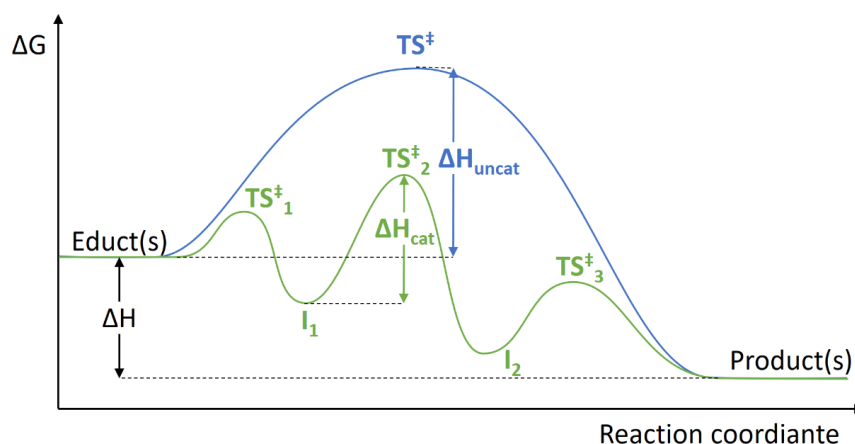
The catalytic efficacy of yeasts in facilitating the fermentation of sugars into alcohol has been recognized since ancient times, with applications in the controlled production of wine, beer, and vinegar.¹ While yeasts serve as biocatalysts in this process, the earliest documented instance of inorganic catalysis dates back to a publication from 1561, when Valerius Cordus utilized sulfuric acid to convert ethanol into diethyl ether.² Berzelius linked a plethora of isolated observations of other researchers³, like the dehydration of ethanol on clay at elevated temperatures, the decomposition of ammonia on heated metals, or the inflammation of hydrogen in the presence of platinum sponge at ambient temperature, to a broad concept and defined catalysis in 1835.⁴ Catalysis is derived from the Greek term καταλύω (κατα = down; λύω = dissolution of an object or a group), in contrast to analysis.⁵ The immense importance of catalysis is reflected in the attention it receives in research, but also the presentation of the most important award in science, the Nobel prize. An overview of the most important milestones, that have contributed directly or indirectly to catalysis, is presented in Table 1.⁶

Table 1: Selected Nobel laureates that contributed to the area of catalysis.⁶

Nobel laureate(s)	Year	Prize motivation
Wilhelm Ostwald	1909	"in recognition of his work on catalysis and for his investigations into the fundamental principles governing chemical equilibria and rates of reaction"
Paul Sabatier	1912	"for his method of hydrogenating organic compounds in the presence of finely disintegrated metals"
Alfred Werner	1913	"in recognition of his work on the linkage of atoms in molecules by which he has thrown new light on earlier investigations and opened up new fields of research especially in inorganic chemistry"
Fritz Haber	1918	"for the synthesis of ammonia from its elements"
Arthur Harden, Hans K.A.S. von Euler- Chelpin	1929	"for their investigations on the fermentation of sugar and fermentative enzymes"
Karl Ziegler, Guilio Natta	1963	"for their discoveries in the field of the chemistry and technology of high polymers"
Christian B. Anfinsen, Stanford Moore,	1972	"for his work on ribonuclease, especially concerning the connection between the amino acid sequence and the biologically

Nobel laureate(s)	Year	Prize motivation
William H. Stein		active conformation" and "for their contribution to the understanding of the connection between chemical structure and catalytic activity of the active center of the ribonuclease molecule"
Ernst O. Fischer, Geoffrey Wilkinson	1973	"for their pioneering work, performed independently, on the chemistry of the organometallic, so called sandwich compounds"
John Cornforth, Vladimir Prelog	1975	"for his work on the stereochemistry of enzyme-catalyzed reactions" and "for his research into the stereochemistry of organic molecules and reactions"
Sidney Altman, Thomas Cech	1989	"for their discovery of catalytic properties of RNA"
William S. Knowles, Ryoji Noyori, Barry K. Sharpless	2001	"for their work on chirally catalysed hydrogenation reactions" and "for his work on chirally catalysed oxidation reactions"
Robert H. Grubbs, Yves Chauvin, Richard R. Schrock	2005	"for the development of the metathesis method in organic synthesis"
Gerhard Ertl	2007	"for his studies of chemical processes on solid surfaces"
Richard F. Heck, Ei-ichi Negishi, Akira Suzuki	2010	"for palladium-catalyzed cross couplings in organic synthesis"
Benjamin List, David W.C. MacMillan	2021	"for the development of asymmetric organocatalysis"

In contemporary scientific discourse, a catalyst is defined as a compound that accelerates reaction rates without undergoing consumption or affecting the reaction equilibrium.⁷ This acceleration is achieved by modification of the energy hypersurface, opening up alternative reaction pathways with a lower maximum activation energy barrier by splitting into more elemental steps (Scheme 1), thus expanding the scope of viable synthesis routes.^{1b, 8}



Scheme 1: Schematic representation of the free energy (ΔG) for an uncatalyzed (blue) and a catalyzed reaction (green). Conversion of the educt(s) *via* transition states (TS^\ddagger) and possibly intermediates (I). If the largest enthalpy barrier (ΔH_{cat}) for an alternative reaction pathway is smaller than that of the uncatalyzed reaction (ΔH_{uncat}), acceleration of the reaction rate is observed.^{8b-g}

Highlighting the importance of catalysis, as of 2019 it contributes to more than 35% of the global gross domestic product (GDP) of 88 trillion USD.⁹ This share is almost equivalent to the entire chemical industry, as 85% of processes rely on catalysts (Figure 1), and the trend is rising.¹⁰ The production of ammonia by the Haber-Bosch process probably is still the most important development even today, as the obtained fertilizers indirectly feed about half of the world population.^{1a, 11} Typically, classification is employed to distinguish between homogeneous, heterogeneous, and biocatalysis.^{8d, 8g} Additionally, specialized fields such as organocatalysis, photocatalysis, and electrocatalysis, among others, are recognized within the broader scope of catalytic processes.^{8h}

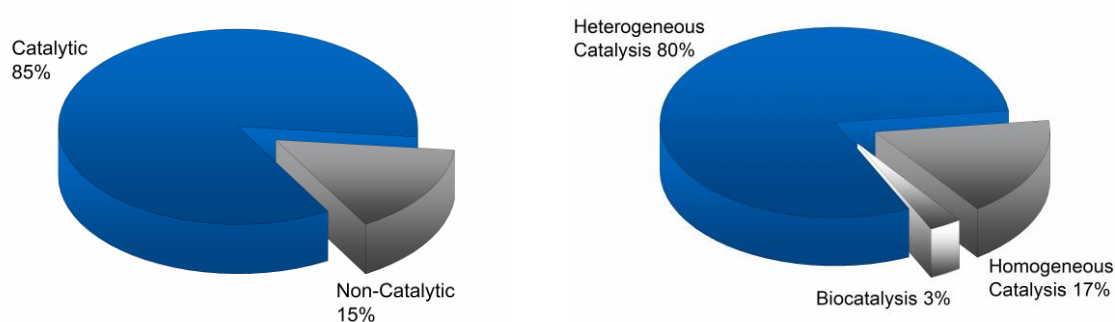


Figure 1: Share of catalysis in chemical processes (left) and quota of the catalytic categories.¹⁰

Each of the categories of catalysis possesses certain strengths while suffering from drawbacks in other aspects (Table 2).^{8d, 12} Heterogeneous catalysts are most commonly employed in industrial processes and consist of active metals or metal oxides that are dispersed over a support like alumina, silica or carbon. This reduces the cost for the frequently expensive active component, as only the surface atoms are accessible for substrates, unlike in homogeneous and biological catalysts, where, at least in theory, all sites are active. Although heterogeneous catalysts generally lack activity, selectivity, and require harsh reaction conditions, they are currently the industry's workhorse as they are highly stable, cheap,

and easily separated from the product, allowing continuous reactor operation. However, the production of fine chemicals and pharmaceuticals, especially with chemo-, regio-, stereo-, or enantioselective transformations frequently requires well-defined homogeneous or biological systems, where particularly homogeneous catalysts allow for tailor-made coordination spheres and hence reactivity.

Table 2: Comparison of heterogeneous, homogeneous and biocatalysts regarding selected properties.^{8d, 12}

Property	Heterogeneous	Homogeneous	Biological
Catalyst	Metal/metal oxides on a support	Molecule, complex	Enzyme, molecule
Phase	Gas or liquid	Liquid	Liquid
Activity	Variable	High	Very high
Selectivity	Variable	High	Very high
Structure	Undefined	Defined	Defined
Reaction conditions	Harsh	Mild	Mild
Diffusion problems	High	None	None
Product separation	Easy	Difficult	Difficult
Tuneability	Low (<i>via</i> promoters)	High (<i>via</i> ligands)	High (<i>via</i> genetics)
Mechanistic understanding	Low	High	High

Even though the definition of catalysts ideally assumes that consumption thereof does not occur, they remain susceptible to decomposition and hence deactivation.¹³ A key figure for the robustness or lifetime of a catalyst is the turnover number (TON) which describes the amount of substrates that are converted per active site, which raises limits for the application in heterogeneous systems (Eq. 1).

$$\text{TON} = \frac{\text{moles [substrate]}}{\text{moles [catalyst]}} \quad (1)$$

The derivative of the TON with respect to time, determines the turnover frequency (TOF), which describes the activity of a catalyst (Eq. 2). The TOF and TON depend on the reaction conditions, complicating the comparison of these figures. Also, the logarithmic reaction rate has to be respected when assessing the TOF, therefore the initial and fastest regime should be used for the calculation of the TOF, which is commonly the steepest slope of a yield-time curve.

$$\text{TOF} = \frac{\text{moles [substrate]}}{\text{moles [catalyst]} \cdot \text{time}} \quad (2)$$

1.2 The Chemistry of Silicones

Silicones are synthetic polysiloxanes, containing a --O--Si--O-- backbone, that are not to be confused with the element silicon and are also fundamentally different than conventional polymers (Figure 2).¹⁴ The remaining valence sites are usually occupied by hydrocarbon moieties, or are used as crosslinks to other siloxanes. The most important polysiloxane is poly(dimethyl)siloxane (PDMS), in which two methyl groups are bound to each silicon.

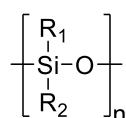


Figure 2: Schematic representation of a generic silicone.^{14b}

Siloxanes and polysiloxanes can exist in various forms, including linear chains, cyclic structures, branched configurations, and network formations with varying degrees of crosslinking.¹⁵ These compounds are classified into different categories of commercial products, such as fluids, compounds, lubricants, resins, and rubbers (= elastomers), based on their structural characteristics.¹⁶ Regarding nomenclature, the building blocks are commonly described by the letters M, D, T, Q (mono, di, tri, and quarternary), which indicate the degree of oxygen substitution at silicon (Table 3).^{14a, 17} The capital letters are often provided with a superscript that specifies silicon-bound groups. Methyl, as the most common substituent is usually not written out.

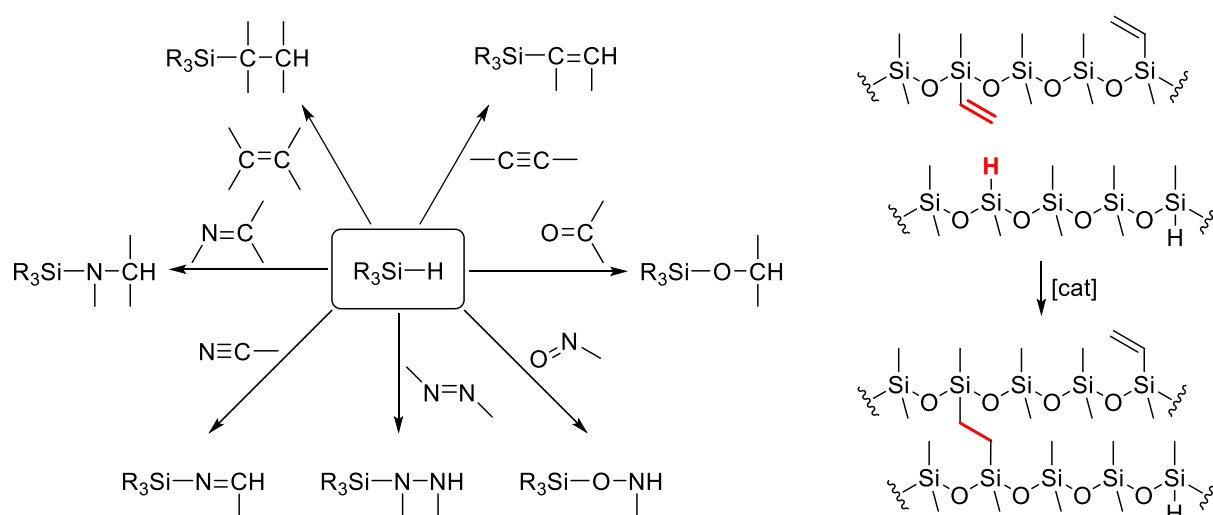
Table 3: Symbol and functionalities of siloxane building blocks.^{14a, 17}

Symbol	M^{Me}	D^{Me}	T^{Me}	Q	D^{MeVi}	D^{MeH}
Functionality	$\begin{array}{c} \text{CH}_3 \\ \\ \text{H}_3\text{C--Si--O}_{0.5} \\ \\ \text{CH}_3 \end{array}$	$\begin{array}{c} \text{CH}_3 \\ \\ \text{H}_3\text{C--Si--O}_{0.5} \\ \\ \text{O}_{0.5} \end{array}$	$\begin{array}{c} \text{CH}_3 \\ \\ \text{O}_{0.5}\text{--Si--O}_{0.5} \\ \\ \text{O}_{0.5} \end{array}$	$\begin{array}{c} \text{O}_{0.5} \\ \\ \text{O}_{0.5}\text{--Si--O}_{0.5} \\ \\ \text{O}_{0.5} \end{array}$	$\begin{array}{c} \text{O}_{0.5} \\ \\ \text{H}_3\text{C--Si--O}_{0.5} \\ \\ \text{O}_{0.5} \end{array}$	$\begin{array}{c} \text{H} \\ \\ \text{H}_3\text{C--Si--O}_{0.5} \\ \\ \text{O}_{0.5} \end{array}$

The distinctive properties of silicones arise from their exceptionally stable inorganic backbone, coupled with organic residues chemically bonded to it, resulting in an amphiphilic character (hybrid semi-inorganic polymer¹⁸).^{14c, 15a, 19} While C–C bonds possess a dissociation energy of roughly $355 \text{ kJ}\cdot\text{mol}^{-1}$, Si–O bonds are significantly more stable at $444 \text{ kJ}\cdot\text{mol}^{-1}$.^{14b, 20} This renders silicones extremely resistant to chemicals and heat and at the same time provides electrical conductivity due to extensive delocalization of electrons along the backbone.²⁰ Additionally, the --O--Si--O-- backbone is highly flexible due to comparatively long Si–C and Si–O bonds²¹, lack of substituents on every second (oxygen) atom of the chain^{15a}, and can therefore even pass through a linear 180° state²². This facilitates the rotation of methyl groups (or other organic groups) towards the polymer surface.²³ Consequently, silicones exhibit a low-tension/energy surface compared to organic polymers, rendering them resistant to reactions with the surrounding environment.^{18, 21} This property makes silicones well-suited for pressure-sensitive release coatings.¹⁸ Other phenomenal properties of silicones include flame

retardancy, biocompatibility, abrasion resistance, weatherability, oxidative stability, gas permeability, radiation resistance, excellent dielectric properties, and physical properties, including glass transition temperatures as low as -120°C , making them the ideal material for a plethora of applications.^{14b, 14c, 16, 17b, 20, 24} This is reflected by the global silicone production that exceeded 8 million metric tons in 2020, correlating to a market valuation of 15.1 billion USD.²⁵

The Direct Process, also known as the Müller-Rochow process²⁶, serves as the pivotal step in generating the essential raw materials necessary for silicone manufacturing.²⁷ This process can occur through condensation or radical polymerization reactions, but also through a transformation called hydrosilylation.^{16b, 17b, 20, 28} A hydrosilylation reaction entails the atom-efficient addition of a Si–H entity to large scope of unsaturated organic functional groups (Scheme 2, left), typically a C=C double bond, under the influence of a catalyst, resulting in that case in the formation of an alkyl silane.²⁹



Scheme 2: Hydrosilylation reaction of diverse unsaturated functional groups (left).^{29a} Crosslinking of two polysiloxane chains (right).^{14a}

The hydrosilylation is of major importance for the crosslinking of polysiloxane chains (Scheme 2, right) for the generation of rubbers or resins, where the properties of the product are not only determined by the nature of the educts but also by the degree of crosslinking. Additionally, fumed silica might be added as filler, reinforcing the materials.^{14a, 15} The process of network formation is also called vulcanization and the products thereof are referred to as silicone rubbers, conceivably due to the fortunate discovery of vulcanization of natural rubber by Goodyear in 1839.^{16b}

1.3 Hydrosilylation Catalysts

1.3.1 Synopsis of the Periodic Table of Elements

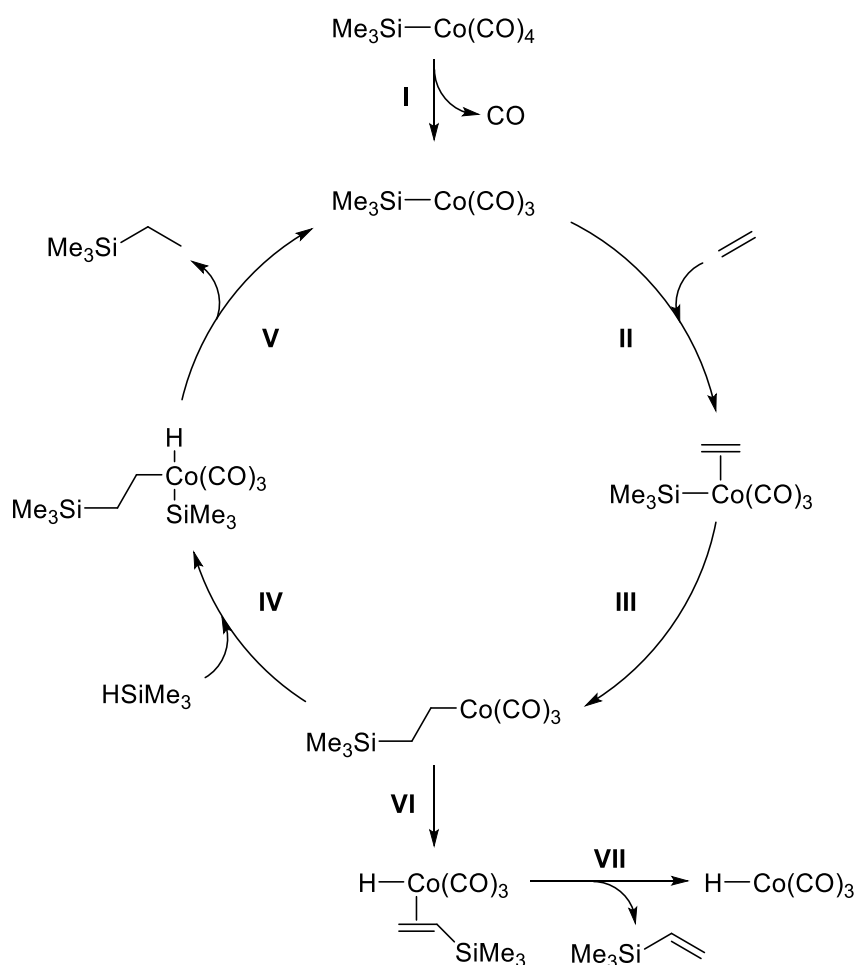
A multitude of compounds are known to be catalytically active in the hydrosilylation reaction, among them free radical initiators (e.g. peroxy compounds), nucleophilic-electrophilic catalysts, strong acids, organic bases such as trialkyl amines and Lewis acids (e.g. AlCl_3 , $\text{B}(\text{C}_6\text{F}_5)_3$).^{29b, 29c, 30} Most prominently transition metal compounds (e.g. Ti, Zr, Hf, Mn, Re, Fe, Ru, Os, Co, Rh, Ir, Ni, Pd, Pt)^{14a, 27b, 29b-d, 30-31}, but also alkali and alkaline earth metals (e.g. Ca, Sr, K)^{29b} and lanthanides (e.g. Y, La, Sm)³⁰ are employed in the hydrosilylation reaction. They are used in the form of homogeneous complexes and heterogeneous catalysts, among them nanoparticles and supported nanoparticles, single atom-site catalysts and immobilized catalysts.^{27b, 30-31} Initiation and control of the reaction is possible by light or temperature, but also microwave, sonic and electrochemically triggered compositions are reported in literature.^{29c}

Until now, platinum-based catalysts remain essential for industrial applications due to their unmatched activity and ability to function effectively under ambient conditions.^{27a} However, encapsulation of the catalyst in cured silicones irreversibly removes up to 6 t/a of platinum³² from the available resources, which are made up of 190 t/a of primary production and 65.4 t/a of recycled platinum³³. If one excludes recycling, the present-day demand would deplete all currently available platinum resources in about 200 years.³³ Yet, the demand for platinum is expected to increase drastically³⁴, which has led to the recycling of platinum, mainly from automotive catalysts³⁵, but also feasibility studies concerning silicones have been conducted³⁶. Furthermore, the utilization of platinum is intertwined with economic, environmental, and human health considerations.³⁷ These factors collectively underscore the imperative to diminish platinum usage, or potentially substitute it with alternative materials.

Efforts to design highly potent catalysts, exploiting vastly available and cheap elements are ongoing and require tailor-made ligands to overcome intrinsic element-specific barriers.^{27b, 29c, 31b, 31c} Additionally, mechanistic considerations of non-platinum catalysts might differ from those of the established platinum catalysts, which has to be reflected during development.³⁸ This also affects the regioselectivity, as platinum catalysts almost exclusively yield the anti-Markovnikov product, while other elements might form the Markovnikov product.^{31b} While the mechanism of platinum-catalyzed hydrosilylation is presented in great detail later on, a superficial review^{30, 38} of non-platinum catalysts and their associated reaction cycles for the hydrosilylation of alkenes has to suffice.

Seitz and Wrighton disclosed the mechanism³⁹ (Scheme 3) of photocatalytically⁴⁰ active $[(\text{CO})_4\text{Co-SiMe}_3]$, building on evidence of the reaction cycle of $[(\eta^5\text{-C}_5\text{Me}_5)(\text{CO})_2\text{Fe-SiR}_3]$ ⁴¹ ($\eta^5\text{-C}_5\text{Me}_5 = \text{Cp}^*$). Removal of one CO entity (**I**) generates the coordinatively unsaturated 16-electron complex $[(\text{CO})_3\text{Co-SiMe}_3]$ as evidenced by FTIR following near-UV photolysis at 77 K.⁴² Subsequent side-on coordination

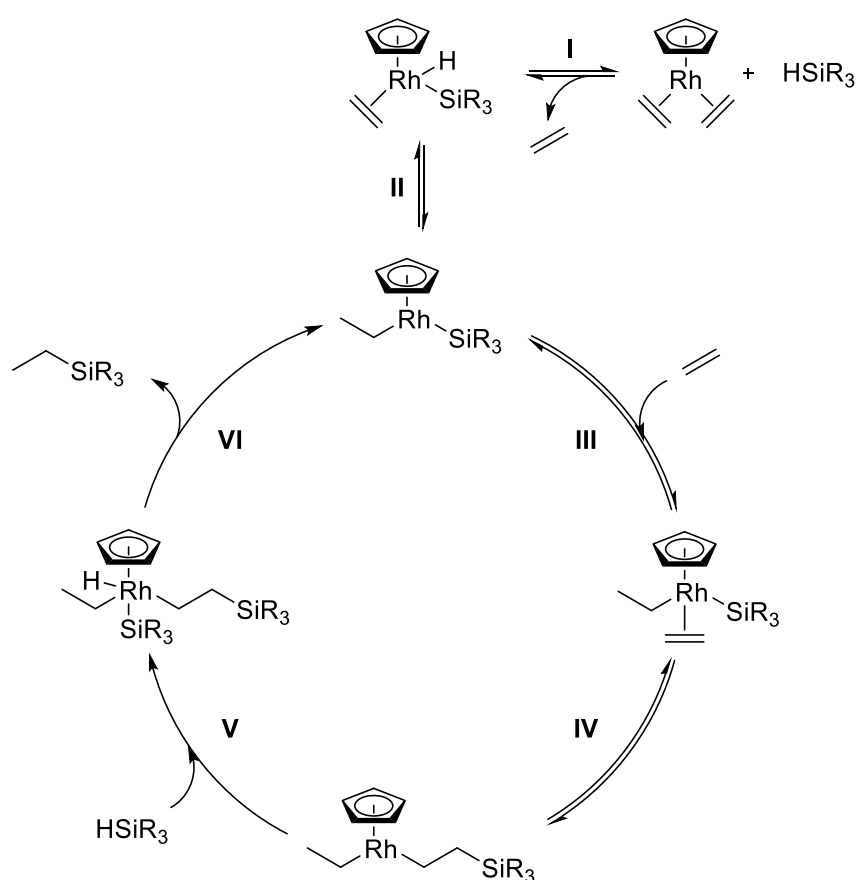
of ethylene (**II**) is accounted for by FTIR analysis, as well as ^1H NMR.³⁹ Migratory insertion of ethylene into the Co–Si bond (silyl migration) (**III**) is succeeded by oxidative addition of silane (**IV**) and completion of the catalytic cycle achieved by C–H reductive elimination (**V**) of the product. Steps **IV** and **V** were further investigated by reaction of $[(\text{CO})_4\text{Co-Me}]$ with HSiMe_3 and analysis by ^1H NMR, which confirmed the generation of CH_4 , not SiMe_4 , the expected product according to the Chalk-Harrod⁴³ mechanism. In the absence of silane, β -H elimination takes place (**VI**), releasing vinyl(triethyl)silane (**VII**), which was detected by GC. Later on, it was reported that the introduction of NHCs as spectator ligands for cobalt complexes significantly alters the reactivity thereof.⁴⁴



Scheme 3: Seitz-Wrighton mechanism for the hydrosilylation and dehydrogenative silylation of alkenes.³⁹

Duckett and Perutz also studied the hydrosilylation of ethylene, however in the presence of $[\eta^5\text{-C}_5\text{H}_5\text{Rh}(\text{C}_2\text{H}_4)_2]$ ⁴⁵ ($\eta^5\text{-C}_5\text{H}_5 = \text{Cp}$; Scheme 4), illuminating two competitive pathways – especially for rhodium complexes – olefin insertion into M–Si vs. M–H bonds³⁰. In addition to Rh, olefin insertion into M–Si bonds has been reported for Fe, Co, and Ru.⁴⁶ Photolysis of $[\text{CpRh}(\text{C}_2\text{H}_4)_2]$ in the presence of silane (**I**)⁴⁷, particularly at low temperatures⁴⁸, generates $[\text{CpRh}(\text{C}_2\text{H}_4)(\text{SiR}_3)\text{H}]$, reflecting the basic structure that is also required in the Chalk-Harrod mechanism⁴³. A (1,3)-H shift (**II**) yields a 16-electron species that reversibly coordinates ethylene (**III**), succeeded by a (1,3)-silyl shift (**IV**) that is also

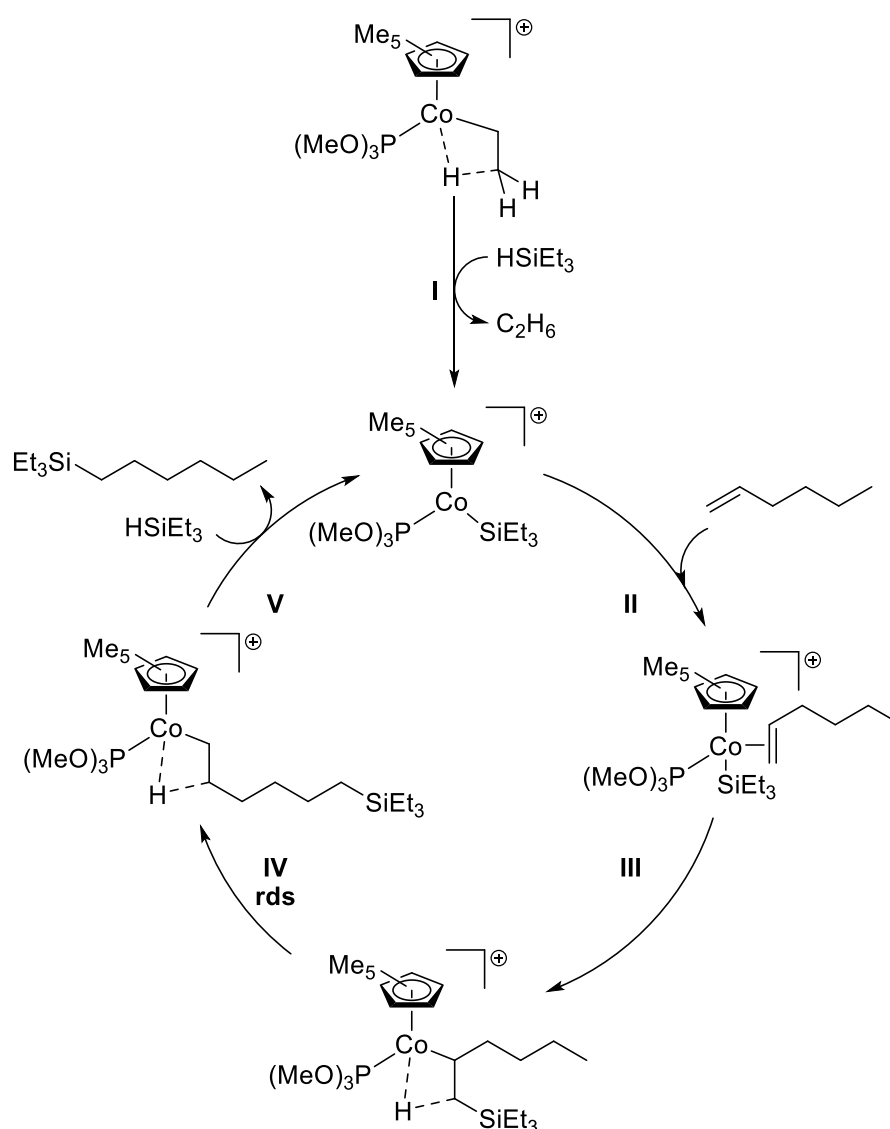
reversible. Oxidative addition of silane (**V**) forms a species that contains two silicon atoms, hence the description as a two-silicon cycle, and rhodium in oxidation state V that is possibly stabilized by a RhSiH or RhCH 3-center-2-electron bond⁴⁹. Related Rh(V) intermediates were earlier reported by Maitlis *et al.*⁵⁰ The reaction cycle is concluded by reductive elimination (**VI**) of the hydrosilylation product and regeneration of the active species. By means of cross-alkene, cross-silane, and deuterium labeling experiments, it was determined that (1) silyl migration is a key step, (2) $[\text{CpRh}(\text{C}_2\text{H}_4)(\text{SiR}_3)\text{H}]$ is not involved in the catalytic cycle, and (3) the ethyl group is retained as a spectator ligand. Indeed, this sequence mirrors the one proposed by Seitz and Wrighton³⁹, with $[\text{Co}(\text{CO})_3]$ substituted by $[\text{CpRhEt}]$. Despite the presence of silylation products in the hydrosilylation system examined by Duckett and Perutz⁴⁵, no mechanistic route was suggested for their generation, unlike for Seitz and Wrighton³⁹.



Scheme 4: Duckett-Perutz mechanism (two-silicon cycle) for the hydrosilylation of alkenes.⁴⁵

“Direct evidence for a silyl migration pathway” was also provided by Brookhart and Grant.⁵¹ Initially they found that electrophilic Co(III) complexes efficiently catalyze olefin oligomerization and polymerization reactions⁵², as well as hydrogenation⁵¹ thereof. Parallels between H_2 and silanes prompted investigation of hydrosilylation properties of $[\text{Cp}^*(\text{P}(\text{OMe})_3)\text{CoCH}_2\text{CH}_2-\mu\text{-H}][\text{BAR}_4]$ ($[\text{BAR}_4]^- = \text{B}[3,5-(\text{CF}_3)_2\text{C}_6\text{H}_3]_4^-$) and resulted in the elucidation of the reaction mechanism (Scheme 5) by identification of two key intermediates, in conjunction with kinetic and deuterium labeling experiments.⁵¹ Variable temperature ^1H NMR experiments revealed the formation of ethane as initial

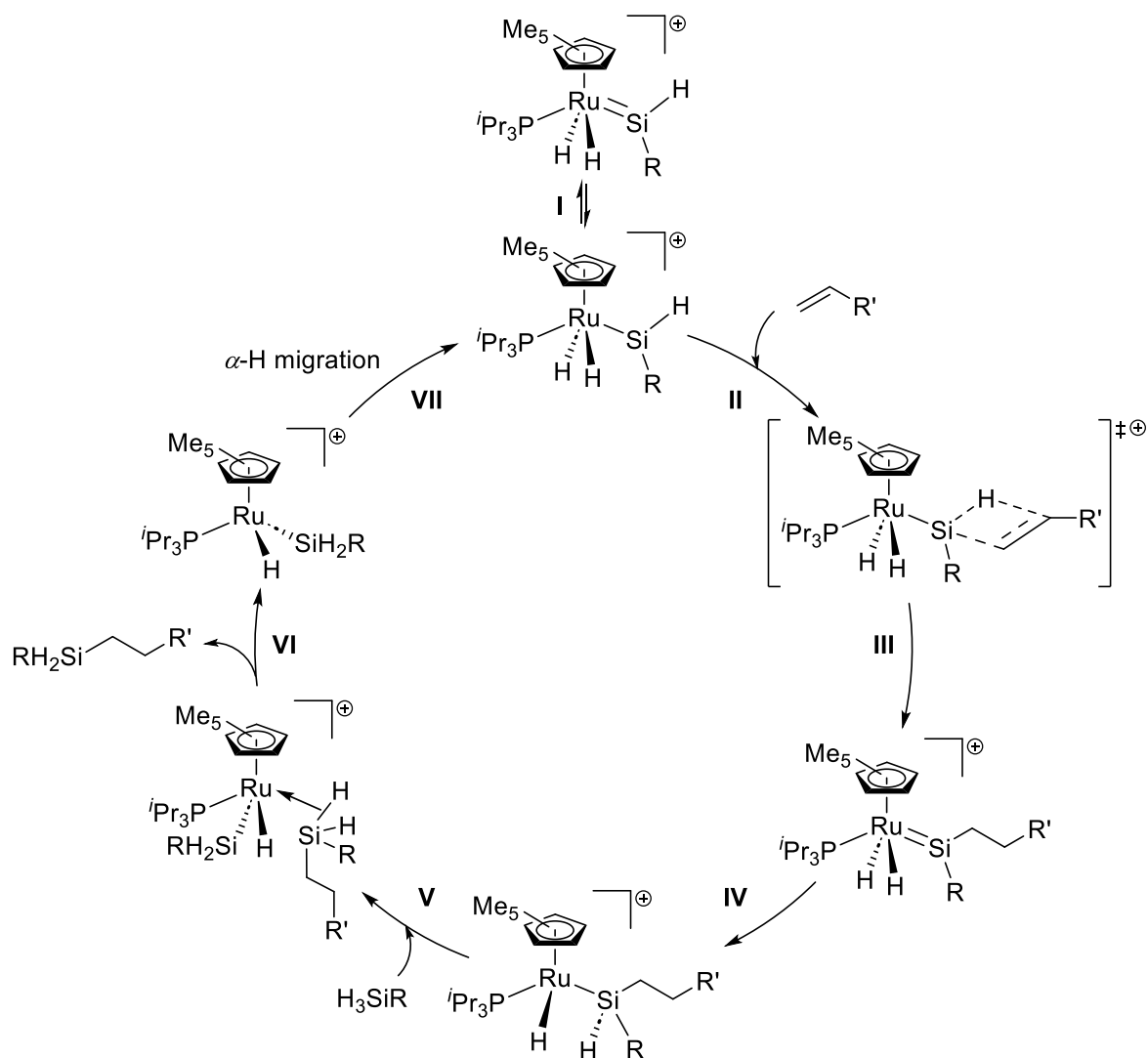
step in the presence of silane (I). Side-on coordination of hex-1-ene (II) would be succeeded by oxidative addition if this mechanism would proceed according to the Seitz-Wrighton³⁹ (Co(III)) or Duckett-Perutz⁴⁵ (Rh(V)) mechanism. However, Co(V) might be avoided herein and σ -bond metathesis (III) would retain Co(III) with an agostic stabilization. This species, as well as the one after the rate-limiting isomerization (IV), were spectroscopically identified and in a final conversion with silane (V), the catalytic cycle is concluded. In conclusion, the herein discussed mechanisms of Seitz and Wrighton³⁹, Duckett and Perutz⁴⁵, and Brookhart and Grant⁵¹ rely on silyl migration as key transformation, thereby avoiding a metal alkene silyl hydride intermediate in the catalytic cycle as in the Chalk-Harrod⁴³ mechanism.



Scheme 5: Brookhart-Grant mechanism for the hydrosilylation of hex-1-ene. [BAR₄]⁻ omitted for clarity.⁵¹

Glaser and Tilley reported ruthenium-catalyzed hydrosilylation that proceeds *via* silylene extrusion, the transfer of a silylene unit from H₃SiR to the ruthenium center (Scheme 6).⁵³ Charge distribution stabilizes the cationic ruthenium fragment (I) that readily adds the sp² Si-H bond to an alkene (II, III).

1,2-Migration of hydrogen from ruthenium to silicon (**IV**), Si-H bond activation (**V**) and reductive product elimination (**VI**) with subsequent α -H migration (**VII**) complete the catalytic cycle.⁵³⁻⁵⁴ Consistent with the Chalk-Harrod mechanism⁴³, there is compatibility with highly substituted alkenes, strict anti-Markovnikov selectivity, and cis-addition of Si-H entities to alkenes, however, exclusively primary silanes are converted by this mechanism.⁵³⁻⁵⁴



Scheme 6: Glaser-Tilley mechanism for the hydrosilylation of 1-alkenes by primary silanes. [B(C₆F₅)₄]⁻ omitted for clarity.⁵³⁻⁵⁴

1.3.2 Supremacy of Platinum Catalysts

Platinum catalysts are by far most often used in industry due to their excellent properties that offset the financial drawback compared to other elements by a long way.^{27a} A significant share of the references in this section are patents, rather than research articles, acknowledging the applied nature and significant industrial research on the topic of platinum-based hydrosilylation catalysis. In this context, the review on hydrosilylation from an industrial point of view from Troegel and Stohrer from the Wacker Chemie AG is illuminating in dissecting advances and actual challenges.^{27a}

Only ten years after the discovery of radical-mediated hydrosilylation by Sommer⁵⁵ in 1947, Speier found that a solution of chloroplatinic acid hexahydrate in isopropanol is catalytically active in the hydrosilylation reaction (Figure 3).⁵⁶ CpPtMe₃ of Robinson and Shaw adopts a piano stool⁵⁷ arrangement and was synthesized for purely structural-chemical reasons and without direct application intentions.⁵⁸ Kinetic decomposition experiments later revealed relatively labile Pt–Me bonds at about 164 kJ·mol⁻¹.⁵⁹ The photohydrosilylation properties of CpPtMe₃ were commercially protected by patent registration⁶⁰, expanding the scarcely investigated area of light-induced hydrosilylation with pioneers like Faltynek⁶¹, Wrighton³⁹, Trogler⁶², and Eckberg⁶³, especially by elucidation of the activation mechanism⁶⁴. The volatility of CpPtMe₃ allows simple purification by sublimation⁵⁸, application in organometallic chemical vapor deposition (OMCVD)⁶⁵, but also poses problems with respect to workplace safety, due to the inherent toxicity of the compound^{27a}. These issues are resolved by introduction of silyl substituents or alkyl moieties at the Cp ligand^{60a, 66}, while the quantum efficiency is improved by extension of the π -system⁶⁷ or addition of auxiliary radical photoinitiators⁶⁸, or a combination thereof⁶⁷. Returning from photocatalysis to thermally-induced hydrosilylation, the system of Speier was further developed by Lamoreaux, extending the range of alcohols to 1-octanol but also isoamyl, 2-ethylhexyl, hexyl, and pentyl alcohols.⁶⁹ Willings patented a platinum hydrosilylation catalyst in 1968, that is formed by heating a mixture of divinyltetramethyldisiloxane (dvtms, M^{Vi}M^{Vi}) and chloroplatinic acid hexahydrate⁷⁰. Karstedt improved Willings catalysts by including ethanol and sodium bicarbonate into the synthesis that was optimized to remove inorganic halogens⁷¹. In this context it is noteworthy that solutions of M^{Vi}M^{Vi}-Pt(0) complexes in excess vinylsiloxane are referred to as solution A.^{71b, 71c} To this day, Karstedt's catalyst remains the benchmark system for newly developed catalysts as it represents the most established and versatile catalyst in the industrial repertoire.^{27a} Consequently, an in-depth mechanistic presentation is provided further below. In retrospect of the last chapter, it is worth noting, that the nickel equivalent of Karstedt's catalyst favors dehydrogenative silylation, while the "original" platinum version exhibits high selectivity for the hydrosilylation reaction.⁷² Ashby patented a cyclic D^{Vi}₄-Pt(0) catalyst which is closely related to Karstedt's catalyst on behalf of the General Electric Company, like

Karstedt and Lamoreaux before.^{29d, 73} By contrast, Willing and Speier worked for Dow Corning Corporation. NHCs were used for the first time by Markó which resulted in more selective catalysts.⁷⁴ The stronger NHC ligands prevent colloidal platinum formation that was observed for weakly coordinating olefinic Pt catalysts. Colloidal platinum was found to deactivate the catalyst, reduce selectivity but also lessen product quality by yellowing.^{17c, 75} The great importance of Markó-type complexes for this work is acknowledged by a detailed account of the catalytic performance and overall reactivity further below. More recently silylene ligands were employed by Kato and Baceiredo⁷⁶ and Iwamoto⁷⁷, which gave both highly active and selective catalysts.

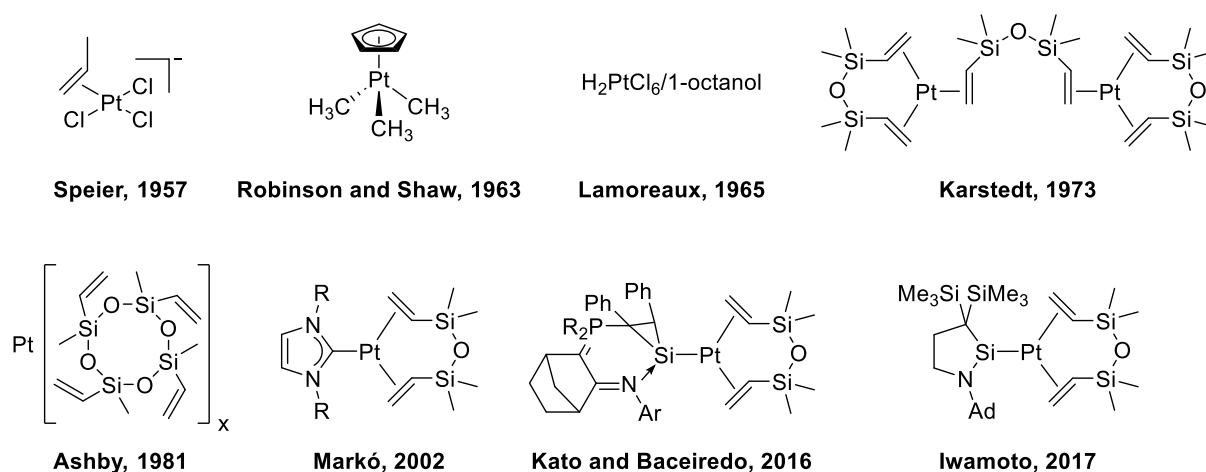


Figure 3: Selected hydrosilylation catalysts of industrial and academical importance.

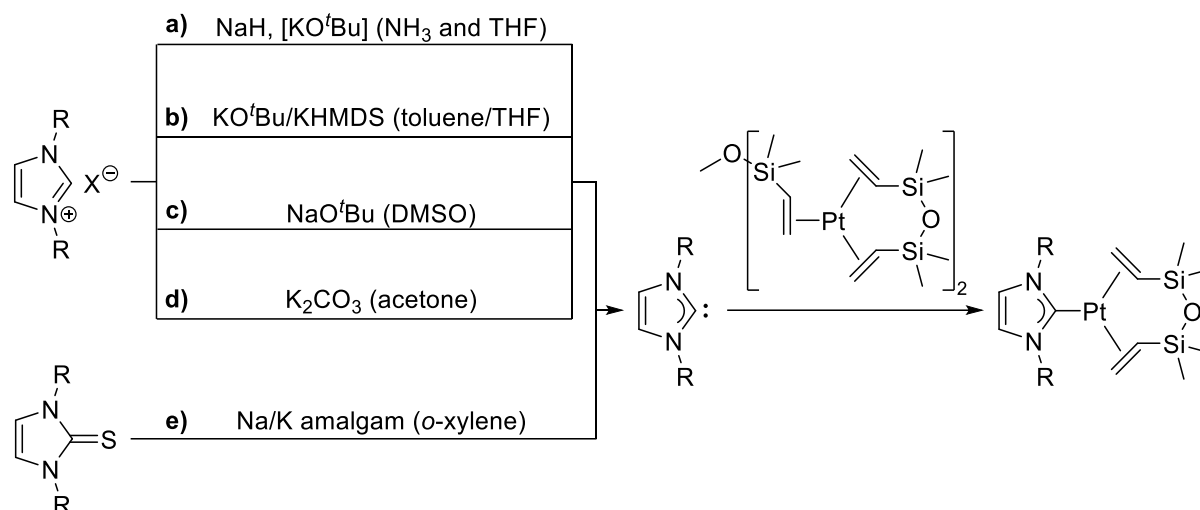
1.3.3 Markó-type Complexes

In 2002, Markó *et al.* addressed limitations associated with Karstedt's catalyst, including inadequate stability leading to colloidal platinum formation, resulting in yellowing of the reaction mixture and reduced selectivity.^{74a} This was achieved by incorporating NHC spectator ligands, which, while slightly diminishing the catalyst's activity, enabled tolerance of a broad spectrum of functional groups and hydrosilylation of their alkenes with absolute regioselectivity.⁷⁴ The hydrosilylation kinetics of these complexes are characterized by sigmoidal behavior due to the rate-determining initiation step, as they are "slow-release" precursors of the catalytically active platinum species.⁷⁸ The air and moisture-stable 16-electron Pt(0) complexes of the general formula (NHC)Pt(dvtms) are easily accessible, but are sensitive towards light, especially in solution.^{74a, 79} Initially, their phosphine congeners, (R₃P)Pt(dvtms), were also investigated and although Karstedt's activity is not quite matched, the Markó-type complexes are easily outclassed in terms of activity.^{74a} However, the rate of isomerization remains high, and colloidal platinum formation indicates displacement of the phosphine ligand at least to some extent. Additionally, phosphines are readily oxidized, which directed the focus of further research to the NHC complexes^{78, 80}, also attracting great attention of other groups^{75a, 79, 81}. The long-held assumption that no platinum colloid is formed during catalysis^{74a, 78} has recently been challenged by UV-vis data of Nahra and Nolan *et al.*⁸² However, it is estimated that platinum colloids play a subordinate role, as selectivity is maintained at an excellent level.

In Markó-type complexes, the dvtms chelate coordinates to platinum in a bidentate fashion, spanning a hexagon, that adopts chair conformation. In combination with the carbene, platinum is in a characteristic, distorted trigonal planar environment, improving π^* -backbonding to the vinyl groups due to better overlap.⁷⁸ Indeed, the C=C bond distance serves as a probe for the degree of backbonding from platinum, and hence as an indicator of electron density at the central atom.⁷⁸

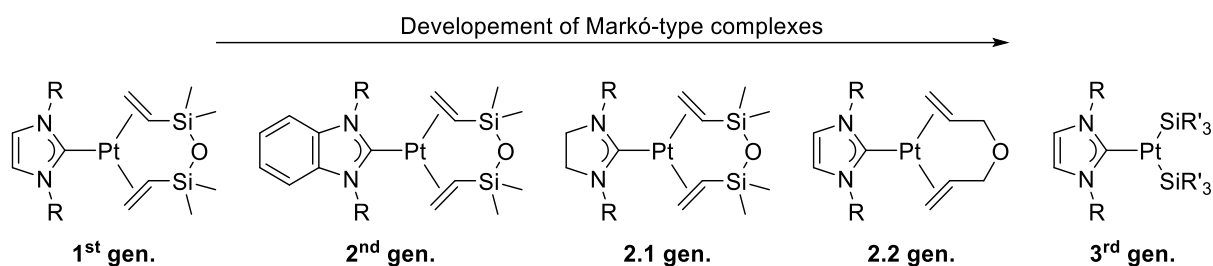
Initially⁷⁸, the synthesis of these complexes from an imidazolium salt and Karstedt's catalyst *via* the free carbene was conducted in accordance with an arduous procedure of Herrmann *et al.*⁸³ (Scheme 7, a), at -40 °C in a mixture of liquid ammonia and THF (5:1) and in the presence of stoichiometric amounts of NaH with catalytic amounts of KO^tBu. As a matter of fact, imidazolium salts are much more soluble in the presence of liquid ammonia, than in pure organic solvent, and also hydrogen bonding enhances the acidity of the carbenoid proton. The selected bases form simple alkaline salts as byproducts, that are easily removed after evaporation of all volatiles and filtration as diethyl ether or hexane solution, rendering this route ideal for large-scale synthesis of free carbenes. Most commonly, a strong base (e.g. KO^tBu) is combined with an aprotic and rather apolar (e.g. toluene) solvent, leading to product formation after 16 h.^{78, 81c, 81g, 81k} The use of sulfonated NHCs, however, requires a highly polar, yet aprotic solvent, like DMSO, in combination with NaO^tBu for improved solubility, granting

access to hydrosilylation reactions in aqueous media.^{81e, 81f} Recently, the weak-base route was proposed as a more sustainable alternative, employing K_2CO_3 as a base in acetone, which requires 60 °C for 20 h and gives the target complexes in good yields. The final synthesis route generates a free carbene by reduction of the corresponding thiourea in the presence of Na/K amalgam after 20 d and is merely employed in the case of challenging access to certain imidazolium salts.^{80a}



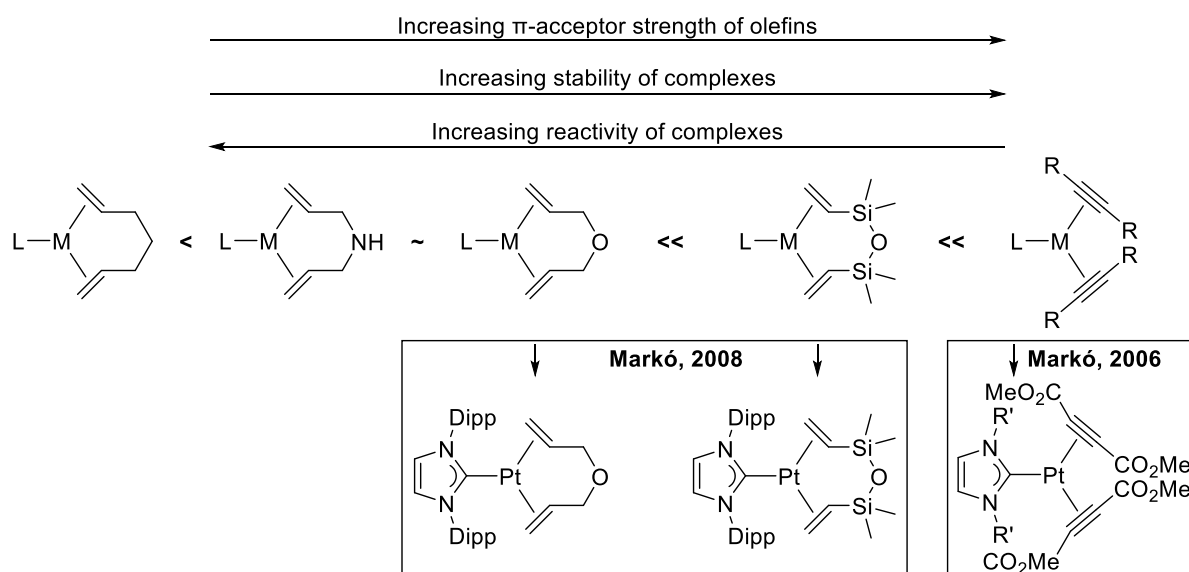
Scheme 7: Synthesis strategies for the access of Markó-type complexes *via* generation of a free carbene, which reacts with Karstedt's catalyst. a) procedure of Herrmann *et al.* where a 5:1 mixture of liquid NH_3 and THF is used with stoichiometric amounts of NaH as base and catalytical amounts of KO^tBu at -40 °C.^{78, 83} b) most common: combination of a strong base and (rather) apolar, aprotic solvent.^{78, 81c, 81g, 81k} c) combination of a strong base and polar, aprotic solvent for highly polar (e.g. sulfonated) NHCs.^{81e, 81f} d) weak-base method, using K_2CO_3 and acetone at 60 °C for 20 h.⁸⁴ e) reduction of the thiourea over Na/K amalgam for 20 d at RT.^{80a}

As previously noted, early investigations involved phosphine complexes; however, they were discontinued due to stability concerns, rendering (imidazole-2-ylidene)Pt(dvtms) complexes as the first-generation of Markó-type complexes (Scheme 8).^{74a} At remarkably low catalyst loadings of 30 ppm, terminal alkenes are efficiently and selectively hydrosilylated, while epoxides, alcohols, ketones, esters, and protecting groups tetrahydropyranyl ether and *t*-butyl dimethylsilyl ether are tolerated, achieving TONs beyond 10^6 .⁷⁴ The duration of the induction period correlates with the steric bulkiness of the substituents attached to the NHC moiety. Consequently, initiation phases are prolonged in the presence of bulky NHC-wingtips but also aromatic wingtips compared to alkyl substituents. Once activated, the rate of reaction is inversely proportional to the steric demand, resulting in activity series $Me < Cy < ^tBu$ for alkyl NHC-wingtips, and $Mes < Dipp$ for aromatic NHC-wingtips.^{74b, 78} The first-generation of Markó-type complexes was also employed in the hydrosilylation of alkynes, where it was found that the electronic influence of the NHC on the regioselectivity (β -(E) vs. α) is negligible, and only the steric demand of the NHC-wingtips increases the β -(E)/ α -ratio.^{80b}



Scheme 8: Generations of Markó-type complexes with modifications of the NHC spectator and diene- or silyl-ligands.

Subsequently, in the second-generation of Markó-type complexes, stronger σ -donors based on benzimidazole-2-ylidene were employed only in combination with alkyl NHC-wingtips, and the resulting catalysts were found to be superior to their parent complexes.^{80a} This concept was expanded by incorporation of 4,5-dihydroimidazol-2-ylidenes⁸⁵, which are even stronger σ -donors than benzimidazole-2-ylidenes in a herein-called generation 2.1.⁷⁸ This study validated the observed trend wherein ligands possessing greater σ -donating abilities result in complexes with platinum centers that are more electron-rich. This phenomenon correlates with extended induction periods while concurrently enhancing activity. Instead of altering the NHC, in generation 2.2 (herein) the dtms chelate is substituted by allyl ether, giving significantly more active complexes, which were only subjected to the hydrosilylation of alkynes.⁸⁶ Reason is, the nature of the diene inherently determines the rate-limiting de-coordination of itself during the activation procedure, also affecting the overall stability of the (L)-Pt-(η^2 -alkene)₂ complexes.^{78, 87} Hence, the synthesis of generation 2.2 cannot occur by exchange of the dtms moiety of the first-generation as a post-modification, but rather by reduction of H₂PtCl₆ in the presence of the respective diene analogous to the synthesis of Karstedt's catalyst with subsequent coordination of the NHC.^{86a} The exerted influence of the (*bis*)olefin on the stability and reactivity of complexes is shown in Scheme 9 with the related reports of Markó *et al.*^{80b, 86, 87f}

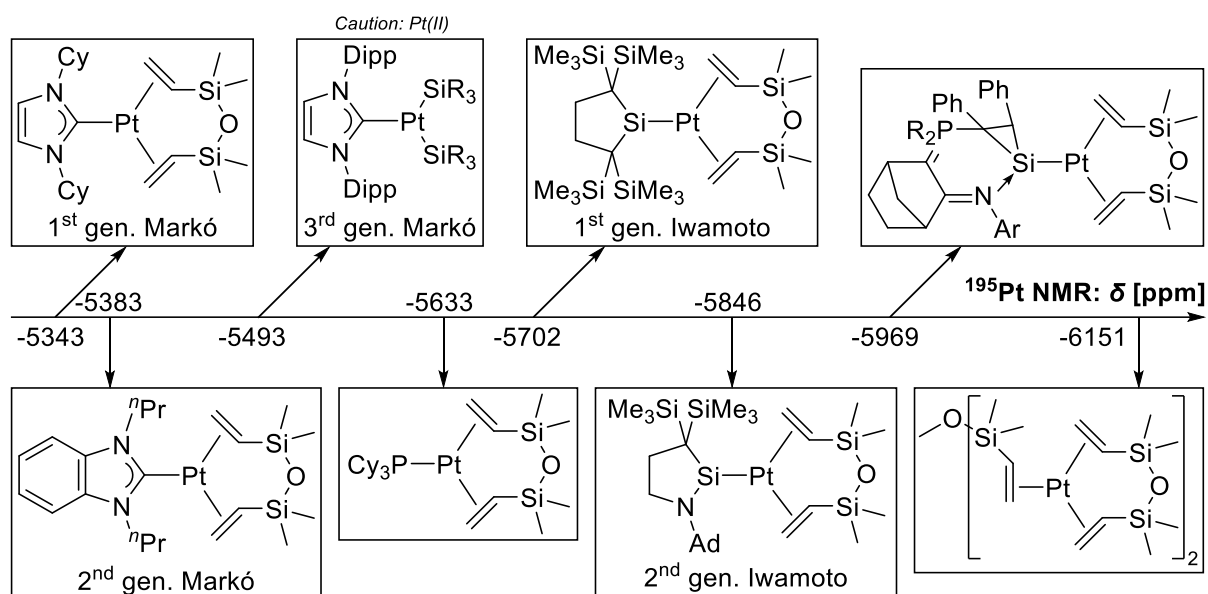


Scheme 9: Acceptor properties of varying (*bis*)olefins on the stability and reactivity of complexes, combined with the associated studies of Markó *et al.*^{80b, 86, 87f}

In this context, it is worth noting, that the second-generation^{80a} and generation 2.2⁸⁸ are both specified as the second-generation by Markó *et al.*, which might lead to poor comprehensibility when accessing literature. Additionally, with regard to NMR, upfield and downfield are used inaccurately.⁷⁸ Hence, upfield is defined as the shift to lower ppm (more shielded), and downfield is defined as the shift to higher ppm (less shielded) to avoid misconceptions.

In the third-generation, the established imidazole-2-ylidene is applied once more and the diene chelate is substituted by two silyl groups, resulting in a unique Y-shaped tricoordinate Pt(II) complex.⁸⁸⁻⁸⁹ The compound was published in 2009 as a coordination curiosity⁸⁹ and it then took six years to discover its exceptional catalytic properties⁸⁸ for the hydrosilylation of alkenes and alkynes. Although the mechanism of formation is not yet confirmed, it is presumed that after the initial hydrosilylation of the diene and oxidative addition of one silane entity a Pt(II) species is formed that subsequently generates the target compound either by σ -bond metathesis of the Pt–H and the Si–H bond of a fresh silane, or by another oxidative addition of silane, which gives Pt(IV), and successive reductive elimination of dihydrogen. The resulting catalyst is highly active and selective in the hydrosilylation reaction of alkynes and under identical conditions, [(Im^{Dipp})Pt(SiR₃)₂] as the third-generation catalyst outperforms his predecessors by far (3rd gen. >> 2.2 gen > 1st gen.), both in activity and selectivity. Unfortunately, the third-generation catalyst requires exclusion of light and high vacuum for storage purposes that exceed two days⁸⁸, unless dissolved in excess silane, where it is stable even under ambient conditions for several weeks⁸⁹.

The electronic environment of the catalytically active platinum atom is conveniently assessed using sensitive ¹⁹⁵Pt NMR spectroscopy⁹⁰ and influenced by two main factors. Ligands exhibiting σ -donor properties contribute to an increase in electron density around the platinum center, generating a more shielded nucleus with resonances that are upfield shifted to lower ppm, while those with π^* -acceptor properties have the opposite effect.⁷⁸ Comparing the first-generation catalyst, (Im^{Dipp})Pt(dvtms), with a chemical shift of $\delta = -5340$ ppm⁷⁸, to the generation 2.2 catalysts, (Im^{Dipp})Pt(allyl ether), with $\delta = -5574$ ppm^{86b}, the ¹⁹⁵Pt NMR data validates the sequence of olefin acceptor strength as depicted in Scheme 9^{87f}. Indeed, there exists an overall correlation between the ¹⁹⁵Pt shift and the activity of complexes in the hydrosilylation reaction. Specifically, compounds displaying highfield shifts tend to demonstrate higher activity.⁷⁸ An overview of platinum catalysts and their ¹⁹⁵Pt shift is presented in Scheme 10, where the shift-activity-correlation is generally abided by.^{71b, 77-78, 89, 91} The highfield shift of silylene-compounds therein acknowledges the surpassing donor properties of silylenes compared to NHCs and phosphines.^{54b, 76, 92} Careful consideration is warranted for the third-generation Markó catalyst due to its Pt(II) nature, in contrast to all other compounds that feature Pt(0), as Pt(II) species typically exhibit more pronounced downfield shifts in their NMR spectra.⁹⁰



Scheme 10: Chemical shift of ^{195}Pt in selected compounds.^{71b, 77-78, 89, 91}

Extended reactivity of Markó-type complexes is discussed in conjunction with the activation and reaction mechanism (*vide infra*).

1.3.4 Bimetallic Hydrosilylation – An Emerging Prospect

Metalloproteins are vital for carrying out numerous reactions efficiently and selectively in living organisms to sustain essential biological functions.⁹³ These elaborate metal complexes are coordinated by endogenous biological ligands *via* nitrogen, oxygen, and sulfur atoms of amino acids, and thereby anchored to the polypeptide backbone, constituting prosthetic groups.^{93a} Protein-bound metal sites might be essential for (1) the configuration of the tertiary and/or quaternary structure, (2) uptake, storage, and release of metals, (3) uptake, storage, and release of electrons, (4) reversible O₂ binding, and (5) catalytic activation and turnover of substrates.^{93a} Bimetallic sites, where two metal ions are closely positioned, often demonstrate the ability to overcome reaction barriers under physiological conditions, that remain challenging even in artificial non-protein systems.⁹³ Selected bimetallic sites of metalloproteins are depicted in Figure 4 that fulfill points 3 to 5 in the prior recital of functions.⁹³⁻⁹⁴

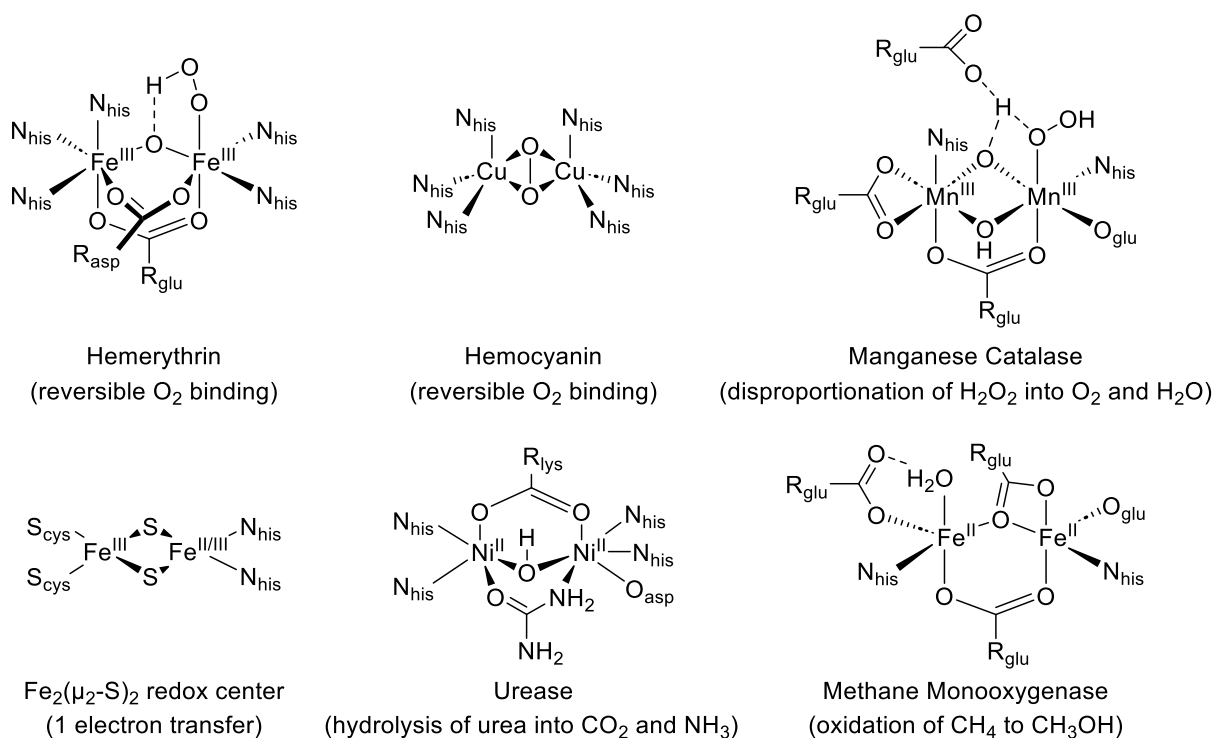


Figure 4: Selected bimetallic sites of metalloproteins and their functions.⁹³⁻⁹⁴

Many biomimetic studies have been inspired by these proteins, highlighting the importance of considering the larger protein structure in addition to the first coordination sphere.^{94a, 94c, 94d, 95} The recognition of synergistic or cooperative effects⁹⁶ between metals in close proximity (Figure 5) has spurred investigations into a wide array of bimetallic complexes in catalysis, aiming to replicate and enhance the activity and selectivity observed in natural metalloproteins.⁹⁷ Artificial systems are not restricted to bioavailable metals and ligands and might therefore utilize a greater variety of structures that expand reactivity patterns of biological systems.^{94a}

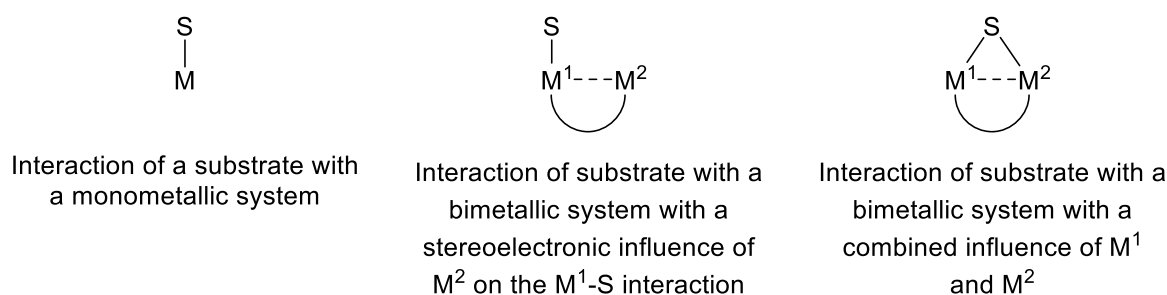


Figure 5: Interaction modes between a substrate and monometallic and bimetallic systems. S = substrate, M = metal ⁹⁶

Bimetallic catalysts also pose an emerging prospect for the hydrosilylation reaction, with a plethora of studied complexes (Figure 6; exhaustive display of literature reports) that exploit the reactivity of Rh, Pt, Ir, and Co but also of oddities like the early transition metals Ti, Zr, Nb, and Ta.⁹⁸ While platinum catalysts are prevalent in industrial applications (*vide supra*), Ishii *et al.*'s Pt-Ir heterobimetallic complexes stand out as the sole platinum-containing bimetallic complexes to catalyze hydrosilylation thus far.⁹⁹

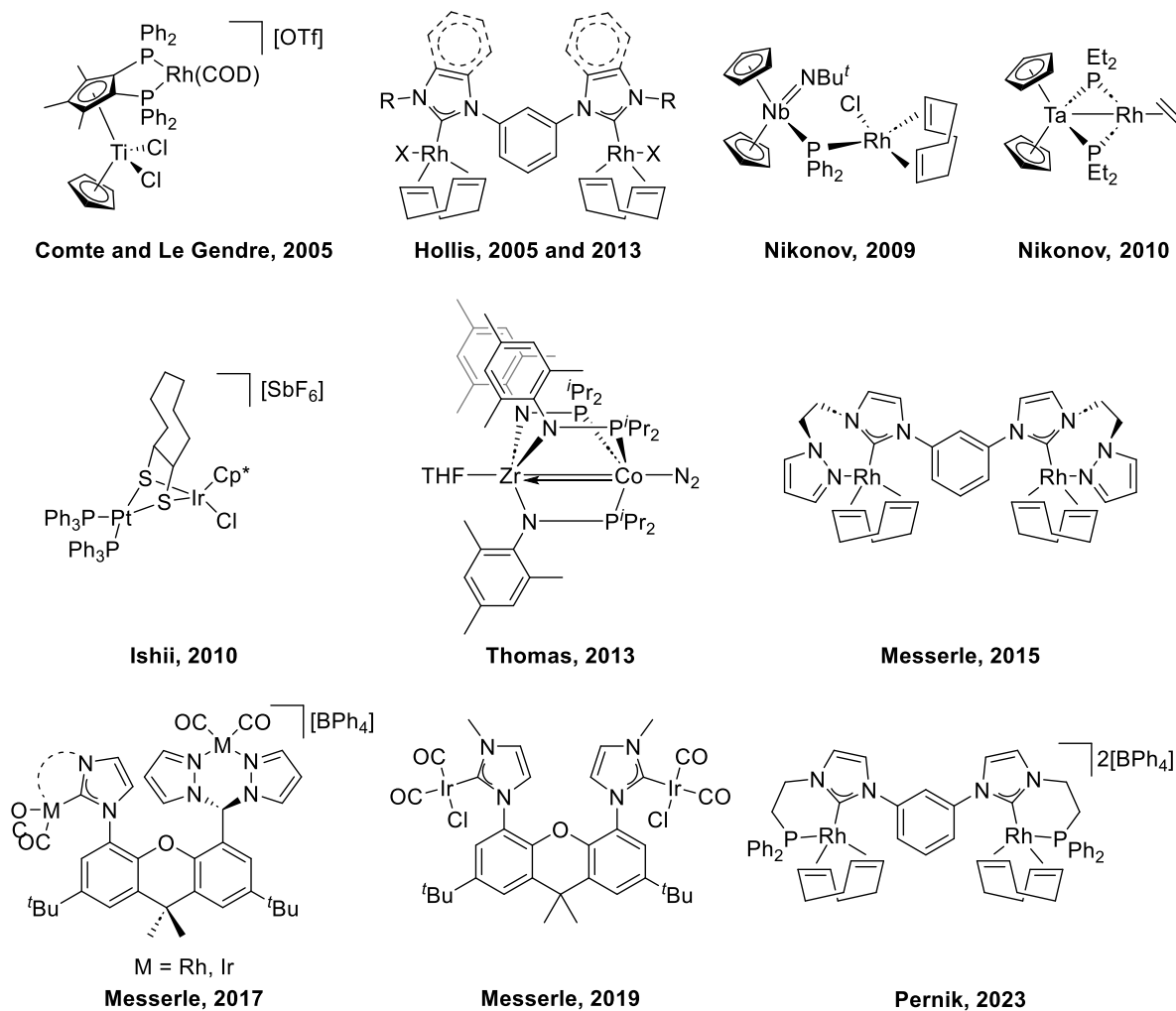


Figure 6: Bimetallic hydrosilylation pre-catalysts.⁹⁸⁻⁹⁹

The Rh-Ti heterobimetallic complex of Comte and Le Gendre *et al.* successfully catalyzes the hydrosilylation of aromatic ketones, surpassing the respective monometallic rhodium complex in

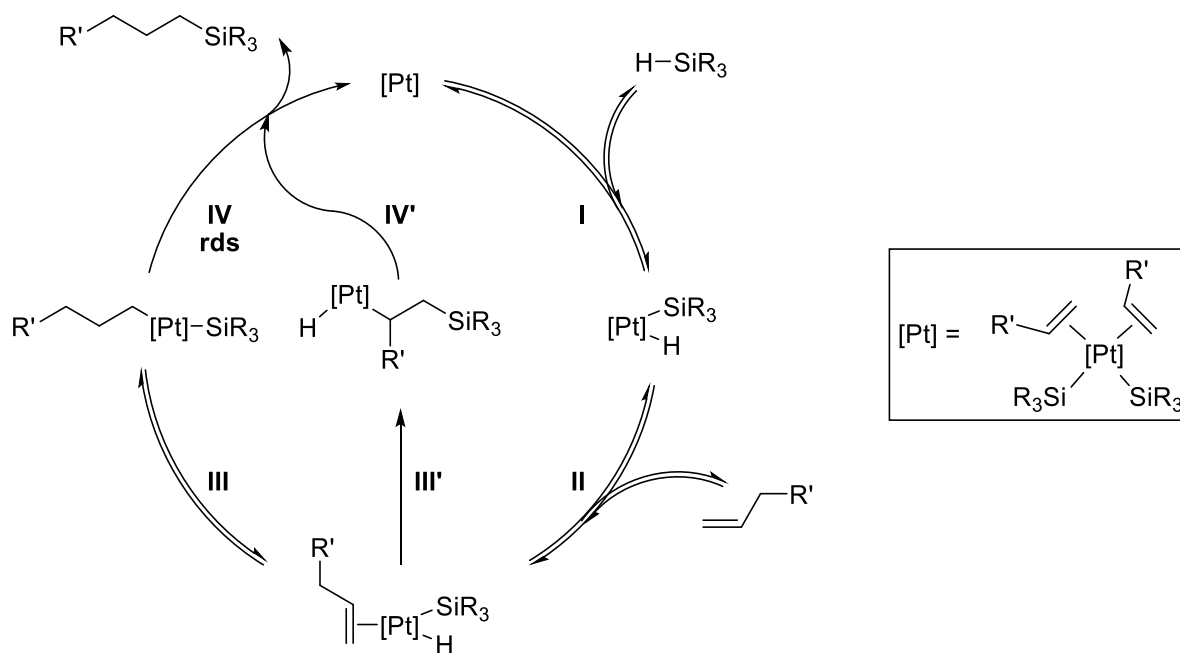
terms of activity and final product yield.^{98b} Although comprehension of the effect of the titan component is deficient, it is noteworthy that the induction period remains virtually unaffected upon incorporation of titanium into the monometallic rhodium complex, whilst the TOF doubles. Ishii *et al.*'s Pt-Ir heterobimetallic complexes excel in the stereoselective hydrosilylation of terminal alkynes, exclusively forming β -(Z) vinylsilanes under the right conditions.⁹⁹ The basic 1,3-*bis*(imidazol-2-ylidene-1-yl)benzene scaffold has found extensive application for the synthesis of homobimetallic rhodium complexes and dangling, or rhodium-coordinating groups at the NHCs have been explored, as well as extension of the aromatic system in the shape of benzimidazol-2-ylidene.^{98c, 98d, 98h, 98j, 98k} The hydrosilylation of a vast variety of substrates like alkenes, aldehydes, ketones, acyl chlorides, α,β -unsaturated carbonyls, nitriles, nitro groups, isocyanates, and tertiary amides is efficiently catalyzed by this complex class.^{98k} Also, a cooperative increase in the TOF has been determined, *inter alia*, by altering the scaffold to 1,4-*bis*(imidazol-2-ylidene-1-yl)benzene to exclude metal-metal interactions.^{98d} Most importantly, insights into the mechanism revealed that the main catalytic cycle is the same for mono- and bimetallic complexes, but the pre-catalyst activation follows different sequences, which is in certain cases the origin of the synergistic effect.^{98h} In the monometallic complex, dissociation of the COD (cycloocta-1,5-diene) is required for complex activation, while the energetically favorable hydrogen transfer between adjacent COD moieties results in disproportionation to cycloocta-1,3,5-triene and cyclooctene to generate a free coordination site at the rhodium center. The catalytic mechanism of hydrosilylation with bimetallic complexes is – so far – based on the Chalk Harrod mechanism, with only one pivotal metal atom in a catalytic cycle, further indicating that mainly the induction period is affected by our bimetallic complexes.^{98d, 98h, 99} An exception, however, is the hydrosilylation of ketones by a Co/Zr heterobimetallic complex, where a mechanism based on ketyl radicals was proposed.⁹⁸ⁱ

1.4 Mechanistic considerations of Platinum-Catalyzed Alkene Hydrosilylation

Understanding the activation of the pre-catalysts and mechanism of catalytic (by-)product formation, along with stability issues and the role of platinum colloids is of major importance for the improvement of catalysts and in particular ligand design. Equally affected is the development of proper methodology for the catalytic evaluation of complexes to account for the analysis of key compounds and to avoid methodic mistakes. Hence, this chapter about the mechanistic considerations will be presented in great detail.

1.4.1 The (Modified) Chalk-Harrod Mechanism

Platinum-catalyzed hydrosilylation seized a pivotal role in silicone chemistry since the discovery of Speier's catalyst⁵⁶ in 1957 and was first mechanistically described by Chalk and Harrod⁴³ in 1965 with a simple model that is still commonly accepted today (Scheme 11) but that was complemented by further mechanistic work^{17c, 100}.

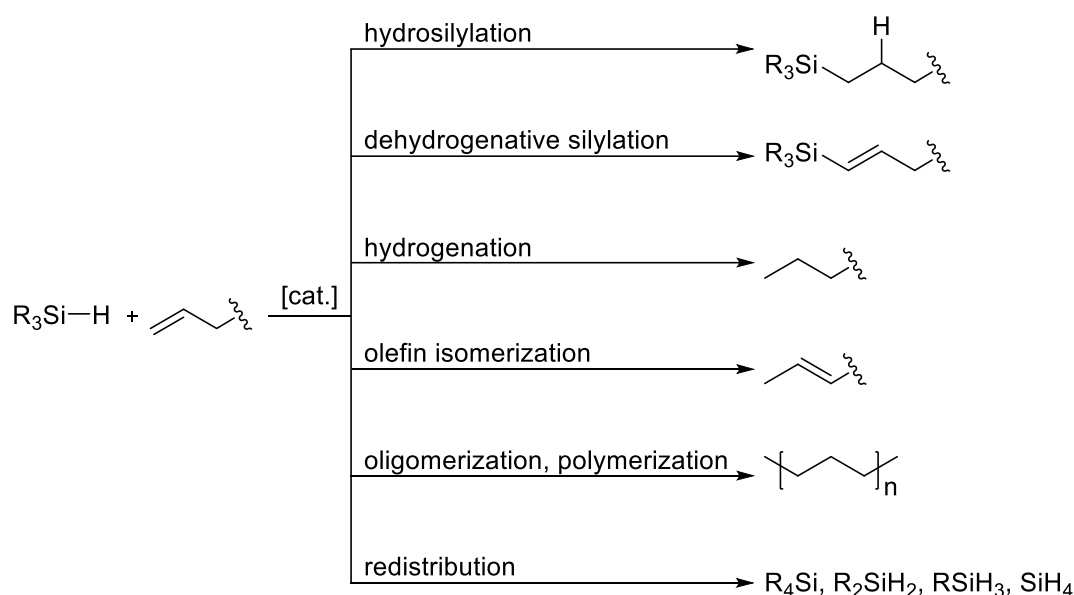


Scheme 11: Left: Catalytic cycle of the Chalk-Harrod mechanism⁴³ (outer cycle) and the modified Chalk-Harrod mechanism¹⁰¹ (inner cycle via III' and IV'). Right: Proposed structure of the catalytically active species. ^{17c, 79, 100a}

The mechanistic cycle begins with a catalytically active platinum species that is depicted as [Pt]. The catalytic cycle involves oxidative addition of a hydrosilane (I), thereby increasing the oxidation state of Pt from 0 to +II. Introduction of an olefin into the coordination sphere of platinum (II) facilitates the preferred migratory insertion into the Pt-H bond, rather than silyl migration, yielding a Pt-C sigma bond (III). The hydrosilylation product is finally reductively eliminated (IV), re-generating free coordination sites for a new catalytic cycle. An extension of this mechanism involves insertion of the alkene into the Pt-Si bond (III', silyl migration), as is common for non-platinum metals (*vide supra*), followed by reductive elimination of the product (IV') and is referred to as the modified Chalk-Harrod

mechanism.¹⁰¹ Reversibility is attested to steps **I-III**, while **IV** is believed to be the rate-determining step.^{17c, 79, 100a, 101b, 102} Investigations of the active species revealed Pt-C and Pt-Si bonds, while no proof of Pt-H bonds was detected, which led to the proposal of a *bis*(alkenyl)-*bis*(silyl)-complex.^{17c, 79, 100a}

Fundamentally, the rate of conversion is dependent on electronic and steric factors of the substrates. The rate is increased for electron-rich olefins and electron-poor silanes, while strongly coordinating olefins, especially chelates, decrease the reaction rate.^{17c, 103} Unfortunately, the Chalk-Harrod mechanism is not strictly obeyed in platinum-catalyzed hydrosilylation and is often accompanied by side reactions that significantly reduce the yield of the desired product.^{27a, 29b} Byproducts are formed by dehydrogenative silylation, hydrogenation, olefin isomerization, oligomerization, polymerization, and redistribution of hydrosilanes (Scheme 12).^{29b} This requires further purification steps, or in the case of silicone materials imposes adverse effects on product quality.^{29b}



Scheme 12: Catalytic hydrosilylation of an alkene and competing side reactions.^{29b}

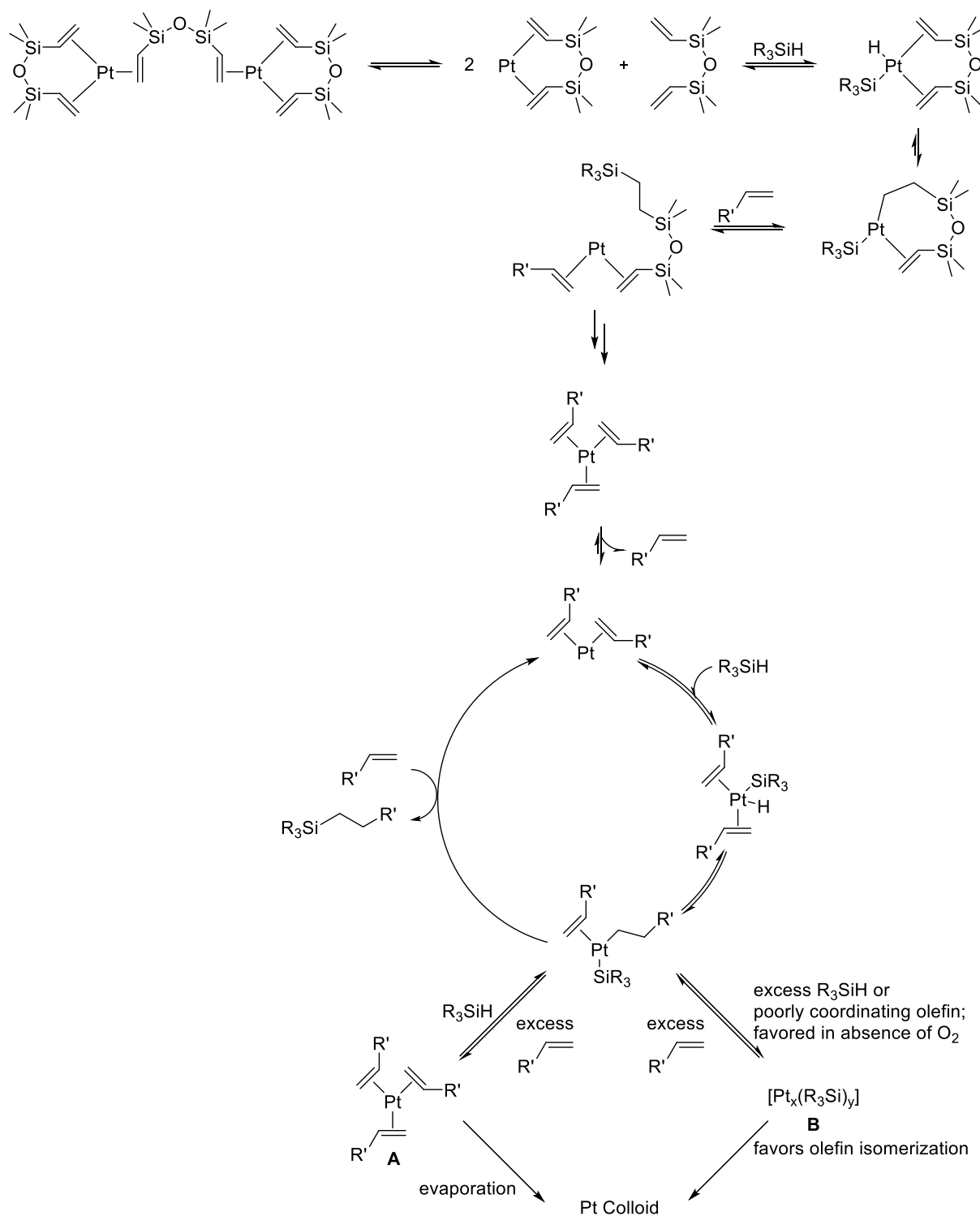
Additionally, several phenomena remain unaddressed by the mechanism of Chalk and Harrod, like the induction period, the formation of colored bodies, the oxygen effect, and the formation of vinylsilanes.^{17a, 17c, 103a, 104} The duration of the induction period depends on the characteristics of both the olefin and silane and also the platinum pre-catalyst and their concentrations. Especially the oxidation state of the platinum compound is of major importance, as $H_2[PtCl_6] \cdot 6H_2O$ for instance needs to undergo reduction prior to hydrosilylation.^{17c}

1.4.2 Activation and Decomposition of Karstedt's catalyst – An In-Depth Study

Furthermore, the nature of platinum-catalyzed hydrosilylation catalysis^{100a} – whether mononuclear and homogenous^{17a, 17c} or at the surface of platinum colloids^{103, 105} – has been the subject of lively discussions. Stein and Lewis *et al.* determined the mononuclear nature of platinum-catalyzed

hydrosilylation in 1999 and revealed the errors that led to the assumption of colloid catalysis.^{17c} The transmission electron microscopy (TEM) and high-resolution electron microscopy (HREM) images^{103a, 105-106} that evidenced colloids were based on evaporated solutions after completion of the reaction and a false positive mercury poisoning test^{105a} was observed as contact of the platinum catalyst to mercury for 7 h prior to catalysis led to decomposition and amalgamation of the catalyst precursor and therefore showed no activity. Done with the correct methodology, mercury demonstrates no adverse effect on the catalytic properties of platinum catalysts.^{17c} Platinum colloids, however, can still be detected upon completion of the hydrosilylation reaction in certain cases (*vide infra*).^{17c} It was also established that both Speier's and Karstedt's catalysts follow the same sequence of identical steps and form the same platinum products.^{17c} The reaction scheme of Stein and Lewis *et al.* is depicted in Scheme 13 and explained in more detail hereafter due to its importance.

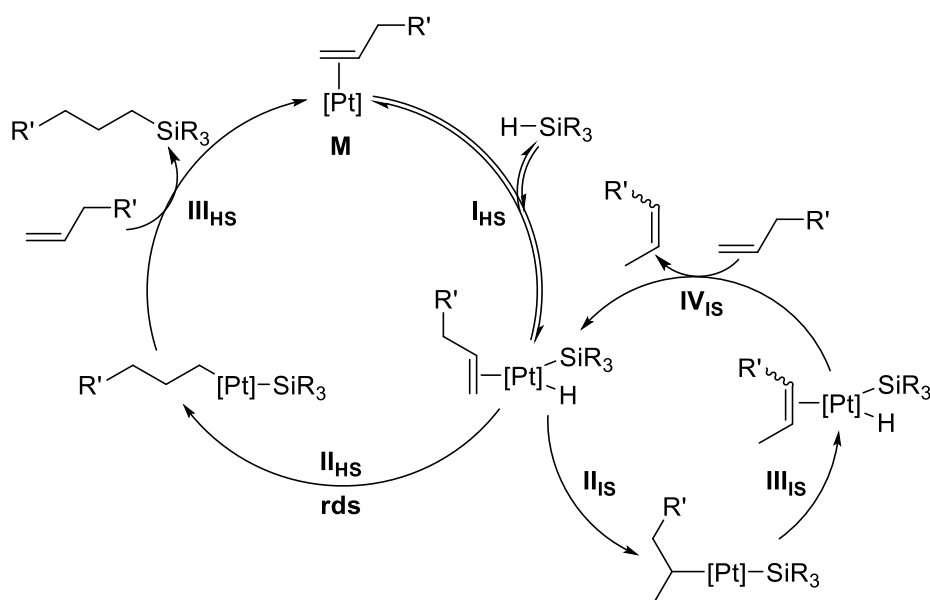
An in-depth study of the reaction cascade of Karstedt's catalyst was conducted using extended X-ray absorption fine structure (EXAFS), small-angle X-ray scattering (SAXS), X-ray photoelectron spectroscopy (XPS), ultraviolet-visible (UV-vis) spectroscopy, HREM, deuteration experiments and the kinetic isotope effect¹⁰⁷ (KIE), and variation of substrates and their stoichiometry.^{17c} In the induction period, de-coordination of the bridging dtms moiety of Karstedt's catalyst is succeeded by hydrosilylation of the dtms chelate in the presence of silane which leads to the active species that proceeds according to the Chalk-Harrod mechanism. Upon completion of the reaction, two different species form dependent on the ratio of silane and olefin and the coordination strength of the olefin. An excess of olefin forms a Pt(alkene)₃ species (**A**), while excess of silane or poorly coordinating olefins favors the formation of **B**, where platinum is bound in a silicon-rich environment. Interconversion of **A** and **B** is possible by addition of the required substrate, but both species are susceptible to colloid formation. The previous assumption, that colloids are the active species^{103a, 103b, 105} is reversed and inactivity and isomerization^{17c} are linked to platinum colloids. The oxygen effect^{103a, 103b, 108} has also been revised and evidence was provided that oxygen disassembles and prevents^{17c} the formation of multinuclear platinum species.



Scheme 13: Reaction scheme for the hydrosilylation of alkenes by Karstedt's catalyst, including the activation procedure, catalytic cycle and transformation of platinum species at the end of catalysis when platinum colloids are frequently formed.^{17c}

1.4.3 State of the Art Kinetic and Mechanistic Considerations

Further investigations of Karstedt's catalyst remain scarce as common laboratory techniques are hampered by the nature of said compound that requires excess vinylsiloxanes^{17c, 78} to avoid decomposition to platinum black (colloids)^{17a, 71b}, the sensitivity towards temperature, light, and atmospheric conditions^{71b}. Additionally, the characterization of intermediates is challenging because of their high activity and susceptible character^{74b, 109}. Understandably enough, the next major mechanistic advance took a while and was put forth by Kühn *et al.* in 2016.¹¹⁰ The study with the objective of gaining more insight into reaction kinetics and the hydrosilylation of internal double bonds presents an improved reaction scheme (Scheme 14) that accounts for isomerization, re-evaluates the reversibility of the olefin into the Pt–H bond (**II_{HS}**) into an irrevocable and rate-determining step. Deuteration experiments and evaluation of the KIE evidence the proposed modifications and are in fact a revised interpretation of the findings of Stein and Lewis *et al.*^{17c} rather than a contradiction.

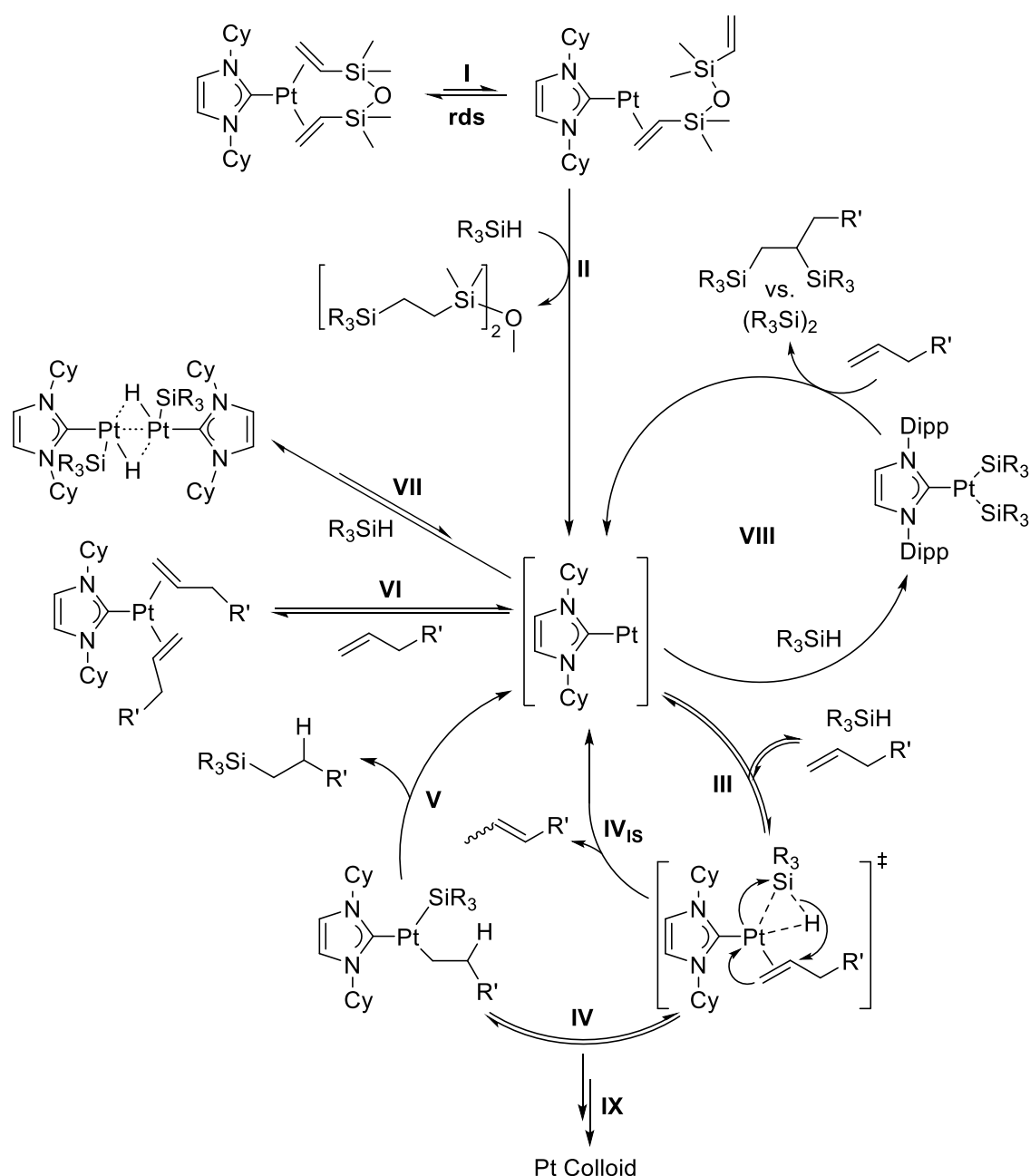


Scheme 14: Revised Chalk-Harrod Mechanism including the hydrosilylation cycle (HS, left) and isomerization cycle (IS, right).¹¹⁰

1.4.4 Mechanistic Aspects and Reactivity of Markó-type Complexes

Markó-type complexes pose an integral part of this work, hence a concise introduction into the reactivity of this complex class is appropriate. The activation *via* partial de-coordination of the dtms chelate (**I**, Scheme 15^{78, 88-89, 111}) poses the rds of the overall reaction mechanism and is succeeded by two-fold hydrosilylation of said moiety. The initiation period is significantly prolonged compared to Karstedt's catalyst, hence Markó-type complexes are described as “slow-release precursors”.⁷⁸ This raises the dilemma of a strongly bound NHC to achieve high selectivities and activities, but at the same time π^* -backbonding from electron-rich platinum to the dtms ligand impedes activation of the parent complex.⁷⁸ The main catalytic cycle (**III-V**) proceeds based on the Chalk-Harrod mechanism with concerted oxidative addition and 1,2 migratory insertion of the educts. Additionally, isomerized

2-alkenes might form in step **IV_{IS}**. At high olefin concentrations, the active species is deactivated by formation of $\text{Im}^{\text{Cy}}\text{Pt}(\text{olefin})_2$ (**VI**), but deactivation occurs also by dimer formation in the presence of silane (**VII**). In the absence of olefin, the formation of a Y-shaped tricoordinate *bis*(silyl)platinum complex in cycle **VIII** was observed (caution: here $\text{Im}^{\text{Dipp}}\text{Pt}(\text{dvtms})$ is the starting compound), which catalyzes the hydrosilylation of alkenes in without an induction period.⁸⁸⁻⁸⁹ Upon exposure to olefin, reductive elimination of disilane or *bis*-silylation of the olefin occurs, re-generating the active species. No proof for the formation of colloids has been available for a long time^{74, 78, 80a} but recent experimental data⁸² suggests minor agglomeration thereof (**IX**), though without major impact on catalysis.



Scheme 15: Activation, equilibria, and hydrosilylation mechanism for Markó-type complexes, including isomerization of alkenes.^{78, 88-89, 111} Although the reaction scheme is explicitly drawn for $\text{Im}^{\text{Cy}}\text{Pt}(\text{dvtms})$, apart from generation of Y-shaped tricoordinate *bis*(silyl)platinum complex in cycle **VIII** which was investigated for $\text{Im}^{\text{Dipp}}\text{Pt}(\text{dvtms})$, it is believed that other Markó-type complexes react according to this scheme.

2 Objective

Indeed, the hydrosilylation reaction is of major importance in accessing a multitude of chemical building blocks and forms the backbone of the silicone industry in combination with the Direct process. Platinum-based systems, such as Karstedt's catalyst, exhibit unmatched activity and tolerance to atmospheric conditions, rendering them indispensable for industrial use. The revolutionary introduction of NHCs by Markó *et al.* generates highly selective and efficient catalysts that tolerate a wide range of functional groups while boasting extensive shelf life, albeit accompanied by a notable induction phase.^{74a}

Two strategies are pursued in this thesis (Figure 7) with the aim of overcoming this drawback with the potential of increased activity and selectivity on top: (1) the wingtips at the NHCs of the first-generation Markó catalyst are varied in terms of steric bulk and electronic properties, while presumably hemilabile *N*-donors are also investigated based on promising catalytic reports on compounds with NHC-tethered thioether ligands.¹¹² (2) The established class of Markó-type complexes is extended to a homobimetallic platinum-based system, in anticipation of cooperative, synergistic effects. Such effects have been reported for a range of mostly non-platinum bimetallic compounds⁹⁸⁻⁹⁹, virtually demanding the exploration of auspicious bimetallic platinum catalysts.

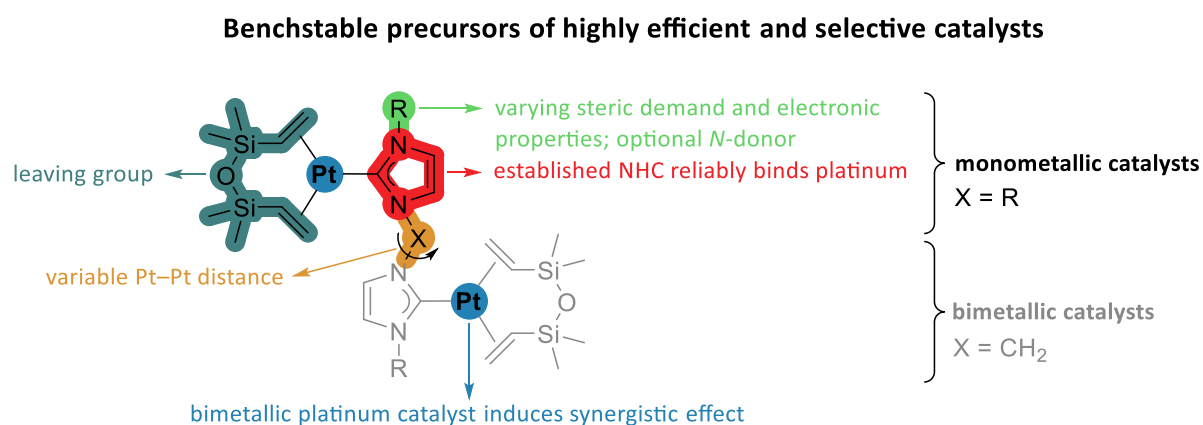


Figure 7: Overcoming the limitations of Markó-type complexes with two strategies. (1) Variation of NHC wingtips in monometallic catalysts and (2) extending the established system to a novel class of bimetallic complexes with prospect of synergistic effects.

Careful selection of framework conditions for the implementation and verification of hydrosilylation benchmark reactions is succeeded by in-depth catalytic evaluation of selected compounds and their comparison by means of key parameters, serving as a starting point for future improvements. Insights into the activation procedure will be generated by pre-catalytic reaction of platinum complexes with silane. Screening of temperature and catalyst loading is expected to provide further information on the properties, while mercury poisoning experiments elucidate stability aspects.

3 Results and Discussion

3.1 Synthesis and Characterization of Markó-type (NHC)Pt(dvtms) Complexes and their Evaluation in the Hydrosilylation Reaction of Alkenes

Michael J. Sauer, Leon F. Richter, Jeff Offorjindu, Robert M. Reich, Fritz E. Kühn*

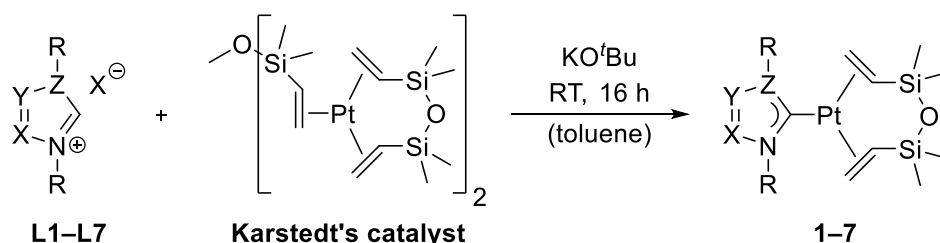
J. Organomet. Chem. **2024**, *1005*, 122995-123005.

3.1.1 Publication Summary

The introduction of NHCs as spectator ligands by Markó *et al.* in the field of platinum-catalyzed hydrosilylation drew great attention due to the selective and efficient nature of the resulting catalysts.⁷⁴ However, these complexes suffer from prolonged induction periods, as the removal of the dtms chelate is the overall rate-determining step, and delays generation of the catalytically active species.⁷⁸ Here, the synthesis and characterization of seven (NHC)Pt(dvtms) complexes (**1–7**; numbering applies only to this publication) by multinuclear NMR spectroscopy, SC-XRD, and elemental analysis is presented in conjunction with an investigation of the catalytic performance in the hydrosilylation of alkenes.¹¹³

To overcome the issue of slow initiation, the wingtips at the NHC moieties are varied in terms of their steric demand. Dangling *N*-donors were attached at the wingtips of the NHCs for **3** and **4** on the basis of research by Huynh and Bernhammer, which demonstrated the efficiency of Pt(II) complexes with hemilabile NHC-tethered thioether ligands in the hydrosilylation reaction.¹¹² Also, an abnormal 1,2,3-triazole-5-ylidene Pt(0) complex (**5**) was designed, where an increase in selectivity and activity⁷⁸ is anticipated due to the stronger σ -donor properties¹¹⁴.

The target complexes are easily accessible, by deprotonation of the respective azolium salt in the presence of potassium *tert*-butoxide as a base, which generates a free carbene, that reacts with Karstedt's catalyst⁷¹, applying an adapted procedure of Markó *et al.* (Scheme 16).⁷⁸



Scheme 16: Synthetic procedure for the preparation of complexes **1–7** from the respective azolium salt and Karstedt's catalyst⁷¹ in the presence of potassium *tert*-butoxide. **1**: X = CH, Y = CH, Z = N, R = *i*Pr, **2**: X = CH, Y = CH, Z = N, R = Ph, **3**: X = CH, Y = CH, Z = N, R = 2-Py, **4**: X = CH, Y = CH, Z = N, R = methylene-1-mesityl-1*H*-1,2,3-triazole, **5**: X = N, Y = (CH₃)N, Z = C, R = 2,4,6-trimethylphenyl (Mes), **6**: X = CH, Y = CH, Z = N, R = Me, **7**: X = CH, Y = CH, Z = N, R = Mes.

3 Results and Discussion

The kinetics of model reaction **A** are characterized by sigmoid time-yield curves due to varyingly pronounced induction periods. The least sterically demanding methyl groups at the NHC for **6** virtually eliminate the induction behavior while that period takes up to 1 h for **3** with pyridyl wingtips. Complexes **3** and **4** exhibit inferior performance in comparison to their non-nitrogen-containing congeners, which is attributed to the stabilization of a Pt(II) species due to coordination of nitrogen to platinum. As expected, an increased selectivity of 95% for **5** compared to 92% for **7** (Table 4) is observed coupled with a prolonged induction period, both factors as a result of the increased σ -donor strength of the 1,2,3-triazole-5-ylidene compared to the imidazole-2-ylidene. The overall best performance is exhibited by **2** with a miniscule induction period and a TOF of 39,000 h⁻¹ and 94% yield of the desired product.

Table 4: Catalytic formation of product (M₂D-oct) by hydrosilylation of oct-1-ene (1.0 eq., 2.024 mmol, 0.5 M) with MD^HM (1.0 eq., 2.024 mmol, 0.5 M) in *p*-xylene at 72 °C with 50 ppm [Pt] and *n*-decane (1.518 mmol) as internal standard (**A**).

Catalyst	Y(M ₂ D-oct) [%]	X(oct-1-ene) [%]	X(MD ^H M) [%]	S [%]	Y(isomerization) [%]	TOF [h ⁻¹]
1	88	92	87	96	4	14,000
2	94	98	93	96	3	39,000
3	82	85	81	97	3	11,000
4	56	60	55	94	2	10,000
5	93	98	92	95	4	12,000
6	83	98	82	84	12	31,000
7	91	98	90	92	4	17,000

Y: yield. X: conversion. S: selectivity regarding oct-1-ene at t = 6 h; Selectivity regarding MD^HM ≥ 99%. Sum of C₈ isomers at t = 6 h. *n*-Octane is included herein. TOF of oct-1-ene calculated at the steepest slope.

3.1.2 Publication Reprint

Journal of Organometallic Chemistry 1005 (2024) 122995



Contents lists available at ScienceDirect

Journal of Organometallic Chemistry

journal homepage: www.elsevier.com/locate/jorganchem

Synthesis and characterization of Markó-type (NHC)Pt(dvtms) complexes and their evaluation in the hydrosilylation reaction of alkenes

Michael J. Sauer^a, Leon F. Richter^a, Jeff Offorjindu^{a,b}, Robert M. Reich^a, Fritz E. Kühn^{a,*}

^a Molecular Catalysis, Department of Chemistry and Catalysis Research Center, TUM School of Natural Sciences, Technische Universität München, Lichtenbergstr. 4, D-85748 Garching bei München, Germany

^b Ausbildungszentrum der Technischen Universität München, Lichtenbergstrasse 4, D-85748 Garching bei München, Germany

ARTICLE INFO

Keywords:

Catalytic optimization
Homogeneous catalysis
Hydrosilylation
Induction period
N-heterocyclic carbenes
Platinum

ABSTRACT

A series of Markó-type complexes of the structure (NHC)Pt(dvtms) were prepared (dvtms = 1,1,3,3-tetramethyl-1,3-divinylidisiloxane, NHC = N-heterocyclic carbene, Im = imidazole, Trz = triazole; NHC = ^tPrIm (1), PhIm (2), 2-PyIm (3), MesTrzMeIm (4) Mes(Me)Trz (5) MeIm (6), MesIm(7)), with 5 being the first reported abnormal 1,2,3-triazole-5-ylidene Pt(0) complex. All these compounds are easily accessible using Karstedt's catalyst [Pt₂(dvtms)₃], the respective azolium salts (L1-7) and potassium *tert*-butoxide. Comprehensive characterization by NMR spectroscopy (¹H, ¹³C, ²⁹Si, ¹⁹⁵Pt), SC-XRD and CHNS analysis is presented. The hydrosilylation reactions of oct-1-ene or MM^{Vi} with MD^HM, respectively, where the latter mimics the cross linking of silicones, are efficiently catalyzed at remarkable low Pt-loadings of 50–100 ppm.

1. Introduction

A hydrosilylation reaction is an atom-efficient addition of a silane to an unsaturated organic compound, most commonly a C=C double bond, to form an alkyl silane (Scheme 1) [1–4]. In combination with the “Direct Process”, also called Müller–Rochow process [5–7], this key transformation is of major importance for the silicone industry [8,9]. The hydrosilylation reaction is efficiently catalyzed by platinum-based systems, such as Speier's (H₂PtCl₆/iPrOH) [10–12] and Karstedt's catalyst (Pt₂dvtms₃) [13–15] on an industrial scale. The latter system represents an improvement in terms of activity, induction period and overall better solubility in polysiloxane matrices [8]. Certain drawbacks like low selectivity and colloidal platinum formation due to deficient stability were countered by the introduction of N-heterocyclic carbene (NHC) spectator ligands by Markó et al. The isolable 16 e[−] Pt(0) complexes of the general formula (NHC)Pt(dvtms) are insensitive towards air and moisture, displaying outstanding selectivity and efficiency [16–19]. In conjunction with a straightforward synthesis [18,20] this class of catalyst precursors has attracted extensive attention in research [21–35].

Platinum loss due to catalyst encapsulation in cross linked silicones [8,36,37] alongside economic and environmental reasons, have sparked efforts to design platinum-free catalysts with great interest in

compounds based on more common and cheaper metals such as Co, Fe and Ni, among others [2,3,38,39]. However, the unparalleled activity of Pt-based catalysts and their applicability under ambient conditions render them - so far - indispensable for industrial use.

Thus, in this work the synthesis and comprehensive characterization of seven (NHC)Pt(dvtms) complexes (1–7) by NMR spectroscopy (¹H, ¹³C, ²⁹Si, ¹⁹⁵Pt), SC-XRD and CHNS analysis and their evaluation in two instructive hydrosilylation model reactions (Fig. 1) is reported. A more exhaustive characterization of PhIm-Pt(dvtms) (2) is presented in combination with hydrosilylation kinetics although the complex has been already reported by Marinetti et al. [26]. Also, MeIm-Pt(dvtms) (6) [16,18] and MesIm-Pt(dvtms) (7) [18] are included in this study as reference systems for comparison to the closely related, novel complexes ^tPrIm-Pt(dvtms) (1) and, to the best of our knowledge, the first abnormal 1,2,3-triazole-5-ylidene Pt(0) complex, Mes(Me)Trz-Pt(dvtms) (5). However, Markó-type complexes with 1,2,4-triazole-ylidene ligands had been reported previously [21,23]. The ligand in 5, is a stronger σ-donor [40–42] which is expected to lower the amount of isomerization [18]. On the basis of Pt(II) complexes with hemilabile NHC-tethered thioether ligands as catalysts for the hydrosilylation reaction, originally reported by Huynh and Bernhammer [43], Pt(0) complexes PyIm-Pt(dvtms) (3) and MesTrzMeIm-Pt(dvtms) (4) were designed. In this work, pyridine or a modified 1,2,3-triazole moiety are attached to the NHC scaffold,

* Corresponding author.

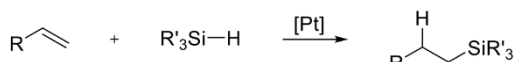
E-mail address: fritz.kuehn@ch.tum.de (F.E. Kühn).

<https://doi.org/10.1016/j.jorganchem.2023.122995>

Received 19 October 2023; Received in revised form 11 December 2023; Accepted 13 December 2023

Available online 14 December 2023

0022-328X/© 2023 Elsevier B.V. All rights reserved.



Scheme 1. Pt-catalyzed hydrosilylation of alkenes.

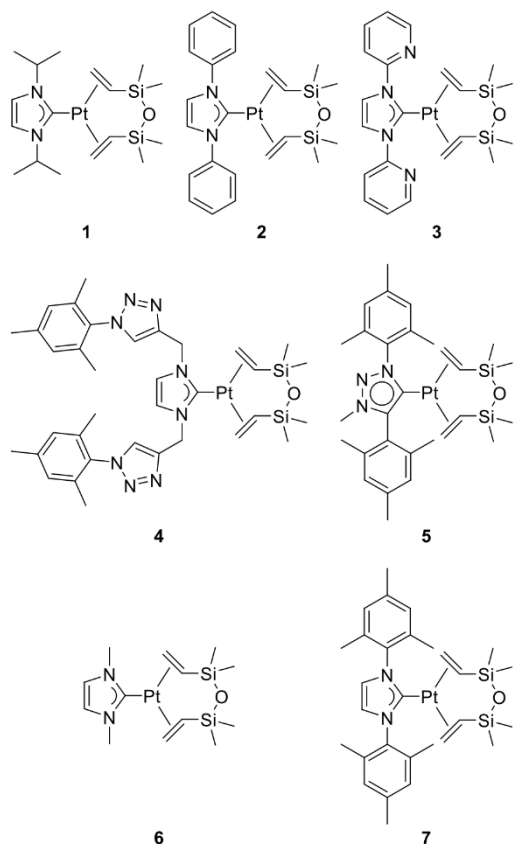


Fig. 1. Structure of (NHC)Pt(dvtms) complexes used in this study. Compounds 2 [26], 6 [16,18] and 7 [18] are literature known.

respectively. The influence of these *N*-donors is discussed based on NMR, SC-XRD and catalysis data.

2. Experimental

2.1. Methods and materials

All reactions were carried out under oxygen free, dry conditions in an argon atmosphere using standard Schlenk and glovebox techniques unless specifically stated otherwise. The solvents were purified, degassed, and dried according to standard purification techniques or obtained from an MBraun solvent purification system (SPS). The ligand precursor salts ¹PrIm-Br (L1) [44], PhIm-PF₆ (L2) [45], PyIm-Br (L3) [46], MesTrzCH₂Im-Br (L4) [47], Mes(Me)Trz-I (L5) [48], MeIm-PF₆ (L6) [49] and MesIm-BF₄ (L7) [50] were prepared from adapted literature procedures. All further chemicals were purchased from Sigma-Aldrich, VWR or abcr and used as received. NMR spectra were recorded on a Bruker Avance Ultrashield 400 MHz spectrometer. All ¹H, ¹³C and ²⁹Si chemical shifts are reported in parts per million (ppm) relative to TMS, with the residual solvent peak serving as internal reference. ¹⁹⁵Pt chemical shifts are externally referenced to K₂PtCl₄ in

H₂O ($\delta = -1628$ ppm). ²⁹Si NMR spectra were recorded via the INEPT technique. Abbreviations for NMR multiplicities are singlet (s), doublet (d), heptet (hept), and multiplet (m). Coupling constants are given in Hz. Catalytic experiments were conducted under atmospheric conditions and GC grade *p*-xylene and *n*-hexane were employed therein. An in depth description of the procedure is provided in the SI. GC analysis was performed with an Agilent Technologies 7890B GC system using an HP-5 column (30 m \times 320 μ m \times 0.25 μ m). Injection volume was 1 μ L at an oven temperature of 50 $^{\circ}$ C and with a split ratio of 30:1. A flow of 0.9 mL min⁻¹ of nitrogen as carrier gas was applied and the system was equipped with an FID detector, that was kept at 50 $^{\circ}$ C. After injection of the sample at 50 $^{\circ}$ C the oven temperature was held for 9 min and subsequently ramped to 80 $^{\circ}$ C at a rate of 6 $^{\circ}$ C min⁻¹. Afterwards the ramp was increased to 15 $^{\circ}$ C min⁻¹ until 205 $^{\circ}$ C were reached and the final temperature of 250 $^{\circ}$ C were reached by heating at 30 $^{\circ}$ C min⁻¹ and then keeping the temperature for 3 min. Elemental analyses were performed at the microanalytical laboratory of the Catalysis Research Center, Technische Universität München. Single crystals were measured in the SC-XRD laboratory of the Catalysis Research Center at Technische Universität München, Germany.

2.2. Synthesis and characterization

2.2.1. General protocol for the synthesis of (NHC)Pt(dvtms) complexes (1–7)

The respective imidazolium salt (1.00 eq.), Karstedt's catalyst (1.00 eq.), potassium *tert*-butoxide (1.50 eq.; 1.05 eq. for 4) and toluene are combined under argon atmosphere. The suspension is stirred overnight under exclusion of light. Under atmospheric conditions, pentane is added and the suspension stirred before filtration over Celite and elution with pentane. Volatiles are removed in vacuo and resulting solid washed with propan-2-ol and pentane, yielding the target compound. A more detailed account is presented in the SI.

2.2.2. ¹PrIm-Pt(dvtms) (1)

Yield: 71%. ¹H NMR (400 MHz, CDCl₃, 298 K): δ [ppm] = 7.05 (s, ⁴J_{Pt,H} = 12.8 Hz, 2H, H_{im}), 4.71 (hept, ³J_{H,H} = 6.8 Hz, 1H, CH₃CHCH₃), 4.63 (hept, ³J_{H,H} = 6.8 Hz, 1H, CH₃CHCH₃), 2.20 (d, ³J_{H,H} = 10.6 Hz, ²J_{Pt,H} = 52.8 Hz, 2H, CH₂CHSi), 1.98–1.72 (m, 4H, CH₂CHSi), 1.31 (d, ³J_{H,H} = 6.6 Hz, 6H, CHCH₃), 1.29 (d, ³J_{H,H} = 6.7 Hz, 6H, CHCH₃), 0.33 (s, 6H, SiCH_{3,eq}), -0.30 (s, 6H, SiCH_{3,ax}). ¹³C{¹H} NMR (101 MHz, CDCl₃, 298 K): δ [ppm] = 179.9 (Pt-C_{car}, ¹J_{Pt,C} = 1387.7 Hz), 116.9 (C_{im}, ³J_{Pt,C} = 37.4 Hz), 51.3 (CH₃CHCH₃), 51.1 (CH₃CHCH₃), 40.6 (CH₂CHSi), ¹J_{Pt,C} = 157.6 Hz), 33.8 (CH₂CHSi, ¹J_{Pt,C} = 119.2 Hz), 23.3 (CHCH₃), 23.2 (CHCH₃), 1.6 (SiCH_{3,eq}), -2.0 (SiCH_{3,ax}). ²⁹Si{¹H} NMR (79 MHz, CDCl₃, 298 K): δ [ppm] = 2.65 (s, ²J_{Pt,Si} = 42.7 Hz, 2 Si). ¹⁹⁵Pt NMR (85 MHz, CDCl₃, 298 K): δ [ppm] = -5379 (s, 1 Pt). Elemental analysis calcd (%) for C₁₇H₃₄N₂OPtSi₂: C 38.26; H 6.42; N 5.25; found: C 38.36; H 6.45; N 5.25.

2.2.3. PhIm-Pt(dvtms) (2)

Yield: 62%. ¹H NMR (400 MHz, CDCl₃, 298 K): δ [ppm] = 7.57–7.48 (m, 4H, H_{ar}), 7.44 (s, ⁴J_{Pt,H} = 10.8 Hz, 2H, H_{im}), 7.34–7.27 (m, 6H, H_{ar}), 1.94 (d, ³J_{H,H} = 10.2 Hz, 2H, ²J_{Pt,H} = 53.2 Hz, CH₂CHSi), 1.76–1.49 (m, 4H, CH₂CHSi), 0.22 (s, 6H, SiCH_{3,eq}), -0.59 (s, 6H, SiCH_{3,ax}). ¹³C{¹H} NMR (101 MHz, CDCl₃, 298 K): δ [ppm] = 185.1 (Pt-C_{car}, ¹J_{Pt,C} = 1400.9 Hz), 140.9 (C_{ar}), 128.7 (C_{ar}), 128.0 (C_{ar}), 124.7 (C_{ar}), 122.5 (C_{im}, ³J_{Pt,C} = 38.4 Hz), 41.6 (CH₂CHSi, ¹J_{Pt,C} = 163.6 Hz), 34.0 (CH₂CHSi, ¹J_{Pt,C} = 123.2 Hz), 1.6 (SiCH_{3,eq}), -2.7 (SiCH_{3,ax}). ²⁹Si{¹H} NMR (79 MHz, CDCl₃, 298 K): δ [ppm] = 2.68 (s, ²J_{Pt,Si} = 41.9 Hz, 2 Si). ¹⁹⁵Pt NMR (85 MHz, CDCl₃, 298 K): δ [ppm] = -5298 (s, 1 Pt). Elemental analysis calcd (%) for C₂₃H₃₀N₂OPtSi₂: C 45.91; H 5.03; N 4.66; found: C 45.67; H 5.00; N 4.70.

2.2.4. PyIm-Pt(dvtms) (3)

Yield: 58%. ¹H NMR (400 MHz, CDCl₃, 298 K): δ [ppm] = 8.63–8.20

(m, 4H, H_{ar}), 8.14 (s, ⁴J_{Pt,H} = 10.4 Hz, 2H, H_{im}), 7.63–7.41 (m, 2H, H_{ar}), 7.29–7.13 (m, 2H, H_{ar}), 2.13 (d, ³J_{H,H} = 11.4 Hz, 2H, ²J_{Pt,H} = 53.8 Hz, CH₂CHSi), 2.02–1.66 (m, 4H, CH₂CHSi), 0.30 (s, 6H, SiCH_{3,eq}), –0.37 (s, 6H, SiCH_{3,ax}). ¹³C{¹H} NMR (101 MHz, CDCl₃, 298 K): δ [ppm] = 186.5 (Pt-C_{car}, ¹J_{Pt,C} = 1372.6 Hz), 152.3 (C_{ar}), 148.0 (C_{ar}), 137.6 (C_{ar}), 122.7 (C_{ar}), 121.2 (C_{im}), 116.8 (C_{ar}), 42.7 (CH₂CHSi, ¹J_{Pt,C} = 163.6 Hz), 35.1 (CH₂CHSi, ¹J_{Pt,C} = 123.2 Hz), 1.6 (SiCH_{3,eq}), –2.6 (SiCH_{3,ax}). ²⁹Si{¹H} NMR (79 MHz, CDCl₃, 298 K): δ [ppm] = 2.85 (s, ²J_{Pt,Si} = 40.3 Hz, 2 Si). ¹⁹⁵Pt NMR (85 MHz, CDCl₃, 298 K): δ [ppm] = –5277 (s, 1 Pt). Elemental analysis calcd (%) for C₂₁H₂₈N₄O₂OSi₂: C 41.78; H 4.67; N 9.28; found: C 41.47; H 4.64; N 9.19.

2.2.5. MesTrzMeIm-Pt(dvtms) (4)

Yield: 64%. ¹H NMR (400 MHz, CDCl₃, 298 K): δ [ppm] = 7.43–7.26 (s, 4H, H_{ar}), 6.96 (s, 4H, H_{ar}), 5.37 (s, 2H, NCH₂C), 5.33 (s, 2H, NCH₂C), 2.33 (s, 6H, *p*-CH₃), 2.22 (d, ³J_{H,H} = 10.2 Hz, 2H, ²J_{Pt,H} = 50.6 Hz, CH₂CHSi), 2.11–1.73 (m, 4H, CH₂CHSi), 1.90 (s, 12H, *o*-CH₃), 0.30 (s, 6H, SiCH_{3,eq}), –0.32 (s, 6H, SiCH_{3,ax}). ¹³C{¹H} NMR (101 MHz, CDCl₃, 298 K): δ [ppm] = 184.4 (Pt-C_{car}, ¹J_{Pt,C} = 1371.6 Hz), 143.5 (C_{ar}), 143.3 (C_{ar}), 140.3 (C_{ar}), 135.0 (C_{ar}), 133.3 (C_{ar}), 129.2 (C_{ar}), 124.3 (C_{ar}), 124.0 (C_{ar}), 121.9 (C_{ar}), 121.4 (C_{ar}), 44.9 (NCH₂C), 41.1 (CH₂CHSi, ¹J_{Pt,C} = 157.6 Hz), 35.2 (CH₂CHSi, ¹J_{Pt,C} = 119.2 Hz), 21.2 (*p*-CH₃), 17.4 (*o*-CH₃), 1.5 (SiCH_{3,eq}), –1.5 (SiCH_{3,ax}). ²⁹Si{¹H} NMR (79 MHz, CDCl₃, 298 K): δ [ppm] = 2.90 (s, ²J_{Pt,Si} = 41.9 Hz, 2 Si). ¹⁹⁵Pt NMR (85 MHz, CDCl₃, 298 K): δ [ppm] = –5386 (s, 1 Pt). Elemental analysis calcd (%) for C₃₅H₄₈N₈O₂OSi₂: C 49.57; H 5.71; N 13.21; found: C 49.62; H 5.77; N 13.11.

2.2.6. Mes(Me)Trz-Pt(dvtms) (5)

Yield: 46%. ¹H NMR (400 MHz, CDCl₃, 298 K): δ [ppm] = 6.92 (s, 2H, H_{ar}), 6.91 (s, 2H, H_{ar}), 3.85 (s, 3H, CH₃N), 2.29 (s, 3H, *p*-CH₃), 2.28 (s, 3H, *p*-CH₃), 2.11 (s, 6H, *o*-CH₃), 2.10 (s, 6H, *o*-CH₃), 1.87 (d, ³J_{H,H} = 11.4 Hz, 2H, ²J_{Pt,H} = 53.4 Hz, CH₂CHSi), 1.69–1.39 (m, 4H, CH₂CHSi), 0.17 (s, 6H, SiCH_{3,eq}), –0.73 (s, 6H, SiCH_{3,ax}). ¹³C{¹H} NMR (101 MHz, CDCl₃, 298 K): δ [ppm] = 168.4 (Pt-C_{car}, ¹J_{Pt,C} = 1274.6 Hz), 145.3 (C_{ar}), 139.8 (C_{ar}), 139.6 (C_{ar}), 138.3 (C_{ar}), 136.9 (C_{ar}), 134.7 (C_{ar}), 129.0 (C_{ar}), 128.7 (C_{ar}), 125.1 (C_{ar}), 40.6 (CH₂CHSi, ¹J_{Pt,C} = 163.6 Hz), 36.1 (CH₃N), 33.9 (CH₂CHSi, ¹J_{Pt,C} = 120.2 Hz), 21.3 (*p*-CH₃), 21.2 (*p*-CH₃), 20.2 (*o*-CH₃), 17.8 (*o*-CH₃), 1.6 (SiCH_{3,eq}), –2.5 (SiCH_{3,ax}). ²⁹Si{¹H} NMR (79 MHz, CDCl₃, 298 K): δ [ppm] = 3.01 (s, ²J_{Pt,Si} = 41.9 Hz, 2 Si). ¹⁹⁵Pt NMR (85 MHz, CDCl₃, 298 K): δ [ppm] = –5306 (s, 1 Pt). Elemental analysis calcd (%) for C₂₉H₄₃N₃O₂OSi₂: C 49.69; H 6.18; N 5.99; found: C 49.83; H 6.25; N 5.90.

2.2.7. MeIm-Pt(dvtms) (6)

Yield: 74%. ¹H NMR (400 MHz, CDCl₃, 298 K): δ [ppm] = 6.99 (s, ⁴J_{Pt,H} = 11.6 Hz, 2H, H_{im}), 3.51 (s, 6H, NCH₃), 2.22 (d, ³J_{H,H} = 11.1 Hz, 2H, ²J_{Pt,H} = 53.0 Hz, CH₂CHSi), 2.01–1.71 (m, 4H, CH₂CHSi), 0.32 (s, 6H, SiCH_{3,eq}), –0.27 (s, 6H, SiCH_{3,ax}). ¹³C{¹H} NMR (101 MHz, CDCl₃, 298 K): δ [ppm] = 184.2 (Pt-C_{car}, ¹J_{Pt,C} = 1375.6 Hz), 121.9 (C_{im}, ³J_{Pt,C} = 37.4 Hz), 39.5 (CH₂CHSi, ¹J_{Pt,C} = 157.6 Hz), 36.9 (NCH₃), 34.2 (CH₂CHSi, ¹J_{Pt,C} = 119.2 Hz), 1.6 (SiCH_{3,eq}), –1.7 (SiCH_{3,ax}). ²⁹Si{¹H} NMR (79 MHz, CDCl₃, 298 K): δ [ppm] = 2.80 (s, ²J_{Pt,Si} = 41.9 Hz, 2 Si). ¹⁹⁵Pt NMR (85 MHz, CDCl₃, 298 K): δ [ppm] = –5392 (s, 1 Pt). Elemental analysis calcd (%) for C₁₃H₂₆N₂O₂OSi₂: C 32.69; H 5.49; N 5.87; found: C 32.67; H 5.37; N 5.89.

2.2.8. MesIm-Pt(dvtms) (7)

Yield: 64%. ¹H NMR (400 MHz, CDCl₃, 298 K): δ [ppm] = 7.14 (s, ⁴J_{Pt,H} = 9.2 Hz, 2H, H_{im}), 6.88 (s, 4H, H_{ar}), 2.27 (s, 6H, *p*-CH₃), 2.15 (s, 12H, *o*-CH₃), 1.91 (d, ³J_{H,H} = 11.6 Hz, 2H, ²J_{Pt,H} = 54.4 Hz, CH₂CHSi), 1.76–1.37 (m, 4H, CH₂CHSi), 0.17 (s, 6H, SiCH_{3,eq}), –0.74 (s, 6H, SiCH_{3,ax}). ¹³C{¹H} NMR (101 MHz, CDCl₃, 298 K): δ [ppm] = 184.4 (Pt-C_{car}, ¹J_{Pt,C} = 1409.0 Hz), 138.6 (C_{ar}), 136.8 (C_{ar}), 135.3 (C_{ar}), 129.0 (C_{ar}), 123.0 (C_{im}, ³J_{Pt,C} = 41.4 Hz), 41.3 (CH₂CHSi, ¹J_{Pt,C} = 165.6 Hz), 35.2 (CH₂CHSi, ¹J_{Pt,C} = 118.2 Hz), 21.1 (*p*-CH₃), 18.2 (*o*-CH₃), 1.6 (SiCH_{3,eq}),

–2.5 (SiCH_{3,ax}). ²⁹Si{¹H} NMR (79 MHz, CDCl₃, 298 K): δ [ppm] = 3.57 (s, ²J_{Pt,Si} = 40.3 Hz, 2 Si). ¹⁹⁵Pt NMR (85 MHz, CDCl₃, 298 K): δ [ppm] = –5368 (s, 1 Pt). Elemental analysis calcd (%) for C₂₉H₄₂N₂O₂OSi₂: C 50.78; H 6.17; N 4.08; found: C 50.64; H 6.20; N 4.09.

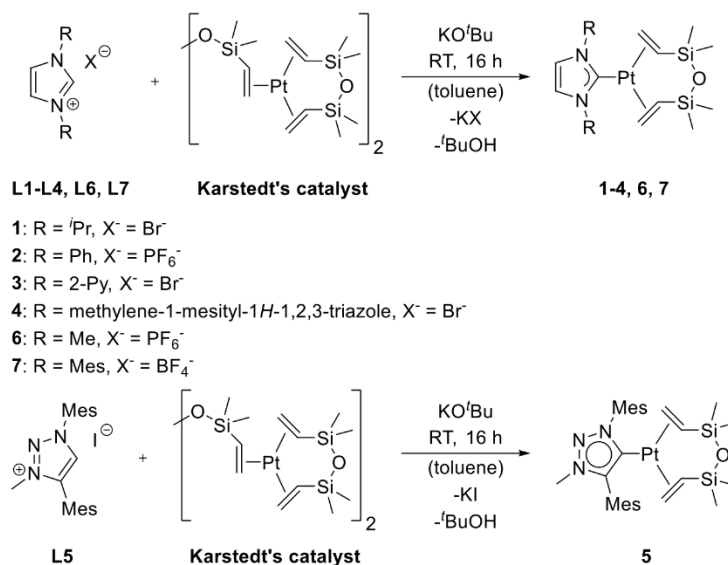
2.3. Single crystal X-ray structure determination

Single crystals of **1** were obtained by layering a solution in dichloromethane with *n*-hexane. Evaporation of a concentrated solution in *n*-pentane gave suitable crystals respectively of **2**, **4** and **5**. Cooling of a hot solution of **3** in *n*-hexane yielded suitable crystals thereof. X-ray crystallographic data was collected on a Bruker D8 Venture single crystal X-ray diffractometer, equipped either with a CMOS detector (k-CMOS) and a TXS rotating anode or a CMOS detector (Bruker Photon-100) and a IMS microsource, both in conjunction with a Helios optic as setup using the APEX4 software package [51]. The measurement used MoK_α radiation (λ = 0.71073 Å) and was performed on single crystals coated with perfluorinated ether. The crystals were fixed on top of a micromount sample holder and frozen under a stream of cold nitrogen at 100 K. A matrix scan was used to determine the initial lattice parameters. Reflections were corrected for Lorentz and polarization effects, scan speed, and background using SAINT [52]. Absorption corrections, including odd and even ordered spherical harmonics were performed using SADABS [53]. Space group assignment was based upon systematic absences, E statistics, and successful refinement of the structure. The structure was solved by direct methods (SHELXT) with the aid of successive difference Fourier maps, and was refined against all data using SHELXL-2015 in conjunction with SHELXLE [54–56]. Hydrogen atoms were calculated in ideal positions as follows: Methyl hydrogen atoms were refined as part of rigid rotating groups, with a C–H distance of 0.98 Å and U_{iso}(H) = 1.5·U_{eq}(C). Other H atoms were placed in calculated positions and refined using a riding model, with methylene, aromatic, and other C–H distances of 0.99 Å, 0.95 Å, and 1.00 Å, respectively and U_{iso}(H) = 1.2·U_{eq}(C). Non-hydrogen atoms were refined with anisotropic displacement parameters. Full-matrix least-squares refinements were carried out by minimizing Σw(F_o–F_c)² with the SHELXL weighting scheme [54]. Neutral atom scattering factors for all atoms and anomalous dispersion corrections for the non-hydrogen atoms were taken from *International Tables for Crystallography* [57]. The unit cell of **4** contains solvent accessible voids of 108 Å³. Therein the PLATON SQUEEZE procedure found seven electrons, which excludes the possibility of cocrystallized solvent [58]. The images of the crystal structures were generated with PLATON [59]. CCDC 2301898–2301902 contain the supplementary crystallographic data for this paper. This data can be obtained free of charge via www.ccdc.cam.ac.uk/data_request/cif, or by emailing data_request@ccdc.cam.ac.uk, or by contacting The Cambridge Crystallographic Data Centre, 12 Union Road, Cambridge CB2 1EZ, UK; fax: +44 1223 336033.

3. Results and discussion

3.1. Synthesis and characterization of (NHC)Pt(dvtms) complexes (1–7)

The (NHC)Pt(dvtms) complexes (**1–7**) were obtained by reaction of the respective azolium salt (**L1–L7**, 1.00 eq.) with potassium *tert*-butoxide (1.50 eq.) and Karstedt's catalyst [**13–15**] (1.00 eq.) in dry toluene at room temperature for 16 h, applying an adapted procedure of Markó et al. (Scheme 2) [18]. An exception, however, is the synthesis of complex **4**, where the amount of potassium *tert*-butoxide was reduced to 1.05 equivalents to avoid potential deprotonation of the triazole wings [60,61]. Two routes were employed for the removal of the formed potassium salts. Filtration over Celite and extraction of a DCM/H₂O system. It was found that filtration is superior as the synthesis of complex **4** for instance was not successful via the extraction route. In any case, hard anions of the parent ligands simplify both routes. Subsequent washing with ¹PrOH and *n*-pentane gives analytically pure products in yields



Scheme 2. Syntheses of complexes 1–7 from Karstedt's catalyst [13–15].

between 46 and 74% (Table 1). In doing so, complexes 1–7 have been isolated and characterized by NMR spectroscopy (¹H, ¹³C, ²⁹Si, ¹⁹⁵Pt), elemental analysis and the structure of complexes 1–5 has been confirmed by SC-XRD. While the syntheses of complexes 1–7 are conducted under inert conditions, the formed products are insensitive to air and moisture and may be stored indefinitely in solid or dissolved state. However, the complexes are sensitive towards light, especially in solution [16,30]. The synthesis of 2 was also attempted via the weak-base route of Nolan, Nahra and Cazin et al. [20,62] in an effort to extend the scope of NHC-HCl pro-ligands to their NHC-HPF₆ cognates, but proved unsuccessful (SI).

NMR spectroscopy of complexes 1–7 reveals a similar nature in comparison to structurally related complexes [16–18,27,35]. The disappearance of the carbenoid proton in the ¹H NMR, upfield shift of the vinyl protons of dvtms from $\delta = 6.17$ – 5.70 ppm for the free molecule to 2.31–1.38 ppm as a bound ligand, along with the parting of the SiMe₂ singlet into two resonances at about $\delta = 0.3$ and -0.5 ppm indicate coordination of the in-situ generated NHC to a Pt(dvtms)₂ moiety of Karstedt's catalyst [18]. The carbene resonances are observed at $\delta = 186.5$ – 179.9 ppm for the imidazolylidene complexes, while the carbene shift of the triazolylidene complex 5 is significantly upfield shifted to $\delta = 168.4$ ppm (Table 2), indicating enhanced donor strength. Comparable triazolylidene carbene shifts of organometallic complexes have been reported in literature [63–65]. The formation of (NHC)Pt(dvtms) complexes is further substantiated by the presence of ¹⁹⁵Pt satellites for several peaks in the ¹H and ¹³C NMR spectra. Connection of platinum to the NHC moiety is proven by a ¹J_{Pt,C} coupling of on average 1371 Hz, along with ⁴J_{Pt,H} and ³J_{Pt,Cim} couplings of Pt and the imidazole backbone protons and carbons, respectively. It is noteworthy, that the weakest

¹J_{Pt,C} coupling of 1274.6 Hz is observed for complex 5. The dvtms ligand provides ¹J_{Pt,C} couplings for the terminal and internal vinyl carbon atoms and ²J_{Pt,H} coupling for the vinyl protons. The extracted data of reference compounds 6 and 7 are in agreement with reported values, apart from the ¹⁹⁵Pt NMR shifts, where deviations of 49 and 29 ppm are observed for 6 and 7, respectively [18]. While ¹H and ¹³C NMR spectroscopy are state of the art for organometallic complexes, the presence of silicon and platinum in the complexes in question enables further analysis. The ²⁹Si NMR shifts are quite similar ($\delta = 3.57$ – 2.65 ppm), due to the distance of silicon from the varying NHC-moieties. However, the downfield shift from $\delta = -3.07$ ppm of free dvtms and a ²J_{Pt,Si} coupling of on average 42 Hz reinforces the claim of NHC-Pt (dvtms) formation. Also, dvtms is bound symmetrically, since a singlet is observed. The electronic environment of the catalytically active center, the platinum atom, is obtained by sensitive ¹⁹⁵Pt NMR spectroscopy [66,67]. Electron density is increased by the σ -donor properties of ligands and reduced by π -acceptor properties of the ligands [18]. The recorded ¹⁹⁵Pt NMR shifts range from $\delta = -5277$ to -5392 ppm, typical for Pt(0) complexes [67]. Complex 2 with phenyl wingtips and complex 3 with 2-pyridine wingtips are closely related, with ¹⁹⁵Pt NMR shifts of $\delta = -5298$ and -5277 ppm, respectively. The less shielded platinum center in 3 may be attributed to energetically lowered LUMO of 2-pyridine compared to phenyl in 2 and therefore increased π -acceptor properties, apparently outweighing potential intra- or intermolecular interaction of the nitrogen lone pair with platinum. However, the ¹J_{Pt,C} coupling constant of 1400.9 Hz for 2 compared to 1372.6 Hz for 3 indicates a stronger carbene-platinum bond for 2. Also structurally similar are complexes 5 and 7 with an abnormally coordinating triazolylidene- and imidazolylidene-carbene, respectively. Although abnormally coordinating carbenes are generally considered to possess stronger σ -donor properties [40–42], ¹⁹⁵Pt NMR shifts of $\delta = -5306$ (5) and -5368 ppm (7) are recorded, with a de-shielded 5 compared to 7. Also, the lowest and the largest ¹J_{Pt,C} coupling in the series of 1–7 are found with 1274.6 Hz (5) and 1409.0 Hz (7). Complex 4 possesses methylene-1-mesityl-1*H*-1,2,3-triazole wings and a ¹⁹⁵Pt NMR shift of $\delta = -5386$ ppm. Thus, complex 4 is most closely related to 6 in terms of electron density at platinum and coupling constants. The difference in the ¹⁹⁵Pt NMR shift might be attributed to a $-I$ effect of the triazole like the mismatch between 2 and 3, even though the wingtip in 4 is more flexible than in 3 due to the additional methylene bridge.

Table 1
Yields of (NHC)Pt(dvtms) complexes.

Complex	Yield [%]
ⁱ PrIm-Pt(dvtms) (1)	71
PhIm-Pt(dvtms) (2)	62
PyIm-Pt(dvtms) (3)	58
MesTrzMelm-Pt(dvtms) (4)	64
Mes(Me)Trz-Pt(dvtms) (5)	46
MelM-Pt(dvtms) (6)	74
MesIm-Pt(dvtms) (7)	64

Table 2
Key chemical shifts and coupling constants of complexes 1–7 as observed by NMR spectroscopy.

Complex	1	2	3	4	5	6	7
Chemical shifts δ [ppm]							
$^{13}\text{C}_{\text{carbene}}$	179.9	185.1	186.5	184.4	168.4	184.2	184.4
^{29}Si	2.65	2.68	2.85	2.90	3.01	2.80	3.57
^{195}Pt	–5379	–5298	–5277	–5386	–5306	–5392 ^a	–5368 ^b
Coupling constants [Hz]							
$^1J_{\text{Pt,C}}$	1387.7	1400.9	1372.6	1371.6	1274.6	1375.6	1409.0
$^3J_{\text{Pt,Clm}}$	37.4	38.4	n.a.	n.a.	/	37.4	41.4
$^1J_{\text{Pt,CVi}}$ (terminal)	157.6	163.6	163.6	157.6	163.6	157.6	165.6
$^1J_{\text{Pt,CVi}}$ (internal)	119.2	123.2	123.2	119.2	120.2	119.2	118.2
$^4J_{\text{Pt,H}}$	12.8	10.8	10.4	n.a.	/	11.6	9.2
$^2J_{\text{Pt,H}}$	52.8	53.2	53.8	50.6	53.4	53.0	54.4
$^2J_{\text{Pt,Si}}$	42.7	41.9	40.3	41.9	41.9	41.9	40.3

^a Differs by 49 ppm from the previously reported shift of –5343 ppm [18].

^b Differs by 29 ppm from the previously reported shift of –5339 ppm [18].

The molecular structure of 1–5 was confirmed by SC-XRD, showing in all cases the characteristic [18,25,31,35], distorted trigonal planar coordination of platinum by the $\text{C}_{\text{carbene}}$ atom of the NHC ligand and the vinyl groups of the dtvms ligand (Fig. 2). A comparison of selected bond lengths and angles is presented in

Table 3, including the reference complexes 6 [16,18] and 7 [18]. The observed bond lengths of $\text{Pt}-\text{C}_{\text{carbene}}$ lie in the narrow range of 2.038–2.054 Å as is typical for these complexes [18,30,35]. The $\text{Pt}-\text{C}_{\text{carbene}}$ distance in 2 is 2.038(2) Å and significantly shorter in terms of statistic uncertainty (3σ) than the same bond in 3 with 2.0542(19) Å, which is in agreement with the found $^1J_{\text{Pt,C}}$ coupling constants. The $\text{C}=\text{C}-\text{C}=\text{C}$ distance is an indicator for the π^* -backbonding from platinum to the dtvms ligand. However, even though the $\text{C}=\text{C}-\text{C}=\text{C}$ bond in 2 appears somewhat elongated compared to 3, this finding is not statistically relevant. The largest difference of $^1J_{\text{Pt,C}}$ coupling constants is observed for 5 and 7 (*vide supra*), however the found $\text{Pt}-\text{C}_{\text{carbene}}$ bond lengths of 2.054(3) and 2.046(4) Å, respectively, do not reflect that mismatch. Contrasting the complexes in terms of the torsion angle that is stretched by the NHC and $\text{Pt}(\text{dtvms})$ plane was pioneered by Markó et al., and is referred to as “tilt” angle Θ [18]. In sterically unhindered complexes such as 6, the possible maximum of $\Theta = 90.00^\circ$ is achieved. Bulky ligands force a rotation along the $\text{Pt}-\text{C}_{\text{carbene}}$ axis to reduce steric strain between the NHC wingtips and the dtvms group. The mesityl wingtips of 5 and 7 render the complexes in question as the sterically most encumbered ones. Although 4 also incorporates mesityl moieties, the methylene linker acts as a joint that allows rotation away from the dtvms ligand, resulting in $\Theta = 80.85^\circ$. The tilt angles for 5 and 7 are even lower at $\Theta = 59.00$ and 64.67° , respectively. In this context the $\text{N}-\text{C}_{\text{carbene}}-\text{C}$ angle of $101.6(3)^\circ$ of the triazolylidene 5 and the $\text{N}-\text{C}_{\text{carbene}}-\text{N}$ angle of $103.1(3)^\circ$ of the imidazolylidene 7 is relevant. This indicates that the mesityl groups in 5 point further away from the dtvms unit than in 7, which should in theory allow a larger tilt angle Θ . This contradiction is attributed to the methyl group at the triazole backbone in 5 that prevents the mesityl moiety in proximity to tilt as far as the mesityl group in 7, where hydrogen atoms are symmetrically bound to the backbone of the NHC. This feature increases the actual bulk of the mesityl wings in 5 compared to 7 and therefore lowers the tilt angle Θ . Using an excessively bulky ligand, Žak et al. described $\text{IPr}^{\text{Ph}}-\text{Pt}(\text{dtvms})$ (where $\text{IPr}^{\text{Ph}} = 1,3\text{-bis}(2,4,6\text{-tris}(\text{diphenylmethyl})\text{phenyl})\text{imidazol-2-ylidene}$) where the steric demand accounts for $\Theta = 53.03^\circ$ [34].

3.2. Catalytic hydrosilylation of alkenes

The performance of compounds 1–7 in the hydrosilylation reaction was evaluated in the model reaction of oct-1-ene and 1,1,3,5,5-heptamethyltrisiloxane (MD^{HM}) that was established by Markó et al. (Scheme 3), where MD^{HM} mimics a PMHS (polymethylhydrosiloxane) [16,17]. This reaction will be referred to as model reaction A and proceeds at relatively mild conditions. However, in terms of selectivities regarding

oct-1-ene, the catalysts compete for minimal formation of isomerized C_8 alkenes and the reduction to *n*-octane. Linking both educts might also yield byproducts [16,17], though they are neglected in this work, as their combined yields always total $< 1\%$. To simulate the industrial three-dimensional silicone network formation *via* platinum-catalyzed addition-cure crosslinking, model reaction B was established (Scheme 4). The vinyl siloxane group is represented by 1,1,1,3,3-pentamethyl-3-vinylidisiloxane (MM^{VI}) and the hydrosilane group by MD^{HM} as in model reaction A [3,68]. Due to the nature of this reaction harsher conditions are required and unlike in A mainly linked byproducts [69] are formed. The hydrosilylation experiments were carried out under ambient conditions but due to the homogeneous and well-defined character of the catalyst and of the reaction mechanism [17,18], respectively, the occurrence of the beneficial “oxygen” effect [70,71] is ruled out. Furthermore, no visual discoloration of the reaction mixtures, that would indicate the formation of colloidal Pt species [71], was observed as is in agreement with literature reports for these (NHC)Pt(dtvms) complexes [16]. However, the “cocktail” nature of a similar catalytic system was suggested on the basis of UV-vis data, but excellent selectivity indicates a minor contribution of Pt-colloids in that case [72].

The kinetics of the hydrosilylation model reaction A at 72°C with 50 ppm catalyst and equimolar amounts of oct-1-ene and MD^{HM} are characterized by sigmoid time-yield curves that are caused by the induction period of the initial hydrosilylation of dtvms of the catalyst precursors (Fig. 3) [18]. $\text{MeIm}-\text{Pt}(\text{dtvms})$ (6) shows virtually no induction period, which is attributed to the sterically least demanding wingtips among the examined complex series. This trait is accompanied by a low selectivity regarding oct-1-ene of merely 84%, which results in the by far highest amount of C_8 byproducts of 12% (Table 4). A minor induction period is observed for 1, where the wingtip ligands are iso-propyl entities. This change causes a harsh drop in the TOF (turnover frequency) from 31,000 to 14,000 h^{-1} from 6 to 1, respectively. However, the selectivity is improved from 84 to 96% and therefore only 4% C_8 byproducts are formed. Due to varying induction kinetics the apparent TOF values have to be handled with caution, as different amounts of the catalyst precursor might have been converted to the active platinum species, which is not reflected in the TOF [18]. A concise overview of TOFs of platinum catalysts for A was published by Bai and Zhang et al. [73]. Complex 4 as the last non-aromatic substituted congener is closely related to 6 in terms of electronics (*vide supra*), but the catalytic performance differs significantly. A prolonged induction period for 4 is attributed to the steric demand of the NHC wingtips in solution and after 6 h solely 60% of oct-1-ene are converted to yield 56% $\text{M}_2\text{D}-\text{oct}$ with the lowest TOF of 10,000 h^{-1} . A noticeable loss in activity after around 2 h, where more than half of the educt amount is still present indicates the deactivation of the active species. Coordination of an $\text{N}_{\text{triazole}}$ to the metal center [47] might form a stabilized Pt(II) species [74,75] that is eliminated from the pool of active Pt catalyst. The most active catalyst in this series is formed by 2 with a TOF of 39,000 h^{-1} and a

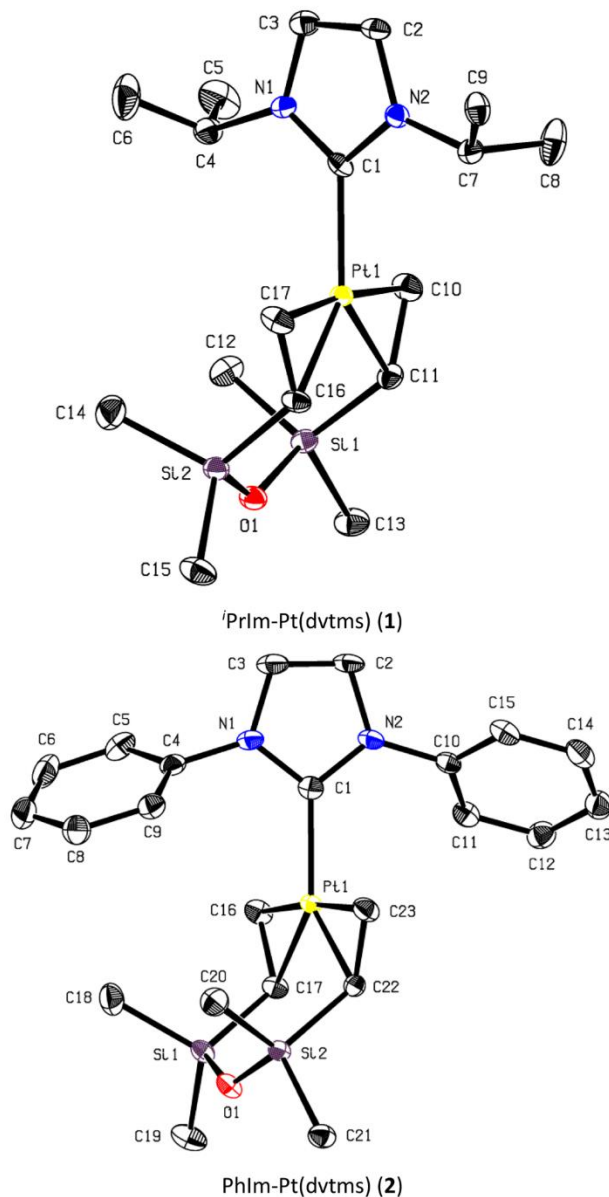


Fig. 2. ORTEP style molecular structure representation of complexes 1–5. Thermal ellipsoids are given at a 50% probability level. Hydrogen atoms are omitted for clarity. One of the two crystallographically independent molecules is shown for 1.

miniscule induction period, especially if compared to other complexes with aromatic wingtips. Despite the high reactivity, the selectivity remains excellent at 96% and a yield of 4% C_8 byproducts. Replacing the phenyl wingtips of **2** with 2-pyridine in **3** severely impedes the initial hydrosilylation of dvtms and results in an induction period of 1 h. This behavior is attributed to the coordination of N_{2-py} to the platinum center [74,75] upon dissociation of one dvtms vinyl moiety [18] during the initiation process. Unfortunately, the deactivated species of **3** and **4** remained elusive and could thus not be characterized. Finally, the comparison of **5** and **7** shows slightly improved induction properties for the triazolylidene complex **5**, which is in agreement with the ^{195}Pt NMR data (*vide supra*). However, due to the inherent activity of **7** with a TOF

of $17,000\text{ h}^{-1}$ the time-yield curve outpaces its congener (**5**: $\text{TOF} = 12,000\text{ h}^{-1}$) in the middle section of the catalysis. Due to enhanced selectivity of **5** at 95% compared to **7** at 92% the kinetic curves cross once more just before the 3 h mark. In conclusion, the catalytic performance depends both on steric and electronic factors of the NHC ligand in accordance with literature known reports [18,21,32] with the additional finding, that N -donors impose a detrimental effect due to the formation of unduly stabilized Pt species.

Sigmoid time-yield curves are also found for model reaction **B** at $100\text{ }^\circ\text{C}$ and a catalyst loading of 100 ppm with equimolar amounts of MM^{vi} and MD^{HM} (Fig. 4; complete kinetic in SI). Table 5 summarizes the results of the kinetic study with generally higher TOFs than for **A** due to

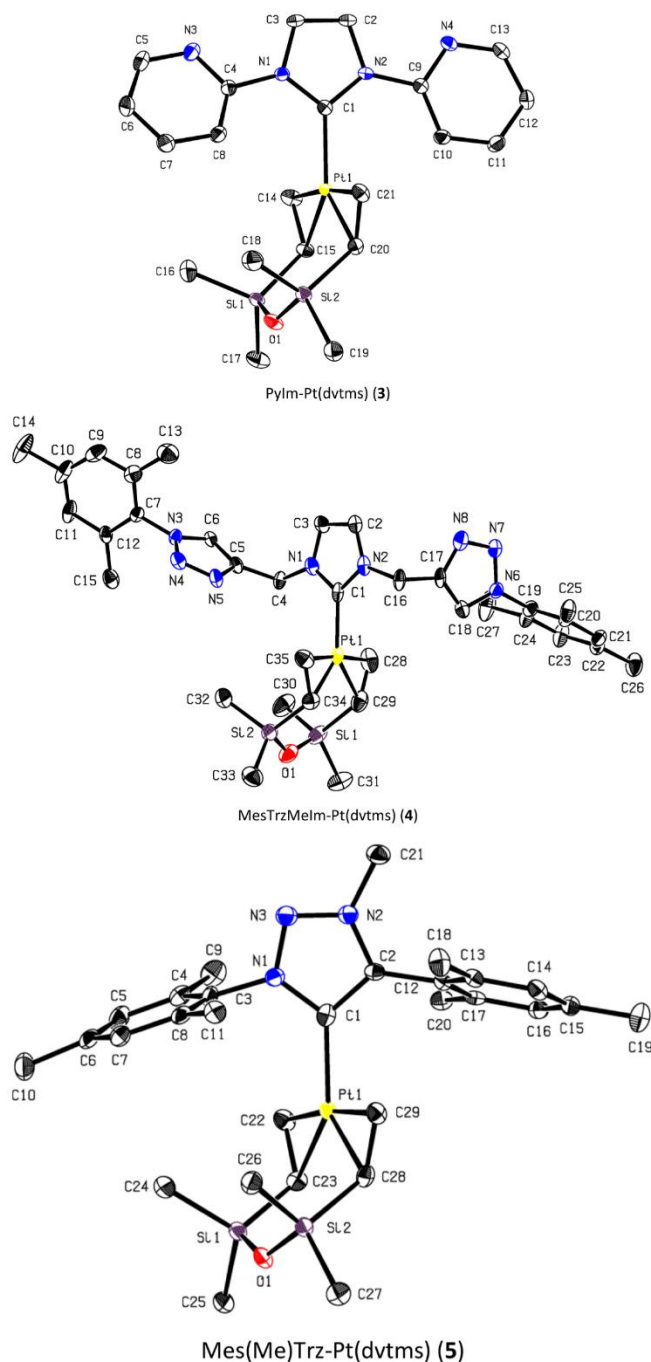


Fig. 2. (continued).

the increased temperature. Also, in model reaction **B** merely a maximum yield of 72% of product $\text{MM}(\text{C}_2\text{H}_4)\text{DM}_2$ is obtained for **2**, compared to 94% of the desired product $\text{M}_2\text{D-oct}$ in model reaction **A**, which was also achieved by **2**. Complex **4** exhibits the same deactivation trait as in **A**, which is indicated by a stagnation in yield, while the conversion of MM^{VI} (82%) and MD^{HM} (79%) has not reached quantitative levels yet. Nevertheless, **4** exhibits the highest selectivity of $S(\text{MM}^{\text{VI}}) = 81\%$ in the

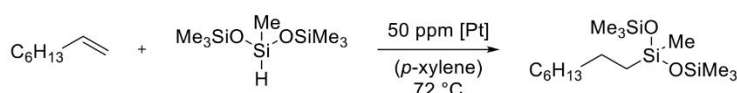
investigated series. In contrast to **A**, **1** and **6** show less profound differences in selectivities and also **5** not only reveals a shorter induction period compared to **7**, but also a higher TOF of $16,000 \text{ h}^{-1}$ for **5** in comparison to a TOF of 9000 h^{-1} for **7**. Moreover, the highest TOFs of $50,000$, $47,000$ and $44,000 \text{ h}^{-1}$ are achieved by **6**, **1** and **4**, respectively, which are the non-aromatic substituted NHC complexes in the order of their steric demand. The percentage share of three major, unidentified

Table 3

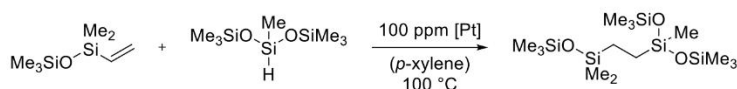
Relevant crystallographic data of novel complexes (1–5) in comparison to literature known complexes (6 [16,18], 7 [18]).

Complex	1 ^c	2	3	4	5 ^d	6 ^e	7 ^f
Bond lengths (Å)							
Pt–C _{carbene}	2.046(3)	2.038(2)	2.0542(19)	2.039(8)	2.054(3)	2.050(11)	2.046(4)
Pt–C _{C=C} (terminal a)	2.118(3)	2.121(2)	2.1210(19)	2.121(8)	2.114(3)	2.103(15)	2.141(5)
Pt–C _{C=C} (terminal b)	2.117(3)	2.120(2)	2.1265(19)	2.111(8)	2.116(3)	2.103(15)	2.138(5)
Pt–C _{C=C} (internal a)	2.127(3)	2.132(2)	2.1387(18)	2.138(8)	2.140(3)	2.178(11)	2.146(4)
Pt–C _{C=C} (internal b)	2.137(3)	2.138(2)	2.1265(19)	2.135(7)	2.139(3)	2.178(11)	2.148(5)
C _{carbene} –N (a)	1.355(4)	1.364(3)	1.368(2)	1.350(9)	1.373(4)	1.34(2)	1.360(5)
C _{carbene} –N (b)	1.362(3)	1.361(3)	1.373(2)	1.367(9)	1.404(4)	1.34(2)	1.367(7)
C _{im} –N (a)	1.388(4)	1.390(3)	1.398(2)	1.397(9)	1.349(4)	1.35(2)	1.377(7)
C _{im} –N (b)	1.387(3)	1.398(3)	1.402(2)	1.377(10)	1.358(4)	1.35(2)	1.390(7)
C _{im} –C _{im}	1.335(4)	1.338(3)	1.331(3)	1.348(10)	1.324(4)	1.34(3)	1.332(8)
C _{C=C} –C _{C=C} (a) ^g	1.436(4)	1.435(3)	1.430(3)	1.415(12)	1.431(5)	1.491(13)	1.437(7)
C _{C=C} –C _{C=C} (b) ^g	1.437(4)	1.435(3)	1.426(3)	1.441(10)	1.435(5)	1.491(13)	1.419(7)
Angles (°)							
N–C _{carbene} –N	104.0(2)	103.50(18)	103.33(15)	103.1(6)	101.6(3)	104.8(10)	103.1(3)
tilt angle θ NHC–Pt(dvtms)	83.43	70.00	79.94	80.85	59.00	90.00	64.67
Torsion (°)							
N–C _{im} –C _{im} –N	–0.5(3)	0.7(3)	0.5(2)	–0.9(8)	0.4(3)	0.0(7)	0.4(6)
C _{C=C} –C _{C=C} –C _{C=C} –C _{C=C}	2.1(3)	–0.3(2)	–1.3(2)	–0.2(8)	0.0(3)	0.0(1)	4.3(5)

c Data is only given for one of two crystallographically independent molecules. d Atom types are not necessarily identical, as 5 is a triazolylidene. The equal position as in an imidazolylidene is described. e Data was extracted from CCDC 197066 [16,18]. f Data was extracted from CCDC 275306 [18]. g Refers to the distance between the two olefinic carbons.



Scheme 3. Model reaction A is the hydrosilylation of oct-1-ene (1.0 eq., 2.024 mmol, 0.5 M) with MD^HM (1.0 eq., 2.024 mmol, 0.5 M) in *p*-xylene at 72 °C with 50 ppm [Pt] and *n*-decane (1.518 mmol) as internal standard, where M₂D-oct is formed.



Scheme 4. Model reaction B is the hydrosilylation of MM^{VI} (1 eq., 2.024 mmol, 0.5 M) with MD^HM (1 eq., 2.024 mmol, 0.5 M) in *p*-xylene at 100 °C with 100 ppm [Pt] and *n*-decane (1.518 mmol) as internal standard, where MM(C₂H₄)DM₂ is formed.

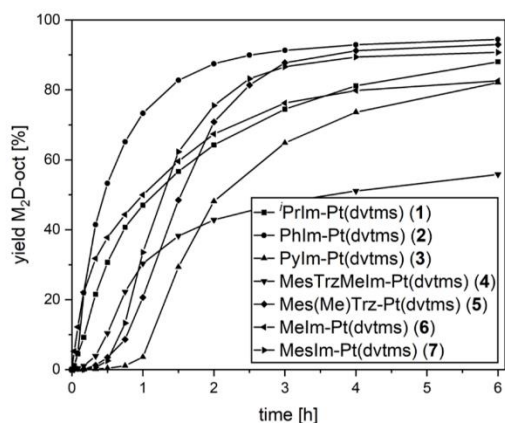


Fig. 3. Time dependent catalytic formation of product (M₂D-oct) by hydrosilylation of oct-1-ene (1.0 eq., 2.024 mmol, 0.5 M) with MD^HM (1.0 eq., 2.024 mmol, 0.5 M) in *p*-xylene at 72 °C with 50 ppm [Pt] and *n*-decane (1.518 mmol) as internal standard (A). Analysis by GC-FID.

byproducts was evaluated and an odd composition was found for 4, which coincides with the high selectivity of the complex in question (see SI).

Table 4

Catalytic formation of product (M₂D-oct) by hydrosilylation of oct-1-ene (1.0 eq., 2.024 mmol, 0.5 M) with MD^HM (1.0 eq., 2.024 mmol, 0.5 M) in *p*-xylene at 72 °C with 50 ppm [Pt] and *n*-decane (1.518 mmol) as internal standard (A). Analysis by GC-FID.

Catalyst	Y (M ₂ D-oct) [%]	X (oct-1-ene) [%]	X (MD ^H M) [%]	S [%] ^h	Y (isomerization) [%] ⁱ	TOF [h ⁻¹] ^j
1	88	92	87	96	4	14,000 ^k
2	94	98	93	96	3	39,000
3	82	85	81	97	3	11,000
4	56	60	55	94	2	10,000
5	93	98	92	95	4	12,000
6	83	98	82	84	12	31,000 ^l
7	91	98	90	92	4	17,000

Y: yield. X: conversion. S: selectivity. ^h Selectivity regarding oct-1-ene at *t* = 6 h; Selectivity regarding MD^HM \geq 99%. ⁱ Sum of C₈ isomers at *t* = 6 h. *n*-Octane is included herein. ^j "Apparent" TOF of oct-1-ene calculated at the steepest slope. ^k calculated from *t* = 2 to 20 min. ^l calculated from *t* = 0 to 5 min.

4. Conclusion

Seven Markó-type complexes of the structure (NHC)Pt(dvtms) were prepared, among them ⁱPrIm-Pt(dvtms) (1), PyIm-Pt(dvtms) (3), MesTrzMeIm-Pt(dvtms) (4) and Mes(Me)Trz-Pt(dvtms) (5) for the first

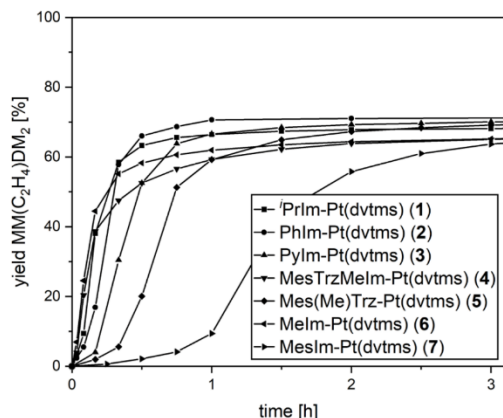


Fig. 4. Time dependent catalytic formation of product $\text{MM}(\text{C}_2\text{H}_4)\text{DM}_2$ by hydrosilylation of MM^{VI} (1.0 eq., 2.024 mmol, 0.5 M) with MD^{HM} (1.0 eq., 2.024 mmol, 0.5 M) in *p*-xylene at 100 °C with 100 ppm [Pt] and *n*-decane (1.518 mmol) as internal standard (B). Analysis by GC-FID. An uncapped kinetic for the duration of 6 h is included in the SI.

Table 5

Catalytic formation of product $\text{MM}(\text{C}_2\text{H}_4)\text{DM}_2$ by hydrosilylation of MM^{VI} (1.0 eq., 2.024 mmol, 0.5 M) with MD^{HM} (1.0 eq., 2.024 mmol, 0.5 M) in *p*-xylene at 100 °C with 100 ppm [Pt] and *n*-decane (1.518 mmol) as internal standard (B). Analysis by GC-FID. Evaluation of selected byproducts is included in the SI.

Catalyst	Y(MM (C ₂ H ₄) DM ₂) [%]	X (MM ^{VI}) [%]	X (MD ^{HM}) [%]	S(MM ^{VI}) [%]	S(MD ^{HM}) [%]	TOF [h ⁻¹] ^m
1	69	98	99	71	70	47,000
2	72	98	≥99	73	72	33,000
3	71	93	92	76	77	20,000
4	66	82	79	81	84	44,000
5	71	96	98	74	73	16,000
6	66	98	≥99	68	66	50,000
7	68	94	94	72	72	9000

Y: yield. X: conversion. S: selectivity. All data given at $t = 6$ h. ^m Apparent TOF of MM^{VI} calculated at the steepest slope.

time. Compound **5** is the first described abnormal 1,2,3-triazole-5-ylidene Pt(0) complex to the best of our knowledge. The structures of these complexes alongside PhIm-Pt(dvtms) (**2**) were investigated by SC-XRD and the whole ensemble of this study was characterized by NMR spectroscopy (¹H, ¹³C, ²⁹Si, ¹⁹⁵Pt) and CHNS analysis. The performance of these compounds as catalyst precursors was studied in two different hydrosilylation reactions. The reaction of either oct-1-ene (A) or MM^{VI} (B) with MD^{HM} are employed as references to literature and to mimic the crosslinking of silicones, respectively. Among the examined complexes, the presumed hemilabile *N*-donors in **3** and **4** displayed a detrimental effect on the catalytic capabilities that indicate a blockade of the catalytic cycle by stabilization as a Pt(II) species with a Pt-N bond. The best performance was obtained with PhIm-Pt(dvtms) (**2**), achieving the highest yield of the products of model reaction A and B, at 94 and 72%, respectively after a very short induction period.

Declaration of Competing Interest

The authors declare that they have no known competing financial interests or personal relationships that could have appeared to influence the work reported in this paper.

Acknowledgments

M.J.S. and L.F.R. thank the TUM Graduate School and WACKER Chemie AG for financial support. J.O. gratefully acknowledges the support of AuTUM (Ausbildungszentrum der Technischen Universität München) and all authors thank AuTUM for the cooperation during J. O.'s apprenticeship.

Supplementary materials

Supplementary material associated with this article can be found, in the online version, at [doi:10.1016/j.jorganchem.2023.122995](https://doi.org/10.1016/j.jorganchem.2023.122995).

References

- [1] B. Marciniak, H. Maciejewski, C. Pietraszuk, P. Pawluć, Hydrosilylation and related reactions of silicon compounds, in: B. Cornils, W.A. Herrmann, M. Beller, R. Paciello (Eds.), *Applied Homogeneous Catalysis With Organometallic Compounds*, WILEY-VCH, 2017, pp. 569–620.
- [2] Y. Nakajima, S. Shimada, Hydrosilylation reaction of olefins: recent advances and perspectives, *RSC Adv.* 5 (2015) 20603–20616, <https://doi.org/10.1039/C4RA17281G>.
- [3] R.J. Hofmann, M. Vlatković, F. Wiesbrock, Fifty years of hydrosilylation in polymer science: a review of current trends of low-cost transition-metal and metal-free catalysts, non-thermally triggered hydrosilylation reactions, and industrial applications, *Polymers* 9 (2017) 534, <https://doi.org/10.3390/polym9100534>.
- [4] R.Y. Lukin, A.M. Kuchkaev, A.V. Sukhov, G.E. Bekmukhamedov, D.G. Yakhvarov, Platinum-catalyzed hydrosilylation in polymer chemistry, *Polymers* 12 (2020) 2174, <https://doi.org/10.3390/polym12102174>.
- [5] E.G. Rochow, Preparation of organosilicon halides, US2380995A, August, 7, 1945.
- [6] E.G. Rochow, The direct synthesis of organosilicon compounds, *J. Am. Chem. Soc.* 67 (1945) 963–965, <https://doi.org/10.1021/ja01222a026>.
- [7] R. Müller, One hundred years of organosilicon chemistry, *J. Chem. Educ.* 42 (1965) 41, <https://doi.org/10.1021/ed042p41>.
- [8] D. Troegel, J. Stohrer, Recent advances and actual challenges in late transition metal catalyzed hydrosilylation of olefins from an industrial point of view, *Coord. Chem. Rev.* 255 (2011) 1440–1459, <https://doi.org/10.1016/j.ccr.2010.12.025>.
- [9] Y. Naganawa, K. Inomata, K. Sato, Y. Nakajima, Hydrosilylation reactions of functionalized alkenes, *Tetrahedron Lett.* 61 (2020), 151513, <https://doi.org/10.1016/j.tetlet.2019.151513>.
- [10] J.L. Speier, J.A. Webster, G.H. Barnes, The addition of silicon hydrides to olefinic double bonds. Part II. The use of group VIII metal catalysts, *J. Am. Chem. Soc.* 79 (1957) 974–979, <https://doi.org/10.1021/ja01561a054>.
- [11] J.L. Speier, D.E. Hook, Process for the Production of Organosilicon Compounds, US2823218, February 11, 1958.
- [12] R.A. Benkeser, J. Kang, The composition of Speier's catalyst, *J. Organomet. Chem.* 185 (1980) C9–C12, [https://doi.org/10.1016/S0022-328X\(00\)94412-7](https://doi.org/10.1016/S0022-328X(00)94412-7).
- [13] B.D. Karstedt, Platinum Complexes of Unsaturated Siloxanes and Platinum Containing Organopolysiloxanes, US3775452, November 27, 1973.
- [14] G. Chandra, P.Y. Lo, P.B. Hitchcock, M.F. Lappert, A convenient and novel route to bis(η -alkyne)platinum(0) and other platinum(0) complexes from Speier's hydrosilylation catalyst $\text{H}_2[\text{PtCl}_6] \cdot x\text{H}_2\text{O}$. X-ray Structure of $[\text{Pt}(\eta\text{-CH}_2 = \text{CHSiMe}_2)_2\text{O}](\text{P-}t\text{-Bu}_3)]$, *Organometallics* 6 (1987) 191–192, <https://doi.org/10.1021/om00144a036>.
- [15] P.B. Hitchcock, M.F. Lappert, N.J.W. Warhurst, Synthesis and structure of a rac-tris (divinylsiloxane)diplatinum(0) complex and its reaction with maleic anhydride, *Angew. Chem. Int. Ed.* 30 (1991) 438–440, <https://doi.org/10.1002/ange.199104381>.
- [16] I.E. Markó, S. Stérin, O. Buisine, G. Mignani, P. Branlard, B. Tinant, J.-P. Declercq, Selective and efficient platinum(0)-carbene complexes as hydrosilylation catalysts, *Science* 298 (2002) 204–206, <https://doi.org/10.1126/science.1073338>.
- [17] I.E. Markó, S. Stérin, O. Buisine, G. Berthon, G. Michaud, B. Tinant, J.-P. Declercq, Highly active and selective platinum(0)-carbene complexes. efficient, catalytic hydrosilylation of functionalised olefins, *Adv. Synth. Catal.* 346 (2004) 1429–1434, <https://doi.org/10.1002/adsc.200404048>.
- [18] G. Berthon-Gelloz, O. Buisine, J.-F. Brière, G. Michaud, S. Stérin, G. Mignani, B. Tinant, J.-P. Declercq, D. Chapon, I.E. Markó, Synthetic and structural studies of NHC–Pt(dvtms) complexes and their application as alkene hydrosilylation catalysts (NHC = *N*-heterocyclic carbene, dvtms = divinyltetramethylsiloxane), *J. Organomet. Chem.* 690 (2005) 6156–6168, <https://doi.org/10.1016/j.jorganchem.2005.08.020>.
- [19] O. Buisine, G. Berthon-Gelloz, J.-F. Brière, S. Stérin, G. Mignani, P. Branlard, B. Tinant, J.-P. Declercq, I.E. Markó, Second generation *N*-heterocyclic carbene–Pt(0) complexes as efficient catalysts for the hydrosilylation of alkenes, *Chem. Commun.* (2005) 3856–3858, <https://doi.org/10.1039/B506369H>.
- [20] B.P. Maliszewski, N.V. Tzouras, S.G. Guillet, M. Saab, M. Beliš, K. Van Hecke, F. Nalra, S.P. Nolan, A general protocol for the synthesis of Pt-NHC (NHC = *N*-heterocyclic carbene) hydrosilylation catalysts, *Dalt. Trans.* 49 (2020) 14673–14679, <https://doi.org/10.1039/D0D103480K>.
- [21] G. De Bo, G. Berthon-Gelloz, B. Tinant, I.E. Markó, Hydrosilylation of alkynes mediated by *N*-heterocyclic carbene platinum(0) complexes, *Organometallics* 25 (2006) 1881–1890, <https://doi.org/10.1021/om050866j>.

- [22] S. Dierick, D.F. Dewez, I.E. Markó, IPr⁺(2-Np)—An exceedingly bulky *N*-heterocyclic carbene, *Organometallics* 33 (2014) 677–683, <https://doi.org/10.1021/om4008955>.
- [23] V. Lillo, J. Mata, J. Ramirez, E. Peris, E. Fernandez, Catalytic dimerization of unsaturated molecules with platinum(0)–NHC: selective synthesis of 1,2-dihydroxysulfones, *Organometallics* 25 (2006) 5829–5831, <https://doi.org/10.1021/om060666n>.
- [24] V. Lillo, J.A. Mata, A.M. Segarra, E. Peris, E. Fernandez, The active role of NHC ligands in platinum-mediated tandem hydroboration–cross coupling reactions, *Chem. Commun.* (2007) 2184–2186, <https://doi.org/10.1039/B700800G>.
- [25] N. Schneider, S. Bellemín-Laponnaz, H. Wadepohl, L.H. Gade, A new class of modular oxazoline-NHC ligands and their coordination chemistry with platinum metals, *Eur. J. Inorg. Chem.* 2008 (2008) 5587–5598, <https://doi.org/10.1002/ejic.200800908>.
- [26] D. Brissy, M. Skander, P. Retailleau, G. Frison, A. Marinetti, Platinum(II) complexes featuring chiral diphosphines and *N*-heterocyclic carbene ligands: synthesis and evaluation as cycloisomerization catalysts, *Organometallics* 28 (2009) 140–151, <https://doi.org/10.1021/om800743r>.
- [27] J.J. Dunsford, K.J. Cavell, B. Kariuki, Expanded ring *N*-heterocyclic carbene complexes of zero valent platinum dvtms (divinyltetramethyldisiloxane): highly efficient hydrosilylation catalysts, *J. Organomet. Chem.* 696 (2011) 188–194, <https://doi.org/10.1016/j.jorganchem.2010.08.045>.
- [28] G.F. Silbestri, J.C. Flores, E. de Jesús, Water-soluble *n*-heterocyclic carbene platinum(0) complexes: recyclable catalysts for the hydrosilylation of alkynes in water at room temperature, *Organometallics* 31 (2012) 3355–3360, <https://doi.org/10.1021/om300148q>.
- [29] A.M. Ruiz-Varilla, E.A. Baquero, G.F. Silbestri, C. Gonzalez-Arellano, E. de Jesús, J. C. Flores, Synthesis and behavior of novel sulfonated water-soluble *N*-heterocyclic carbene (*η*²-diene) platinum(0) complexes, *Dalt. Trans.* 44 (2015) 18360–18369, <https://doi.org/10.1039/C5DT02622A>.
- [30] T.K. Meister, J.W. Küick, K. Riener, A. Pöthig, W.A. Herrmann, F.E. Kühn, Decoding catalytic activity of platinum carbene hydrosilylation catalysts, *J. Catal.* 337 (2016) 157–166, <https://doi.org/10.1016/j.jcat.2016.01.032>.
- [31] P. Žak, M. Bolt, J. Lorkowski, M. Kubicki, C. Pietraszuk, Platinum complexes bearing bulky *N*-heterocyclic carbene ligands as efficient catalysts for the fully selective dimerization of terminal alkynes, *ChemCatChem* 9 (2017) 3627–3631, <https://doi.org/10.1002/cctc.201700580>.
- [32] P. Žak, M. Bolt, M. Kubicki, C. Pietraszuk, Highly selective hydrosilylation of olefins and acetylenes by platinum(0) complexes bearing bulky *N*-heterocyclic carbene ligands, *Dalt. Trans.* 47 (2018) 1903–1910, <https://doi.org/10.1039/C7DT04392A>.
- [33] P. Žak, M. Bolt, C. Pietraszuk, Selective hydrosilylation of dienes, enynes, and diynes catalyzed by a platinum complex with a very bulky NHC ligand—The crucial role of precise tuning of the reaction conditions, *Eur. J. Inorg. Chem.* 2019 (2019) 2455–2461, <https://doi.org/10.1002/ejic.201900217>.
- [34] P. Žak, M. Bolt, B. Dudzic, M. Kubicki, Synthesis of (*E*)-1,4-disilsequioxylsubstituted but-1-en-3-yne via platinum-catalyzed dimerization of ethynylsiloxylsiloxanes, *Dalt. Trans.* 48 (2019) 2657–2663, <https://doi.org/10.1039/C8DT05142A>.
- [35] S.A. Rzhveskiy, M.A. Topchii, K.A. Lyssenko, A.N. Philippova, M.A. Belaya, A. A. Agheshina, M.V. Bermeshev, M.S. Nechaev, A.F. Asachenko, New expanded-ring NHC platinum(0) complexes: synthesis, structure and highly efficient dimerization of terminal alkenes, *J. Organomet. Chem.* 912 (2020), 121140, <https://doi.org/10.1016/j.jorganchem.2020.121140>.
- [36] D. Friedman, T. Masciangioli, S. Olson, *The Role of the Chemical Sciences in Finding Alternatives to Critical Resources: A Workshop Summary*, The National Academies Press, Washington, DC, 2012.
- [37] H.U. Sverdrup, K.V. Ragnarsdóttir, A system dynamics model for platinum group metal supply, market price, depletion of extractable amounts, ore grade, recycling and stocks-in-use, *Resour. Conserv. Recycl.* 114 (2016) 130–152, <https://doi.org/10.1016/j.resconrec.2016.07.011>.
- [38] L.D. de Almeida, H. Wang, K. Jung, X. Cui, M. Beller, Recent advances in catalytic hydrosilylations: developments beyond traditional platinum catalysts, *Angew. Chem. Int. Ed.* 60 (2021) 550–565, <https://doi.org/10.1002/anie.202008729>.
- [39] J.V. Obligacion, P.J. Chirik, Earth-abundant transition metal catalysts for alkene hydrosilylation and hydroboration, *Nat. Rev. Chem.* 2 (2018) 15–34, <https://doi.org/10.1038/s41570-018-0001-2>.
- [40] O. Schuster, L. Yang, H.G. Raubenheimer, M. Albrecht, Beyond conventional *N*-heterocyclic carbenes: abnormal, remote, and other classes of NHC ligands with reduced heteroatom stabilization, *Chem. Rev.* 109 (2009) 3445–3478, <https://doi.org/10.1021/cr8005087>.
- [41] J.D. Crowley, A.-L. Lee, K.J. Kilpin, 1,3,4-trisubstituted-1,2,3-triazol-5-ylidene ‘click’ carbene ligands: synthesis, catalysis and self-assembly, *Aust. J. Chem.* 64 (2011) 1118–1132, <https://doi.org/10.1071/CH11185>.
- [42] D. Schweinfurth, L. Hettmanzyk, L. Suntrup, B. Sarkar, Metal complexes of click-derived triazoles and mesoionic carbenes: electron transfer, photochemistry, magnetic bistability, and catalysis, *Z. Anorg. Allg. Chem.* 643 (2017) 554–584, <https://doi.org/10.1002/zaac.201700030>.
- [43] J.C. Bernhammer, H.V. Huynh, Platinum(II) complexes with thioether-functionalized benzimidazol-2-ylidene ligands: synthesis, structural characterization, and application in hydroelementation reactions, *Organometallics* 33 (2014) 172–180, <https://doi.org/10.1021/om400929t>.
- [44] Y. Zhu, C. Cai, G. Lu, *N*-heterocyclic carbene-catalyzed α -alkylation of ketones with primary alcohols, *Helv. Chim. Acta* 97 (2014) 1666–1671, <https://doi.org/10.1002/hlca.201400076>.
- [45] M.S.S. Jamil, S. Alkaabi, A.K. Brisdon, Simple NMR predictors of catalytic hydrogenation activity for [Rh(cod)Cl(NHC)] complexes featuring fluorinated NHC ligands, *Dalt. Trans.* 48 (2019) 9317–9327, <https://doi.org/10.1039/C9DT01219B>.
- [46] K. Riener, M.J. Bitzer, A. Pöthig, A. Raba, M. Cokoja, W.A. Herrmann, F.E. Kühn, On the concept of hemilability: insights into a donor-functionalized iridium(I) NHC motif and its impact on reactivity, *Inorg. Chem.* 53 (2014) 12767–12777, <https://doi.org/10.1021/ic5016324>.
- [47] M. Hollering, M. Albrecht, F.E. Kühn, Bonding and catalytic application of ruthenium *n*-heterocyclic carbene complexes featuring triazole, triazolylidene, and imidazolylidene ligands, *Organometallics* 35 (2016) 2980–2986, <https://doi.org/10.1021/acs.organomet.6b00504>.
- [48] F. Stein, M. Kirsch, J. Beerhues, U. Albold, B. Sarkar, Mono- and di-mesoionic carbene-boranes: synthesis, structures and utility as reducing agents, *Eur. J. Inorg. Chem.* 2021 (2021) 2417–2424, <https://doi.org/10.1002/ejic.202100273>.
- [49] S. Bauri, A. Ramachandran, A. Rit, Base-catalyzed effective C2-amination of azolium salts using isocyanates under mild conditions, *Chem. Asian J.* 18 (2023), e202201301, <https://doi.org/10.1002/asia.202201301>.
- [50] H. Richter, H. Schwertfeger, P.R. Schreiner, R. Fröhlich, F. Glorius, Thieme chemistry journal awardees - where are they now? Synthesis of diamantane-derived *N*-heterocyclic carbenes and applications in catalysis, *Synlett* 2009 (2009) 193–197, <https://doi.org/10.1055/s-0028-1087676>.
- [51] APEX Suite of Crystallographic Software (Version APEX4), Bruker AXS Inc., 2021.
- [52] SAINT (Version 8.38A), Bruker AXS Inc., 2017.
- [53] SADABS (Version 2016/2), Bruker AXS Inc., 2016.
- [54] C.B. Hübschle, G.M. Sheldrick, B. Dittrich, ShelXle: a Qt graphical user interface for SHELXL, *J. Appl. Crystallogr.* 44 (2011) 1281–1284, <https://doi.org/10.1107/S0021889811043202>.
- [55] G.M. Sheldrick, Crystal structure refinement with SHELXL, *Acta Crystallogr. Sect. C* 71 (2015) 3–8, <https://doi.org/10.1107/S2053229614024218>.
- [56] G.M. Sheldrick, SHELXT - Integrated space-group and crystal-structure determination, *Acta Crystallogr. Sect. A* 71 (2015) 3–8, <https://doi.org/10.1107/S2053273314026370>.
- [57] A.J. Wilson, *International Tables for Crystallography*, Kluwer Academic Publishers, Dordrecht, 1992.
- [58] A. Spek, PLATON SQUEEZE: a tool for the calculation of the disordered solvent contribution to the calculated structure factors, *Acta Crystallogr. Sect. C* 71 (2015) 9–18, <https://doi.org/10.1107/S2053229614024929>.
- [59] A. Spek, Structure validation in chemical crystallography, *Acta Crystallogr. Sect. D* 65 (2009) 148–155, <https://doi.org/10.1107/S090744490804362X>.
- [60] B. Schulze, U.S. Schubert, Beyond click chemistry – supramolecular interactions of 1,2,3-triazoles, *Chem. Soc. Rev.* 43 (2014) 2522–2571, <https://doi.org/10.1039/C3CS60386E>.
- [61] S. Sinn, B. Schulze, C. Friebe, D.G. Brown, M. Jäger, E. Altuntaş, J. Kübel, O. Gunter, C.P. Berlinguette, B. Dietzek, U.S. Schubert, Physicochemical analysis of ruthenium(II) sensitizers of 1,2,3-triazole-derived mesoionic carbene and cyclometalating ligands, *Inorg. Chem.* 53 (2014) 2083–2095, <https://doi.org/10.1021/ic402702z>.
- [62] B.P. Maliszewski, I. Ritacco, M. Belis, I.I. Hashim, N.V. Tzouras, L. Caporaso, L. Cavallo, K. Van Hecke, F. Nahra, C.S.J. Cazin, S.P. Nolan, A green route to platinum *N*-heterocyclic carbene complexes: mechanism and expanded scope, *Dalt. Trans.* 51 (2022) 6204–6211, <https://doi.org/10.1039/D2DT00504B>.
- [63] J.F. Schlagintweit, C.H.G. Jakob, N.L. Wilke, M. Ahrweiler, C. Frias, J. Frias, M. König, E.-M.H.J. Esslinger, F. Marques, J.F. Machado, R.M. Reich, T.S. Morais, J.D.G. Correia, A. Prokop, F.E. Kühn, Gold(I) bis(1,2,3-triazol-5-ylidene) complexes as promising selective anticancer compounds, *J. Med. Chem.* 64 (2021) 15747–15757, <https://doi.org/10.1021/acs.jmedchem.1c01021>.
- [64] J.B. Shaik, V. Ramkumar, B. Varghese, S. Sankaraman, Synthesis and structure of *trans*-bis(1,4-dimesityl-3-methyl-1,2,3-triazol-5-ylidene)palladium(II) dichloride and diacetate. Suzuki–Miyaura coupling of polybromoarenes with high catalytic turnover efficiencies, *Beilstein J. Org. Chem.* 9 (2013) 698–704, <https://doi.org/10.3762/bjoc.9.79>.
- [65] S. Hohloch, F.L. Duecker, M. Van der Meer, B. Sarkar, Copper(I) complexes of mesoionic carbene: structural characterization and catalytic hydrosilylation reactions, *Molecules* 20 (2015) 7379–7395, <https://doi.org/10.3390/molecules20047379>.
- [66] J.R.L. Priqueler, I.S. Butler, F.D. Rochon, An overview of ¹⁹⁵Pt nuclear magnetic resonance spectroscopy, *Appl. Spectrosc. Rev.* 41 (2006) 185–226, <https://doi.org/10.1080/05704920600620311>.
- [67] B.M. Still, P.G.A. Kumar, J.R. Aldrich-Wright, W.S. Price, ¹⁹⁵Pt NMR—Theory and application, *Chem. Soc. Rev.* 36 (2007) 665–686, <https://doi.org/10.1039/B606190G>.
- [68] J.M. Lambert, The nature of platinum in silicones for biomedical and healthcare use, *J. Biomed. Mater. Res. Part B* 78B (2006) 167–180, <https://doi.org/10.1002/jbm.b.30471>.
- [69] K.L. Lee, Aminomethylpyridine complexes for the cobalt-catalyzed anti-markovnikov hydrosilylation of alkoxy- or siloxy(vinyl)silanes with alkoxy- or siloxyhydrosilanes, *Angew. Chem. Int. Ed.* 56 (2017) 3665–3669, <https://doi.org/10.1002/anie.201612460>.
- [70] J. Stein, L.N. Lewis, Y. Gao, R.A. Scott, In situ determination of the active catalyst in hydrosilylation reactions using highly reactive Pt(0) catalyst precursors, *J. Am. Chem. Soc.* 121 (1999) 3693–3703, <https://doi.org/10.1021/ja9825377>.
- [71] L.N. Lewis, On the mechanism of metal colloid catalyzed hydrosilylation: proposed explanations for electronic effects and oxygen cocatalysis, *J. Am. Chem. Soc.* 112 (1990) 5998–6004, <https://doi.org/10.1021/ja00172a014>.

- [72] B.P. Maliszewski, T.A.C.A. Bayrakdar, P. Lambert, L. Hamdouna, X. Trivelli, L. Cavallo, A. Poater, M. Belis, O. Lafon, K. Van Hecke, D. Ormerod, C.S.J. Cazin, F. Nahra, S.P. Nolan, PtII–*N*-heterocyclic carbene complexes in solvent-free alkene hydrosilylation, *Chem. Eur. J.* 29 (2023), e202301259, <https://doi.org/10.1002/chem.202301259>.
- [73] K. Liu, G. Hou, J. Mao, Z. Xu, P. Yan, H. Li, X. Guo, S. Bai, Z.C. Zhang, Genesis of electron deficient Pt(0) in PDMS-PEG aggregates, *Nat. Commun.* 10 (2019) 996, <https://doi.org/10.1038/s41467-019-08804-y>.
- [74] M. Poyatos, A. Maise-François, S. Bellemin-Laponnaz, L.H. Gade, Coordination chemistry of a modular *N,C*-chelating oxazole-carbene ligand and its applications in hydrosilylation catalysis, *Organometallics* 25 (2006) 2634–2641, <https://doi.org/10.1021/om060166u>.
- [75] C. Lu, S. Gu, W. Chen, H. Qiu, Platinum(II) complexes with polydentate *N*-heterocyclic carbenes: synthesis, structural characterization and hydrosilylation catalysis, *Dalt. Trans.* 39 (2010) 4198–4204, <https://doi.org/10.1039/B924587A>.

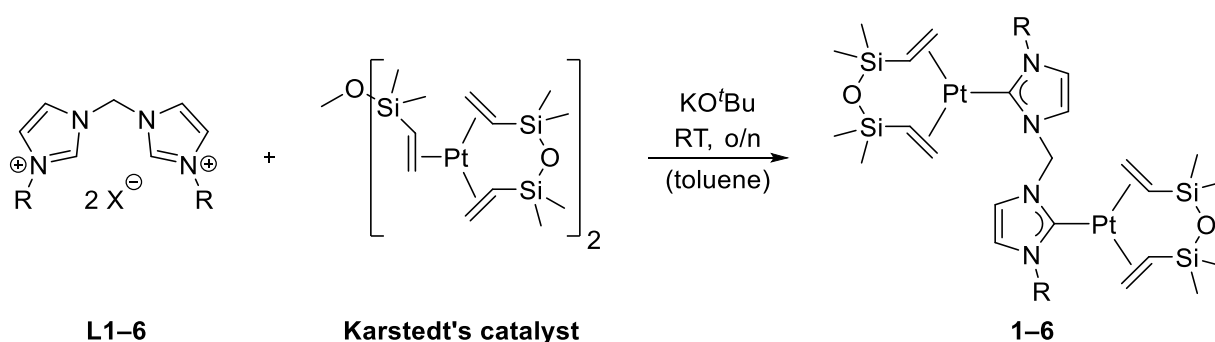
3.2 Homobimetallic *bis*-NHC(Ptdvtms)₂ Complexes for the Hydrosilylation of Alkenes

Michael J. Sauer, Jeff Offorjindu, Greta G. Zámbo, Robert M. Reich, Fritz E. Kühn*

J. Organomet. Chem. **2024**, *1007*, 123030-123044.

3.2.1 Publication Summary

Synergistic or cooperative effects between metals in close proximity, such as in bimetallic complexes, have been recognized to promote activity and selectivity. Based on this, a series of six homobimetallic *bis*-NHC(Ptdvtms)₂ complexes (**1–6**; numbering applies only to this publication) was prepared with the anticipation of cooperative effects and characterization by multinuclear NMR spectroscopy, SC-XRD, and CHNS analysis is reported.¹¹⁵ Due to the remarkable properties of Markó-type complexes, two methylene-bridged imidazolium units were selected as the basic scaffold of this new complex class, that enables a wide range of Pt–Pt–distances by rotation of the central methylene linker. These complexes are prepared following an adapted procedure of Markó *et al.* (Scheme 17).⁷⁸



Scheme 17: Synthetic procedure for the preparation of complexes **1–6** from the respective *bis*-(imidazolium) salt and Karstedt's catalyst⁷¹ in the presence of potassium *tert*-butoxide. **1:** R = Me, X[−] = PF₆[−]; **2:** R = Ph, X[−] = Br[−]; **3:** R = 2-Py, X[−] = PF₆[−]; **4:** R = Mes, X[−] = Br[−]; **5:** R = 2,6-diisopropylphenyl (Dipp), X[−] = PF₆[−]; **6:** R = 4-methylene-1-(2,6-diisopropylphenyl)-1*H*-1,2,3-triazole (MeTrzDipp), X[−] = PF₆[−].

Hindered rotation of the Pt–C bond generates conformational isomers, whereby a rotational barrier of 52.5 kJ·mol^{−1} was determined for **5** based on ¹H variable temperature NMR spectroscopy. Apart from this finding, spectroscopic and crystallographic data indicate a similar chemical environment of platinum in the mono- and bimetallic complexes, which allows catalytic comparison regardless of further parameters.

The bimetallic complexes prove to be potent catalyst precursors and catalyze the hydrosilylation of alkenes efficiently and selectively, outperforming their monometallic congeners due to minuscule initiation periods. The best performance is achieved by **2** with a TOF of 48,000 h^{−1} and a selectivity of 98% (Table 5). However, complexes **1**, **3**, and **6** demonstrate poor suitability for the hydrosilylation of alkenes, as they quickly deactivate. For **3** and **6** this effect is attributed to Pt(II) stabilization by *N*-coordination, but the deactivation of **1** demanded further investigations.

Table 5: Model reaction **A**: Catalytic formation of product (M₂D-oct) by hydrosilylation of oct-1-ene (1.0 eq., 2.024 mmol, 0.5 M) with MD^HM (1.0 eq., 2.024 mmol, 0.5 M) in *p*-xylene at 72 °C with 50 ppm [Pt] and *n*-decane (1.518 mmol) as internal standard. Complex **7** is Im^{Me}Pt(dvtms) as catalytic reference.⁷⁸

Catalyst	Y(M ₂ D-oct) [%]	X(oct-1-ene) [%]	X(MD ^H M) [%]	S [%]	Y(isomerization) [%]	TOF [h ⁻¹]
1	36	43	37	85	2	5000
2	90	92	88	98	3	48,000
3	22	27	23	80	1	12,000
4	90	94	90	96	3	38,000
5	95	99	93	96	3	43,000
6	52	56	51	92	2	5000
7	91	98	90	92	4	17,000

The initiation behavior of mono- and bimetallic complex classes is examined by the pre-catalytic reaction of **4** and **7** with silane (Figure 8). In the case of **4**, a deactivation is observed at first with subsequent reactivation, while selectivity is maintained. On the other hand, **7** is continuously more activated but suffers reduced selectivity at $t_{\text{SiH}} = 16$ and 40 h, which indicates transformation of the active species. This is further investigated by stoichiometric reaction of **1** with a silane, which reveals platinum-bound hydrides. Based on this and considering literature, a di- μ -hydrido complex is postulated. This species provides intermediate stabilization as demonstrated in mercury poisoning experiments contrary to monometallic **7**, which decomposes to platinum colloids under the same conditions. Finally, this also serves as an explanation for the inferior performance of **1** in **A**, where the methyl wingtips of the NHC cannot prevent the formation of an inactive di- μ -hydrido complex under standard conditions.

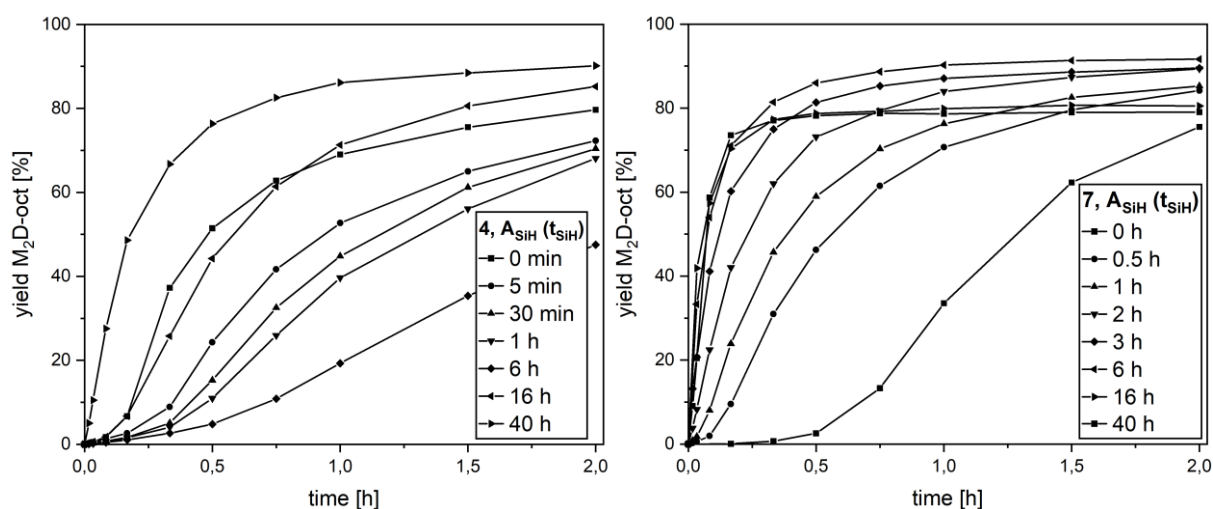


Figure 8: A_{SiH} – Preceding reaction of **4** (left) and **7** (right) with MD^HM for defined durations t_{SiH} . Catalysis is launched upon addition of oct-1-ene. Reaction conditions: oct-1-ene (1.0 eq., 2.024 mmol, 0.5 M) and MD^HM (1.0 eq., 2.024 mmol, 0.5 M) in *p*-xylene at 72 °C with 50 ppm [Pt] and *n*-decane (1.518 mmol) as internal standard.

3.2.2 Publication Reprint

Journal of Organometallic Chemistry 1007 (2024) 123030



Contents lists available at ScienceDirect

Journal of Organometallic Chemistry

journal homepage: www.elsevier.com/locate/jorganchemHomobimetallic *bis*-NHC(Ptdvtms)₂ Complexes for the Hydrosilylation of AlkenesMichael J. Sauer^a, Jeff Offorjindu^{a,b}, Greta G. Zámbo^a, Robert M. Reich^a, Fritz E. Kühn^{a,*}^a Molecular Catalysis, Department of Chemistry and Catalysis Research Center, TUM School of Natural Sciences, Technical University Munich, Lichtenbergstr. 4, D-85748, Garching bei München, Germany^b Ausbildungszentrum der Technischen Universität München, Lichtenbergstr. 4, D-85748, Garching bei München, Germany

ARTICLE INFO

Keywords:

Bimetallic
Induction period
Mercury poisoning
N-heterocyclic carbenes
Platinum
Silanes

ABSTRACT

A series of six bimetallic *bis*-NHC(Ptdvtms)₂ complexes **1–6** (dvtms = 1,1,3,3-tetramethyl-1,3-divinylsiloxane) has been designed by expansion of the monometallic Markó-type system in anticipation of synergistic bimetallic cooperation. The new compounds are easily accessible using Karstedt's catalyst [Pt₂(dvtms)₃] as platinum(0) precursor and the respective *bis*-(imidazolium) salts (**L1–6**), deprotonated by potassium *tert*-butoxide. Characterization via NMR spectroscopy (¹H, ¹³C, ²⁹Si, ¹⁹⁵Pt) and SC-XRD reveals a strong similarity of this new complex class to the parent monometallic complexes. The hydrosilylation reactions of oct-1-ene or 1,1,1,3,3-pentamethyl-3-vinylsiloxane (MM^{Vi}) with 1,1,3,5,5-heptamethyltrisiloxane (MD^HM), respectively, are efficiently and selectively catalyzed with turn-over frequencies (TOF) of up to 78,000 h⁻¹ after a significantly shortened induction period compared to their monometallic relatives. Mercury poisoning experiments demonstrate the superiority of bimetallic compared to monometallic systems in terms of stability when exposed to silanes.

1. Introduction

Metalloproteins are essential in living organisms to perform countless reactions efficiently and, first and foremost, selectively to sustain vital biological functions. Frequently, bimetallic sites are capable of overcoming reaction barriers under physiological conditions that pose problems in artificial non-protein systems [1–4]. A range of biomimetic studies has been inspired by these proteins, indicating the larger protein structure has to be considered in many cases in addition to the first coordination sphere [5–12]. Synergistic or cooperative effects between metals in close proximity have been recognized to promote activity and selectivity [13–17] and led to studies of a plethora of bimetallic complexes in catalysis [18–26]. This also holds true for the hydrosilylation reaction [27–35], where platinum catalysts dominate in industrial applications [36–38]. However, the Pt-Ir heterobimetallic complexes of Ishii *et al.* are the only platinum-containing bimetallic complexes that have been subjected to hydrosilylation so far [39]. The introduction of *N*-heterocyclic carbenes (NHCs) as spectator ligands by Markó *et al.* for monometallic platinum (NHC)Pt(dvtms) complexes proved beneficial in terms of selectivity and stability, reducing colloidal platinum formation under catalytic conditions [40–43]. They do, however, suffer from a pronounced initiation process, which is why they are frequently referred

to as “slow-release” precursors.

In this work the class of Markó-type complexes is extended to homobimetallic systems with the anticipation of cooperative effects and the synthesis and characterization of six *bis*-NHC(Ptdvtms)₂ complexes **1–6** (Fig. 1) is reported. The basic scaffold consists of two methylene-bridged imidazole-2-ylidene-Pt(dvtms) moieties that enable variable distances of the platinum atoms by conformational dynamics. The outer wingtips of the NHCs are altered in terms of steric bulk and contain, *inter alia*, dangling pyridine (**3**) or triazole (**6**) groups as presumed *N*-donors, virtually duplicating monometallic complexes [40,42,44,45]. These compounds are evaluated as catalytic precursors in the hydrosilylation of alkenes and compared to Im^{Mes}Pt(dvtms) (**7**) [41,42,46] as monometallic catalytic reference. A comparison of monometallic and bimetallic complexes is presented, especially in the presence of silanes.

2. Experimental

2.1. Methods and materials

All reactions were carried out under oxygen-free, dry conditions in an argon atmosphere using standard Schlenk and glovebox techniques unless specifically stated otherwise. The solvents were purified,

* Corresponding author.

E-mail address: fritz.kuehn@ch.tum.de (F.E. Kühn).<https://doi.org/10.1016/j.jorganchem.2024.123030>

Received 22 December 2023; Received in revised form 12 January 2024; Accepted 18 January 2024

Available online 24 January 2024

0022-328X/© 2024 The Author(s). Published by Elsevier B.V. This is an open access article under the CC BY-NC-ND license (<http://creativecommons.org/licenses/by-nc-nd/4.0/>).

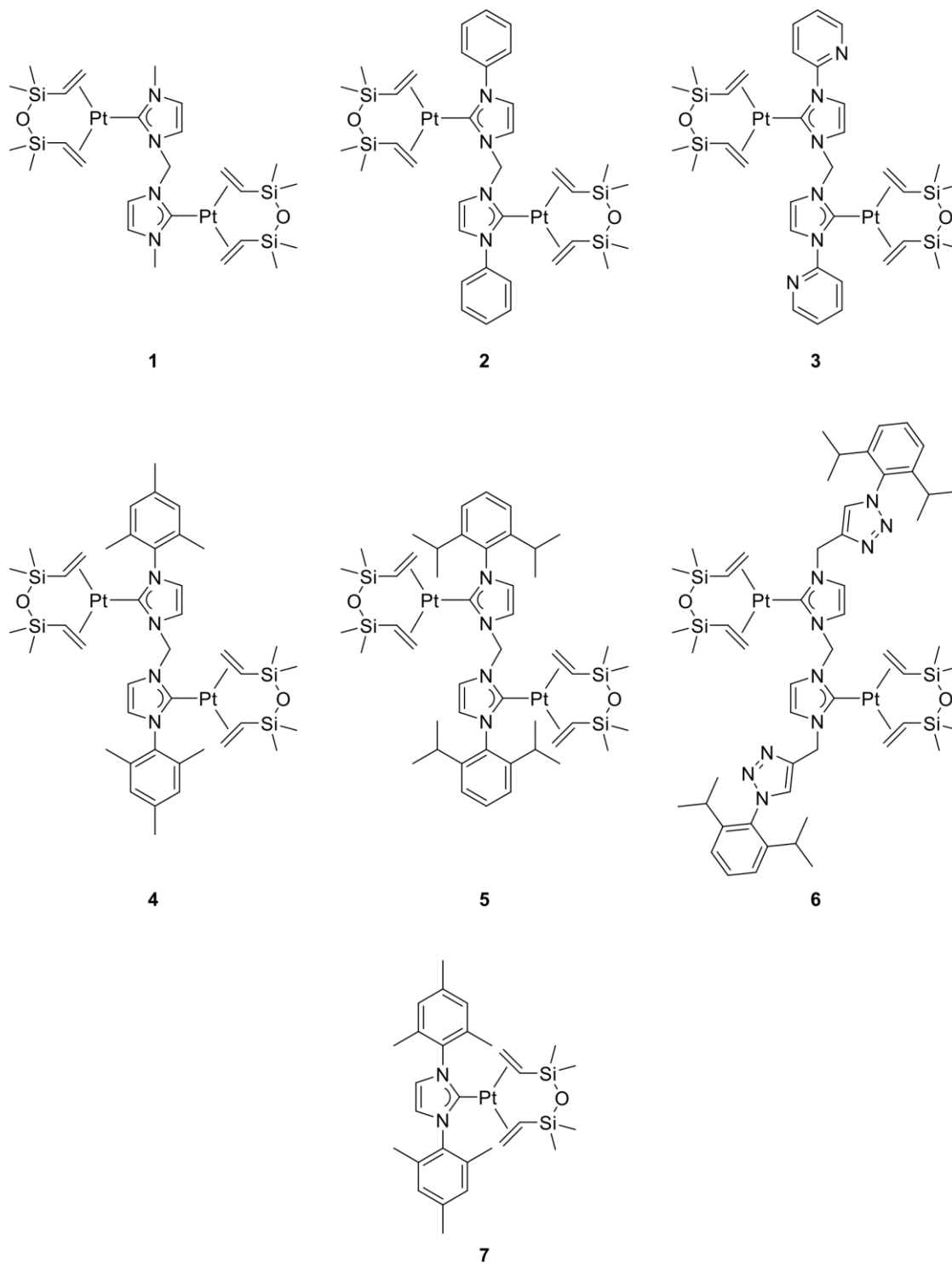


Fig. 1. Structure of NHC(Pt(dvtms)_x)_x (x = 1,2) complexes used in this study. Compound 7 is literature known and used as catalytic reference [42].

degassed, and dried according to standard purification techniques or obtained from an MBraun solvent purification system (SPS). The ligand precursor salts *bis-Im*^{Me}·(PF₆)₂ (**L1**) [47], *bis-Im*^{Ph}·(Br)₂ (**L2**) [48], *bis-Im*^{Py}·(PF₆)₂ (**L3**) [49], *bis-Im*^{Mes}·(Br)₂ (**L4**) [48], *bis-Im*^{Dipp}·(PF₆)₂ (**L5**) [48], *bis-Im*^{MeTrzDipp}·(PF₆)₂ (**L6**) [50] and *Im*^{Mes}·BF₄ (**L7**) [51] were prepared according to literature procedures. Where necessary, the ligand precursor salts were further purified by an anion exchange with 5 eq. NH₄PF₆. All further chemicals were purchased from Sigma-Aldrich, VWR, or abcr and used as received. NMR spectra were recorded on a Bruker Avance Ultrashield 400 MHz and a Bruker DPX 400 MHz spectrometer. All ¹H, ¹³C, and ²⁹Si chemical shifts are reported in parts per million (ppm) relative to TMS, with the residual solvent peak serving as an internal reference. ¹⁹⁵Pt chemical shifts are externally referenced to K₂PtCl₄ in H₂O ($\delta = -1628$ ppm). ²⁹Si NMR spectra were recorded via the INEPT technique. Abbreviations for NMR multiplicities are singlet (s), broad singlet (bs), doublet (d), triplet (t), and multiplet (m). Coupling constants are given in Hz. Catalytic experiments were conducted under atmospheric conditions and GC-grade *p*-xylene and *n*-hexane were employed therein. GC analysis was performed with an Agilent Technologies 7890B GC system using an HP-5 column (30 m × 320 μ m × 0.25 μ m). The injection volume was 1 μ L at an oven temperature of 50 °C and with a split ratio of 30:1. A flow of 0.9 mL·min⁻¹ of nitrogen as carrier gas was applied and the system was equipped with an FID detector, that was kept at 50 °C. After injection of the sample at 50 °C the oven temperature was held for 9 min and subsequently ramped to 80 °C at a rate of 6 °C·min⁻¹. Afterward, the ramp was increased to 15 °C·min⁻¹ until 205 °C was reached and the final temperature of 250 °C was reached by heating at 30 °C·min⁻¹ and then keeping the temperature for 3 min. Elemental analyses were performed at the microanalytical laboratory of the Catalysis Research Center, Technical University Munich. Single crystals were measured in the SC-XRD laboratory of the Catalysis Research Center at Technical University Munich, Germany.

2.2. Synthesis and characterization

2.2.1. General protocol for the synthesis of *bis-NHC*(Ptdvtms)₂ complexes (**1–6**)

Under argon, the respective *bis*-(imidazolium) salt (**L1–L6**, 1.00 eq.), Karstedt's catalyst (2.00 eq. Pt), potassium *tert*-butoxide (3.00 eq.; 2.05 eq. for **6**) and toluene are combined. The resulting suspension is stirred overnight in the dark. Under air, *n*-pentane is added to the reaction mixture and stirred before filtration over Celite. Elution with *n*-pentane and removal of all volatiles *in vacuo* gives crude product. The target compound is obtained by washing with propan-2-ol and *n*-pentane and subsequent drying. A more detailed account is presented in the ESI.

2.2.2. *bis-Im*^{Me}(Ptdvtms)₂ (**1**)

Yield: 53%. ¹H NMR (400 MHz, CDCl₃, 298 K): δ [ppm] = 7.12 (s, 2H, H_{im}), 6.93 (s, 2H, H_{im}), 5.99 (s, 2H, NCH₂N), 3.51 (s, 6H, CH₃), 2.20 (bs, 4H, CH₂CHSi), 2.06–1.82 (m, 8H, CH₂CHSi), 0.34 (s, 12H, SiCH_{3,eq}), -0.27 (s, 12H, SiCH_{3,ax}). ¹³C{¹H} NMR (101 MHz, CDCl₃, 298 K): δ [ppm] = 185.8 (Pt-C_{car}), 122.8 (C_{im}), 120.4 (C_{im}), 61.6 (NCH₂N), 41.4 (CH₂CHSi, ¹J_{Pt,C} = 160.6 Hz), 37.1 (CH₃), 35.5 (CH₂CHSi), 1.6 (SiCH_{3,eq}), -1.6 (SiCH_{3,ax}). ²⁹Si{¹H} NMR (79 MHz, CDCl₃, 298 K): δ [ppm] = 3.11 (s, ²J_{Pt,Si} = 41.1 Hz, 4 Si). ¹⁹⁵Pt NMR (85 MHz, CDCl₃, 298 K): δ [ppm] = -5390 (s, Pt, rotamer), -5395 (s, Pt, rotamer), -5399 (s, Pt, rotamer). Elemental analysis calcd (%) for C₂₅H₄₈N₄O₂Pt₂Si₄: C 31.97; H 5.15; N 5.97; found: C 31.62; H 5.12; N 5.83.

2.2.3. *bis-Im*^{Ph}(Ptdvtms)₂ (**2**)

Yield: 89%. ¹H NMR (400 MHz, CDCl₃, 298 K): δ [ppm] = 7.49–7.35 (m, 6H, H_{ar}), 7.34–7.27 (m, 6H, H_{ar}), 7.17 (s, 2H, H_{ar}), 6.23 (s, 2H, NCH₂N), 2.35–2.08 (m, 4H, CH₂CHSi), 2.03–1.69 (m, 8H, CH₂CHSi), 0.30 (s, 12H, SiCH_{3,eq}), -0.54 (s, 12H, SiCH_{3,ax}). ¹³C{¹H} NMR (101 MHz, CDCl₃, 298 K): δ [ppm] = 186.5 (Pt-C_{car}), 140.4 (C_{ar}), 129.0 (C_{ar}), 128.2 (C_{ar}), 124.6 (C_{ar}), 122.4 (C_{im}), 121.2 (C_{im}), 62.3 (NCH₂N), 42.6

(CH₂CHSi, ¹J_{Pt,C} = 161.6 Hz), 35.3 (CH₂CHSi), 1.6 (SiCH_{3,eq}), -2.5 (SiCH_{3,ax}). ²⁹Si{¹H} NMR (79 MHz, CDCl₃, 298 K): δ [ppm] = 2.98 (s, ²J_{Pt,Si} = 40.1 Hz, 4 Si). ¹⁹⁵Pt NMR (85 MHz, CDCl₃, 298 K): δ [ppm] = -5339 (s, Pt, rotamer), -5356 (s, Pt, rotamer), -5363 (s, Pt, rotamer). Elemental analysis calcd (%) for C₃₅H₅₂N₄O₂Pt₂Si₄: C 39.53; H 4.93; N 5.27; found: C 39.53; H 4.91; N 5.17.

2.2.4. *bis-Im*^{Py}(Ptdvtms)₂ (**3**)

Yield: 16%. ¹H NMR (400 MHz, CDCl₃, 298 K): δ [ppm] = 8.54–8.40 (m, 2H, H_{ar}), 8.40–8.19 (m, 2H, H_{ar}), 8.19–7.91 (m, 2H, H_{ar}), 7.64–7.47 (m, 2H, H_{ar}), 7.43–7.24 (m, 2H, H_{ar}), 7.24–7.17 (m, 2H, H_{ar}), 6.38 (s, 2H, NCH₂N, rotamer), 6.17 (s, 2H, NCH₂N, rotamer), 2.44–2.17 (m, 4H, CH₂CHSi), 2.15–1.74 (m, 8H, CH₂CHSi), 0.35 (s, 12H, SiCH_{3,eq}), -0.31 (s, 12H, SiCH_{3,ax}). ¹³C{¹H} NMR (101 MHz, CDCl₃, 298 K): δ [ppm] = 187.6 (Pt-C_{car}), 151.6 (C_{ar}), 148.1 (C_{ar}), 137.7 (C_{ar}), 122.7 (C_{ar}), 121.1 (C_{ar}), 120.5 (C_{ar}), 116.0 (C_{ar}), 63.0 (NCH₂N), 43.1 (CH₂CHSi, ¹J_{Pt,C} = 161.6 Hz), 36.1 (CH₂CHSi), 1.6 (SiCH_{3,eq}), -1.8 (SiCH_{3,ax}, rotamer), -2.5 (SiCH_{3,ax}, rotamer). ²⁹Si{¹H} NMR (79 MHz, CDCl₃, 298 K): δ [ppm] = 3.11 (s, ²J_{Pt,Si} = 41.1 Hz, 4 Si). ¹⁹⁵Pt NMR (85 MHz, CDCl₃, 298 K): δ [ppm] = -5343 (s, rotamer), -5357 (s, rotamer), -5353 (s, rotamer). Elemental analysis calcd (%) for C₃₃H₅₀N₆O₂Pt₂Si₄: C 37.21; H 4.73; N 7.89; found: C 37.10; H 4.66; N 7.79.

2.2.5. *bis-Im*^{Mes}(Ptdvtms)₂ (**4**)

Yield: 79%. ¹H NMR (400 MHz, CDCl₃, 298 K): δ [ppm] = 7.41 (d, ³J_{H,H} = 2.0 Hz, 2H, H_{im}), 6.86 (d, ³J_{H,H} = 2.0 Hz, 2H, H_{im}), 6.83 (s, 4H, H_{ar}), 6.28 (s, 2H, NCH₂N), 2.31–1.67 (m, 12H, CH₂CHSi), 2.22 (s, 6H, *p*-CH₃), 2.00 (s, 12H, *o*-CH₃), 0.26 (s, 12H, SiCH_{3,eq}), -0.69 (s, 12H, SiCH_{3,ax}). ¹³C{¹H} NMR (101 MHz, CDCl₃, 298 K): δ [ppm] = 187.0 (Pt-C_{car}, ¹J_{Pt,C} = 1381.7 Hz), 139.1 (C_{ar}), 136.3 (C_{ar}), 135.1 (C_{ar}), 129.0 (C_{ar}), 123.2 (C_{ar}), 120.6 (C_{ar}), 62.1 (NCH₂N), 42.3 (CH₂CHSi, ¹J_{Pt,C} = 164.6 Hz), 35.9 (CH₂CHSi, ¹J_{Pt,C} = 119.2 Hz), 21.1 (*p*-CH₃), 18.0 (*o*-CH₃), 1.6 (SiCH_{3,eq}), -2.3 (SiCH_{3,ax}). ²⁹Si{¹H} NMR (79 MHz, CDCl₃, 298 K): δ [ppm] = 3.78 (s, ²J_{Pt,Si} = 40.3 Hz, 4 Si). ¹⁹⁵Pt NMR (85 MHz, CDCl₃, 298 K): δ [ppm] = -5390 (s, Pt). Elemental analysis calcd (%) for C₄₁H₆₄N₄O₂Pt₂Si₄: C 42.92; H 5.62; N 4.88; found: C 43.14; H 5.61; N 4.71.

2.2.6. *bis-Im*^{Dipp}(Ptdvtms)₂ (**5**)

Yield: 55%. ¹H NMR (400 MHz, CDCl₃, 298 K): δ [ppm] = 7.43 (d, ³J_{H,H} = 2.0 Hz, 2H, H_{im}), 7.34 (t, ³J_{H,H} = 7.8 Hz, 2H, H_{ar}), 7.15 (d, ³J_{H,H} = 7.8 Hz, 4H, H_{ar}), 6.96 (d, ³J_{H,H} = 2.0 Hz, 2H, H_{im}), 6.37 (s, 2H, NCH₂N), 2.81–2.52 (m, 4H, CH(CH₃)₂), 2.23–1.95 (m, 4H, CH₂CHSi), 1.92–1.68 (m, 8H, CH₂CHSi), 1.21 (bs, 12H, CH(CH₃)₂), 1.05 (d, ³J_{H,H} = 6.8 Hz, 12H, CH(CH₃)₂), 0.28 (s, 12H, SiCH_{3,eq}), -0.42 (bs, 12H, SiCH_{3,ax}). ¹³C{¹H} NMR (101 MHz, CDCl₃, 298 K): δ [ppm] = 187.5 (Pt-C_{car}), 145.9 (C_{ar}), 135.9 (C_{ar}), 129.8 (C_{ar}), 125.5 (C_{im}), 123.7 (C_{ar}), 119.4 (C_{im}), 62.2 (NCH₂N), 42.5 (CH₂CHSi, ¹J_{Pt,C} = 165.6 Hz), 36.3 (CH₂CHSi, ¹J_{Pt,C} = 120.2 Hz), 28.4 (CH(CH₃)₂), 26.3 (CH(CH₃)₂), 22.4 (CH(CH₃)₂), 1.7 (SiCH_{3,eq}), -1.7 (SiCH_{3,ax}). ²⁹Si{¹H} NMR (79 MHz, CDCl₃, 298 K): δ [ppm] = 3.41 (s, ²J_{Pt,Si} = 41.1 Hz, 4 Si). ¹⁹⁵Pt NMR (85 MHz, CDCl₃, 298 K): δ [ppm] = -5382 (s, Pt). Elemental analysis calcd (%) for C₄₇H₇₆N₄O₂Pt₂Si₄: C 45.83; H 6.22; N 4.55; found: C 45.97; H 6.50; N 4.39.

2.2.7. *bis-Im*^{MeTrzDipp}(Ptdvtms)₂ (**6**)

Yield: 50%. ¹H NMR (400 MHz, CDCl₃, 298 K): δ [ppm] = 7.50 (t, ³J_{H,H} = 7.8 Hz, 2H, H_{ar}), 7.44–7.11 (m, 6H, H_{ar}), 7.29 (d, ³J_{H,H} = 7.7 Hz, 4H, H_{ar}), 6.09 (s, 2H, NCH₂N, rotamer), 5.99 (s, 2H, NCH₂N, rotamer), 5.35 (s, 4H, NCH₂C, rotamer), 5.40 (s, 4H, NCH₂C, rotamer), 2.37–1.80 (m, 4H, CH₂CHSi, 4H, CH(CH₃)₂, 4H, CH₂CHSi), 1.14 (d, ³J_{H,H} = 6.8 Hz, 12H, CH(CH₃)₂), 1.09 (d, ³J_{H,H} = 6.8 Hz, 12H, CH(CH₃)₂), 0.34 (s, 12H, SiCH_{3,eq}), -0.28 (s, 12H, SiCH_{3,ax}). ¹³C{¹H} NMR (101 MHz, CDCl₃, 298 K): δ [ppm] = 186.5 (Pt-C_{car}), 146.0 (C_{ar}), 143.1 (C_{ar}), 142.8 (C_{ar}), 132.9 (C_{ar}), 131.1 (C_{ar}), 124.9 (C_{ar}), 124.0 (C_{ar}), 121.9 (C_{ar}), 120.9 (C_{ar}), 61.8 (NCH₂N), 45.3 (NCH₂C), 42.2 (CH₂CHSi, ¹J_{Pt,C} = 158.6 Hz), 36.3

(CH₂CHSi, rotamer), 35.9 (CH₂CHSi, rotamer), 28.5 (CH(CH₃)₂), 24.2 (CH(CH₃)₂), 24.1 (CH(CH₃)₂), 1.5 (SiCH_{3,eq}), -1.6 (SiCH_{3,ax}). ²⁹Si{¹H} NMR (79 MHz, CDCl₃, 298 K): δ [ppm] = 3.11 (s, 4 Si). ¹⁹⁵Pt NMR (85 MHz, CDCl₃, 298 K): δ [ppm] = -5386 (s, Pt, rotamer), -5391 (s, Pt, rotamer), -5396 (s, Pt, rotamer). Elemental analysis calcd (%) for C₅₃H₈₂N₁₀O₂Pt₂Si₄: C 45.67; H 5.93; N 10.05; found: C 45.62; H 6.00; N 9.88.

2.2.8. Platinum hydride test – reaction of **1** with MD^HM

Under atmospheric conditions **1** (20.0 mg, 21.3 μmol, 1.0 eq.), MD^HM (40.5 μL, 149 μmol, 7.0 eq.) and toluene-*d*₈ (0.3 mL) are reacted for 7 min at 72 °C. Analysis by ¹H NMR reveals four major hydride resonances at δ = -4.25 (¹J_{Pt,H} = 640 Hz), -5.16, -7.18 (¹J_{Pt,H} = 632 Hz) and -9.46 ppm (¹J_{Pt,H} = 652 Hz) with ¹⁹⁵Pt satellites.

2.3. Single crystal X-ray structure determination

Single crystals of **1** were obtained by slow evaporation of a concentrated solution in CDCl₃. The same procedure was successfully applied for **n**-pentane solution of **3**. The layering of a solution of either **2** or **4** in DCM with *n*-pentane gave suitable crystals of the respective compounds. Complex **5** was carefully recrystallized from *n*-hexane at 80 °C. Finally, crystals of **6** were obtained by layering a solution thereof in CDCl₃ with *n*-pentane. X-ray crystallographic data was collected on a Bruker D8 Venture single crystal X-ray diffractometer, equipped either with a CMOS detector (κ-CMOS) and a TXS rotating anode or a CMOS detector (Bruker Photon-100) and an IMS micro source, both in conjunction with a Helios optic as setup using the APEX4 software package [52]. The measurement used MoK_α radiation (λ = 0.71073 Å) and was performed on single crystals coated with perfluorinated ether. The crystals were fixed on top of a micromount sample holder and frozen under a stream of cold nitrogen at 100 K. A matrix scan was used to determine the initial lattice parameters. Reflections were corrected for Lorentz and polarization effects, scan speed, and background using SAINT [53]. Absorption corrections, including odd and even ordered spherical harmonics were performed using SADABS [54]. Space group assignment was based upon systematic absences, E statistics, and successful refinement of the structure. The structure was solved by direct methods (SHELXT) with the aid of successive difference Fourier maps and was refined against all data using SHELXL-2015 in conjunction with SHELXLE [55–57]. Hydrogen atoms were calculated in ideal positions as follows: Methyl hydrogen atoms were refined as part of rigid rotating groups, with a C–H distance of 0.98 Å and U_{iso}(H) = 1.5 · U_{eq}(C). Other H atoms were placed in calculated positions and refined using a riding model, with methylene, aromatic, and other C–H distances of 0.99 Å, 0.95 Å, and 1.00 Å, respectively, and U_{iso}(H) = 1.2 · U_{eq}(C). Non-hydrogen atoms were refined with anisotropic displacement parameters. Full-matrix least-squares refinements were carried out by minimizing Σw(F_o² - F_c²)² with the SHELXL weighting scheme [55]. Neutral atom scattering factors for all atoms and anomalous dispersion corrections for the non-hydrogen atoms were taken from *International Tables for Crystallography* [58]. The images of the crystal structures were generated with PLATON [59]. CCDC 2321225–2321230 contain the supplementary crystallographic data for this paper. This data can be obtained free of charge via www.ccdc.cam.ac.uk/data_request/cif, by emailing data_request@ccdc.cam.ac.uk, or by contacting The Cambridge Crystallographic Data centre, 12 Union Road, Cambridge CB2 1EZ, UK; fax: +44 1223 336033.

3. Results and discussion

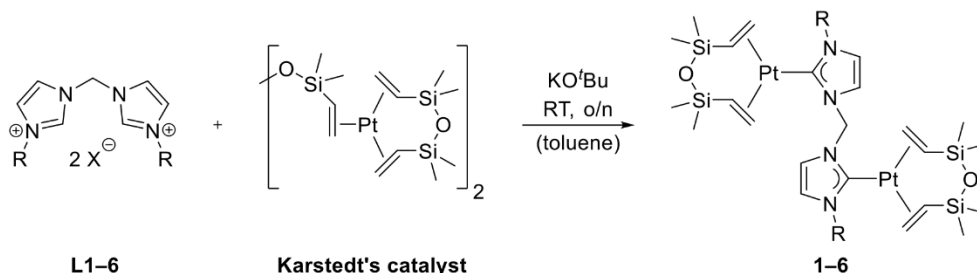
3.1. Synthesis and characterization of bis-NHC(Ptdvtms)₂ complexes (**1**–**6**)

The homobimetallic bis-NHC(Ptdvtms)₂ complexes **1**–**6** are easily accessible by reaction of the respective bis-(imidazolium) salt (**L1**–**L6**,

1.00 eq.) with potassium *tert*-butoxide (3.00 eq.) in the presence of Karstedt's catalyst (2.00 eq. Pt) [37,60,61], based on the synthetic procedure of Markó et al. (Scheme 1) [42]. Solely in the synthesis of **6**, the amount of potassium *tert*-butoxide was reduced to 2.05 equivalents in accordance with the synthesis of a monometallic congener [45] to avoid unintended deprotonation of the triazoles [62,63]. The target compounds, bis-Im^{Me}(Ptdvtms)₂ (**1**, 53%), bis-Im^{Ph}(Ptdvtms)₂ (**2**, 89%), bis-Im^{Py}(Ptdvtms)₂ (**3**, 16%), bis-Im^{Mes}(Ptdvtms)₂ (**4**, 79%), bis-Im^{Dipp}(Ptdvtms)₂ (**5**, 55%) and bis-Im^{MeTrzDipp}(Ptdvtms)₂ (**6**, 50%) were isolated as off-white or colorless, air- and moisture stable compounds. The comparatively low yield of **3** is caused by the low solubility of the desired complex during the filtration step, which was however found to be necessary on top of the washing process to obtain pure product. Improving the yields might be facilitated by the weak base approach in acetone as solvent [64,65], recrystallization [43], precipitation [66,67], or column chromatography [41,68] which have been applied in the purification of related complexes. A potential yield optimization achieved by screening alternative synthetic routes, however, was not the goal of this work.

The chemical composition of **1**–**6** was confirmed by comprehensive NMR spectroscopy (¹H, ¹³C, ²⁹Si, ¹⁹⁵Pt), SC-XRD, and elemental analysis. Complex formation is indicated by vanishing of the carbenoid proton resonances in the ¹H NMR, upfield shifting of the dvtms vinyl protons from δ = 6.17–5.70 ppm for the free molecule to δ = 2.44–1.68 ppm and splitting of the SiMe₂ singlet into two resonances at approximately δ = 0.3 and -0.4 ppm, for equatorial and axial methyl groups, respectively. The ¹³C carbene signal is observed in the narrow range of δ = 187.6–185.8 ppm (Table 1), approving the similar Pt–C bond in the investigated complexes. In addition, a singlet at δ = 3.78–2.98 ppm in the ²⁹Si NMR with ²J_{Pt, Si} = 40.1–41.1 Hz platinum satellites reinforces the claim of (NHC)Pt(dvtms) complex formation. ¹⁹⁵Pt satellites are also observed for the ¹³C resonances at ¹J_{Pt, C, terminal} = 158.6–165.6 Hz and ¹J_{Pt, C, internal} = 119.2–120.2 Hz. These results match with the monometallic Markó-type complexes, for instance **7**, with δ = 184.4 ppm for the carbene signal, ¹J_{Pt, C, terminal} = 165.6 Hz, ¹J_{Pt, C, internal} = 118.2 Hz and for the ²⁹Si resonance δ = 3.57 ppm, with a coupling constant of ²J_{Pt, Si} = 40.3 Hz. This demonstrates a very similar chemical environment for the monometallic and bimetallic systems, which is the prerequisite for a meaningful comparison in catalysis in terms of structure.

The electronic environment of the catalytically active platinum atom is directly probed by highly sensitive ¹⁹⁵Pt NMR, where σ-donor properties of ligands lead to an increase in electron density and π*-acceptor properties of ligands induce the opposite [42,69,70]. The observed resonances range from δ = -5339 for **2** with phenyl wings to -5399 ppm for **1** with methyl wings for the bimetallic complexes and are characteristic for Pt(0) complexes [70]. The ¹⁹⁵Pt shifts of **1** and **6** with aliphatic wingtips at the NHC, although slightly more shielded, resemble their monometallic congeners [45]. Complexes **2**–**5** with terminal aromatic wingtips at the NHC are significantly upfield shifted by Δδ = 22 for **4** and 76 ppm for **3** compared to their monometallic counterparts. This is attributed to the internal methylene bridge that renders these compounds mixed aromatic/aliphatic substituted NHCs and partly introduces a characteristic of Im^{Me}Pt(dvtms) (Im^{Me} = 1,3-dimethylimidazolyl) that exhibits an upfield shifted ¹⁹⁵Pt of δ = -5392 ppm [45]. The most striking feature however is, that for **1**–**3** and **6** three slightly chemically different platinum atoms are observed at room temperature. This behavior was previously reported for asymmetric monometallic (tetrylene)Pt(dvtms) compounds (tetrylene = carbene or silylene) and is induced by a hindered rotation along the Pt–C axis which might result in *syn* and *anti*-conformational isomers [44,46,67,68,71,72]. Our group [46] and Iwamoto et al. [72] investigated the issue for their compounds by variable temperature ¹H NMR from 183 to 363 K and from 203 to 343 K, respectively but no coalescence point was reported. The group of Iwamoto pushed even further and calculated the preference of the *syn* conformation (≠ rotational barrier) by 4.3 kJ·mol⁻¹. Expansion of this concept to incorporate two hindered rotational Pt–C axes is necessary to



Scheme 1. Syntheses of bimetallic complexes 1–6 from Karstedt's catalyst [37,60,61]. 1: R = Me, X⁻ = PF₆⁻; 2: R = Ph, X⁻ = Br⁻; 3: R = 2-Py, X⁻ = PF₆⁻; 4: R = 2,4,6-trimethylphenyl (Mes), X⁻ = Br⁻; 5: R = 2,6-diisopropylphenyl (Dipp), X⁻ = PF₆⁻; 6: R = 4-methylene-1-(2,6-diisopropylphenyl)-1H-1,2,3-triazole (MeTrzDipp), X⁻ = PF₆⁻. Stoichiometry: 1.00 eq. L1–6, 2.00 eq. Pt, 3.00 eq. KO^tBu (2.05 eq. for 6).

Table 1

Chemical shifts of complexes 1–7 as observed by NMR spectroscopy. Main species are highlighted.

Complex	1	2	3	4	5	6	7
Chemical shifts δ [ppm]							
¹³ C _{carbene}	185.8	186.5	187.6	187.0	187.5	186.5	184.4
	-5390	-5339	-5343			-5386	
¹⁹⁵ Pt	-5395	-5356	-5347	-5390	-5382	-5391	-5368 ^a
	-5399	-5363	-5353			-5396	

^a Differs by 29 ppm from the previously reported shift of -5339 ppm [42].

properly describe *bis*-NHC(Pt(dvtms))₂ complexes 1–6 (Fig. 2). This requires three permutations with *syn/syn* as the energetically most favorable according to the SC-XRD results (*vide infra*). Evaluation of the ratio of rotamers is not presented due to improper resolution of the NMR signals. Variable temperature ¹H NMR studies were performed from 233 K to 363 K in steps of 10 K for 5 and 6 to elucidate conformational dynamics (ESD). Complex 5 was selected as it exhibits a clean singlet in the ¹⁹⁵Pt NMR and is sterically more hindered than 4, where also a singlet is observed. It is expected that an increased steric bulk should enhance conformational effects, making them easier to monitor. In contrast, 6 was selected as distinct rotamers are present at room temperature, and, on top of the internal methylene bridge, the external methylene bridges that connect the triazoles to the central scaffold also serve as a probe for conformational dynamics. Analysis of the VT NMR data of 5 reveals the splitting of the NCH₂N bridge into two individual singlets at δ = 5.90 and 5.53 ppm at 233 K. Also, the axial methyl groups of the dvtms moiety separate into singlets at δ = 0.13 and -0.24 ppm at 233 K. Both signal groups coalesce at about 268 K with $\Delta\nu$ = 148 Hz, calculating ΔG^\ddagger = 52.5 kJmol⁻¹ for both barriers using a derivation of the Eyring equation [73,74]. This indicates that these dynamics are linked to one another. Values of similar magnitude were reported for rotation along a metal–NHC bond [75–77]. Lastly, the equatorial methyl groups of dvtms start to separate at 233 K into peaks at δ = 0.77 and 0.69 ppm. The axial methyl groups of dvtms are generally further split as they point towards the NHC ligand and hence their separation is more easily detected, while

the equatorial methyl groups, that point away from the complex, are not that well unraveled [44,72]. The VT NMR data of 6 reveals a more complex behavior, where both the equatorial and axial methyl groups of dvtms split into three, narrowly parted signals each at 233 K at δ = 0.83, 0.81, 0.80 and 0.10, 0.08 and 0.07 ppm, respectively. This contradicts the previously stated findings and is attributed to the introduction of additional degrees of freedom in the form of the methylene bridge on the outer wingtip of the complex scaffold. Coalescence of both peak sets into two singlets is observed at roughly 298 K. At 363 K two singlets at δ = 6.10 and 5.31 ppm in the ratio of 2:4 indicate chemically equivalent protons in each case of the internal and external methylene bridge(s), respectively. The internal methylene bridge exhibits a T_c = 343 K and disintegrates into three peaks at low temperatures, which might be explained by the conformational isomers of Fig. 2. For the outer methylene bridges two consecutive coalescence points are observed at T_c = 333 and 308 K, splitting each peak into two successors repeatedly. Contrary to expectations, the sterically more hindered specimens 4 and 5 don't impose a barrier on the Pt–C rotation at room temperature, while 1–3 are divided into rotamers. This hints at an additional factor that – so far – remains unaccounted for.

Structure elucidation of 1–6 by single crystal XRD reveals coordination of the platinum atoms in characteristic [45,46,66,68,78–80], distorted trigonal planar fashion by the carbene and vinyl groups of the dvtms moiety (Fig. 3). The dvtms groups invariably crystallize in strict *syn/syn* orientation, pointing away from each other, thereby reducing

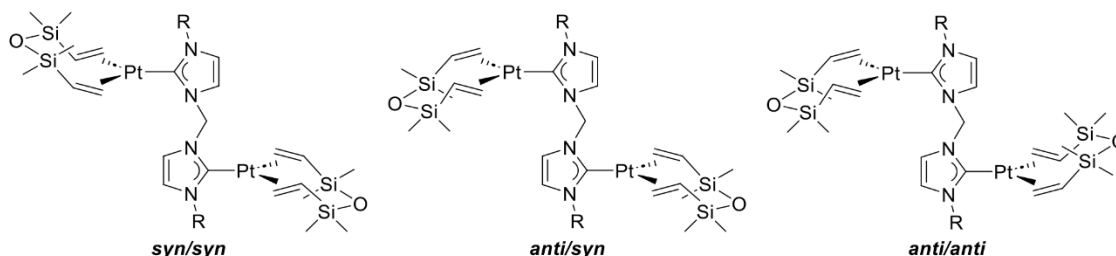


Fig. 2. Conformational isomers produced by hindered rotation along Pt–C_{carbene} axes. *Syn*: the dvtms moiety is pointing towards the NHC wingtip R. *Anti*: the dvtms moiety is pointing away from the NHC wingtip R.

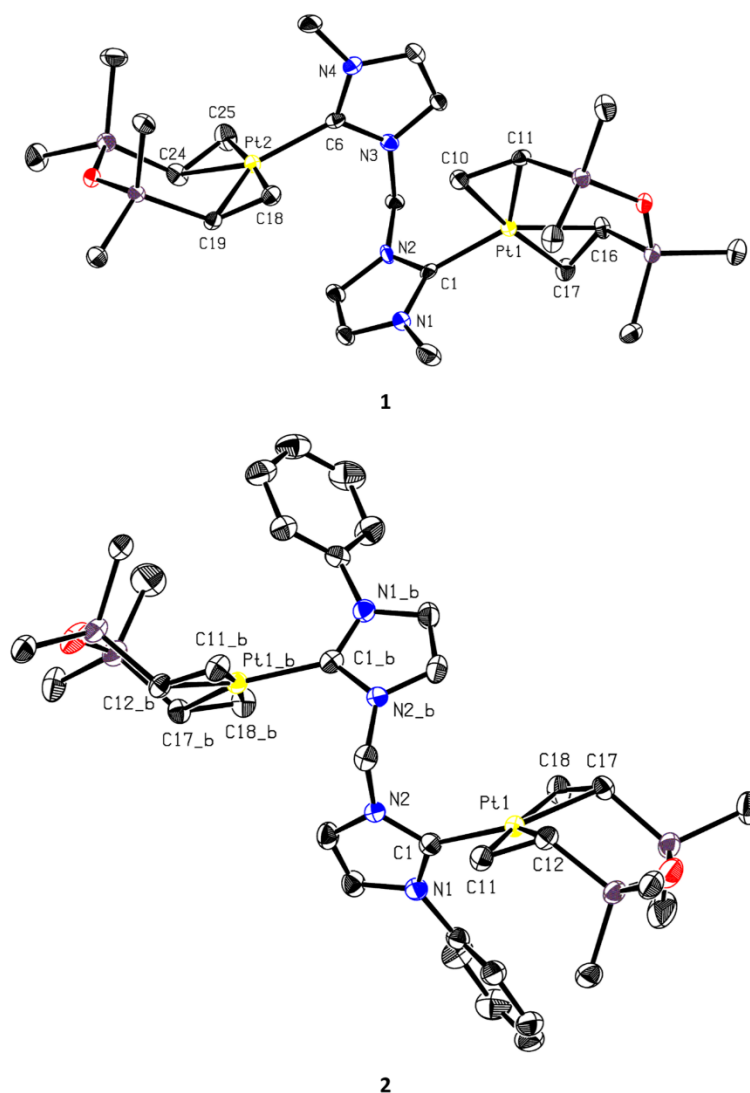
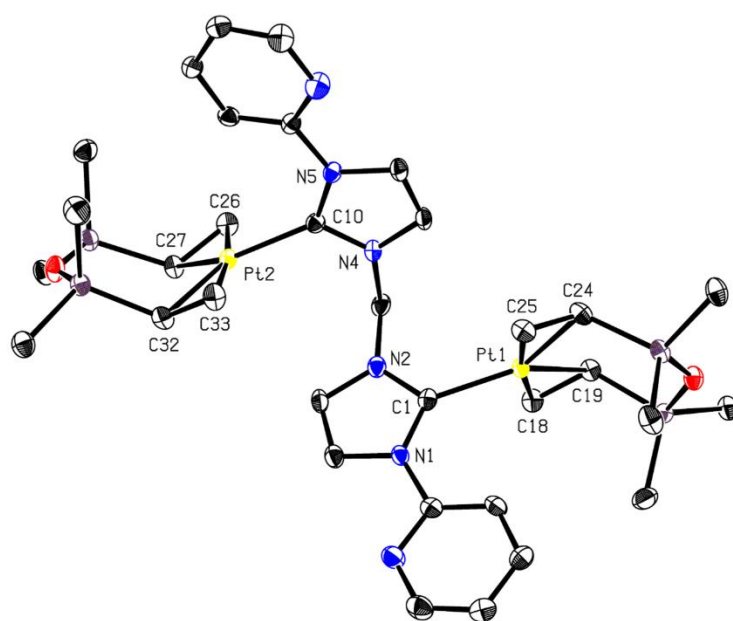


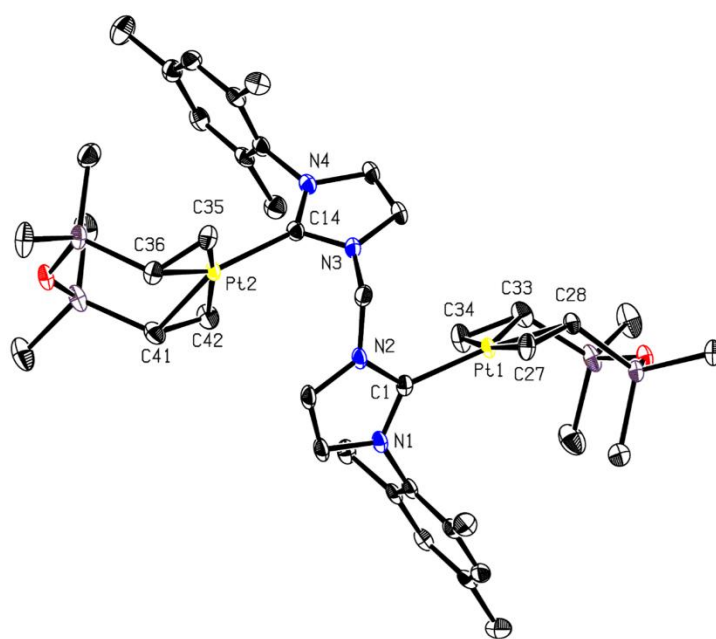
Fig. 3. ORTEP style molecular structure representation of complexes 1–6. Thermal ellipsoids are given at a 50% probability level. Hydrogen atoms are omitted for clarity. One molecule of co-crystallized dichloromethane per unit cell is omitted for 2. Only the mainly occupied site is depicted for the disordered *iso*-propyl group in 5.

steric strain. Therefore, only the most energetically favorable conformation is observed in the crystalline state, which may also be due to packing, while other rotamers may prove viable in solution. The supposedly hemilabile *N*-donors in **3** and **6** are oriented in the opposite direction to the platinum centers, which rules out an intramolecular interaction between the two groups in the solid state. This is consistent with monometallic Markó-type complexes that also contain pyridine or triazole wingtips at the NHC, where no Pt–N interaction was observed either [45]. The main geometric parameters of the bimetallic complexes are summarized in Table 2 and compared to **7** as representative of monometallic complexes. The Pt–C_{carbene} bond lengths lie in the narrow range of 2.022 Å for the sterically least hindered **1** to 2.054 Å for **6** with bulky, though admittedly flexible NHC wingtips. The geometric parameters of the trifold ligated platinum centers are consistent with their monometallic relatives, which further emphasizes the similarity of the

bimetallic and monometallic complexes. However, torsion of the dtvms vinyl groups is generally more pronounced in the bimetallic system, culminating at $-14.7(4)^\circ$ for **5** in this study. This value has so far only been exceeded once in a report by Pietraszuk *et al.* where an extremely bulky ligand forces a distortion of $17.2(6)^\circ$ [79]. Although bound to the identical main scaffold, the Pt–Pt distances vary in the range of 5.787 Å in **1** to 7.004 Å in **6**. For complexes **2**–**5**, which contain aromatic NHC wingtips, the Pt–Pt distance correlates with the Pt–C_{carbene} bond length, indicating that both parameters are affected by steric strain in the same way. Thus, the ideal metal–metal distance for bimetallic catalysis of 3.5–6 Å [19] is partially exceeded but could be realized after the loss of the dtvms moieties and due to conformational dynamics in solution. Interaction of the substrate with both platinum atoms or binding of two reactants in close proximity might still prove beneficial, even if there is no direct interaction between the platinum atoms.



3



4

Fig. 3. (continued).

3.2. Catalytic hydrosilylation of alkenes

3.2.1. Catalytic reaction of oct-1-ene with MD^HM

The performance of the bimetallic catalyst precursors 1–6 was evaluated and compared to 7 as a reference system for monometallic Markó-type complexes in the catalytic hydrosilylation reaction of oct-1-

ene and MD^HM at 72 °C. The bulky MD^HM mimics a PMHS (polymethylhydrosiloxane) in this by Markó *et al.* established benchmark reaction (≡ A, Table 3) [40,41], which finds widespread application in research [45,46,66,81]. The target compound M₂D-oct is formed at very good to excellent yields of up to 98% with respect to the alkene. Linked byproducts are observed at total yields < 1% and are therefore neglected

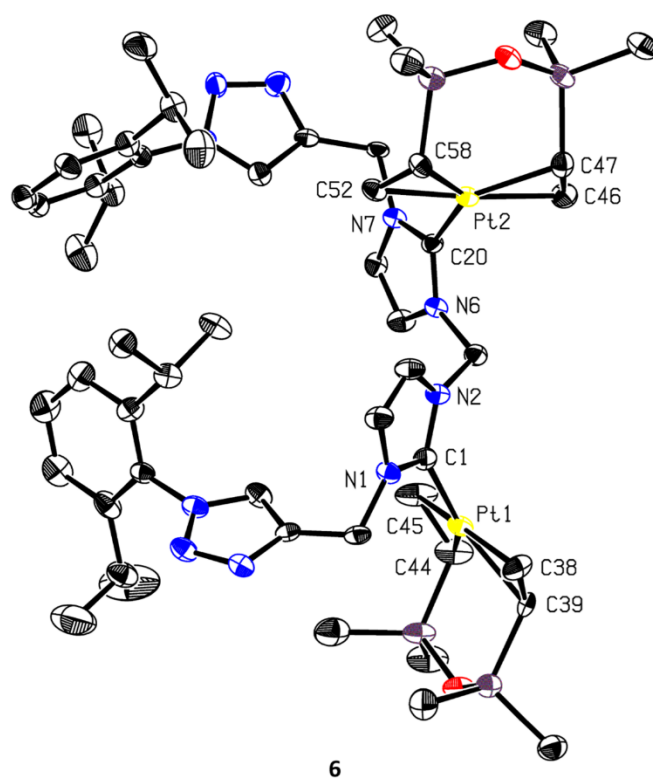
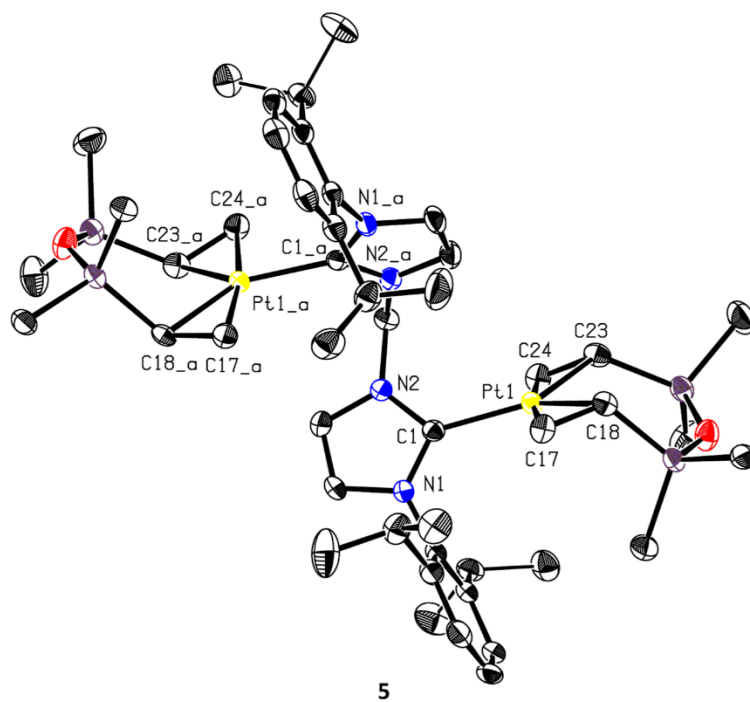


Fig. 3. (continued).

Table 2

Selected crystallographic data of bimetallic complexes (1–6) in comparison to literature known complex 7 [42].

Complex	1	2	3	4	5	6	7 ^b
Bond lengths (Å)							
Pt–C _{carbene}	2.027(5)	2.050(4)	2.050(3)	2.044(3)	2.044(4)	2.054(7)	2.046(4)
Pt–C _{C=C} ^c	2.022(5)		2.042(4)	2.039(3)		2.039(6)	
	2.124(4)	2.133(4)	2.120(4)	2.114(3)	2.124(4)	2.147(6)	2.141(5)
Pt–C _{C=C} ^d	2.110(4)	2.123(4)	2.133(4)	2.129(3)	2.106(4)	2.116(7)	2.138(5)
	2.127(5)		2.138(4)	2.122(3)		2.123(7)	
Pt–C _{C=C} ^d	2.120(6)		2.137(5)	2.130(3)		2.103(7)	
	2.143(5)	2.141(4)	2.140(4)	2.141(3)	2.134(4)	2.151(7)	2.146(4)
C _{C=C} –C _{C=C} ^e	2.121(5)	2.143(4)	2.137(4)	2.142(3)	2.139(4)	2.141(6)	2.148(5)
	2.142(5)		2.140(4)	2.133(3)		2.151(7)	
C _{C=C} –C _{C=C} ^e	2.139(5)		2.147(4)	2.148(3)		2.145(7)	
	1.420(7)	1.436(6)	1.426(5)	1.428(4)	1.429(6)	1.428(9)	1.437(7)
Pt–Pt	1.447(7)	1.429(6)	1.427(6)	1.426(4)	1.425(6)	1.432(11)	1.419(7)
	1.438(7)		1.435(5)	1.433(4)		1.439(9)	
Angles (°)	1.442(8)		1.435(5)	1.427(5)		1.426(9)	
	5.7874(4)	6.7208(8)	6.5177(6)	6.2245(5)	6.396(1)	7.0041(8)	n.a.
N _{im} –CH ₂ –N _{im}	113.4(4)	113.0(4)	114.2(4)	113.8(2)	112.9(4)	112.5(5)	n.a.
tilt angle θ	84.12	70.81	83.32	69.42	61.21	66.11	64.67
NHC–Pt(dvtms)	82.05		78.03	72.80		74.82	
Torsion (°)							
C _{C=C} –C _{C=C} –C _{C=C} –C _{C=C}	5.9(5)	0.0(4)	8.2(4)	–3.8(3)	–14.7(4)	–1.1(7)	4.3(5)
	4.3(5)		–3.4(4)	–4.0(3)		–6.6(7)	

^b Data was extracted from CCDC 275,306 [42].^c Denotes the distance to the terminal carbon.^d Denotes the distance to the internal carbon.^e Denotes the distance between the two olefinic carbons of dvtms.

Table 3

Model reaction A: Catalytic formation of product (M₂D-oct) by hydrosilylation of oct-1-ene (1.0 eq., 2.024 mmol, 0.5 M) with MD^HM (1.0 eq., 2.024 mmol, 0.5 M) in *p*-xylene at 72 °C with 50 ppm [Pt] and *n*-decane (1.518 mmol) as internal standard. Analysis by GC-FID.

Catalyst	Y(M ₂ D-oct) [%]	X(oct-1-ene) [%]	X(MD ^H M) [%]	S [%] ^f	Y(isomerization) [%] ^g	TOF [h ⁻¹] ^h
1	36	43	37	85	2	5000 ⁱ
2	90	92	88	98	3	48,000
3	22	27	23	80	1	12,000 ⁱ
4	90	94	90	96	3	38,000
5	95	99	93	96	3	43,000
6	52	56	51	92	2	5000 ⁱ
7	91	98	90	92	4	17,000

Y = yield. X = conversion. S = selectivity.

^f Selectivity regarding oct-1-ene at t = 6 h; Selectivity regarding MD^HM ≥ 97%.^g Sum of C₈ isomers at t = 6 h. *n*-Octane is included herein.^h TOF of oct-1-ene calculated at the steepest slope.ⁱ Yield used for calculation.

(S_{MDHM} ≥ 97%). However, the catalysts compete for the minimization of C₈ byproducts that are formed by isomerization and reduction of oct-1-ene.

Equimolar amounts of oct-1-ene and MD^HM are reacted under air at 72 °C in the presence of 50 ppm [Pt]. In the case of the bimetallic compounds 1–6, this entails loading the respective complexes at 25 ppm to account for both platinum atoms in them. For 7 on the other hand, loading is fixed at 50 ppm complex, which equals the platinum concentration due to the monometallic nature. This allows comparison of catalytic performance in relation to the amount of platinum sites independent of the catalyst precursor. The reactions were monitored by GC-FID using *n*-decane as an internal standard. The observed time-yield kinetics (Fig. 4) exhibit sigmoidal behavior due to an initiation period in which the active catalyst is formed by hydrosilylation of the dvtms ligand, which is the rate-determining step [42].

This characteristic is most pronounced for 7 and results in < 1%

product formation after 20 min. Classical, monometallic Markó-type (NHC)Pt(dvtms) complexes are therefore described as “slow-release” precursors of catalytically active platinum species [42], a drawback that limits the performance of these complexes and is surpassed by bimetallic complexes 1–6. For instance, a yield of 37% M₂D-oct is obtained for 4 after 20 min, both compounds being related and containing mesityl wingtips at the NHC(s). However, the overall catalytic performance also depends on the inherent activity and stability of the active species. The latter appears to be poor for 1, 3, and 6, as is indicated by flattening of the kinetic curves at yields < 10% in a logarithmic form. Previously, pyridine and triazole wingtips at the NHC moiety proved detrimental in monometallic (NHC)Pt(dvtms) complexes and was attributed to the stabilization of a Pt(II) species [45]. However, these *N*-donor-containing ligands prevent catalysis for bimetallic systems at a different magnitude. An inflection point, caused by increasing activity, around the 1 h mark for 1 and 6 implies another transformation. Investigation and discussion

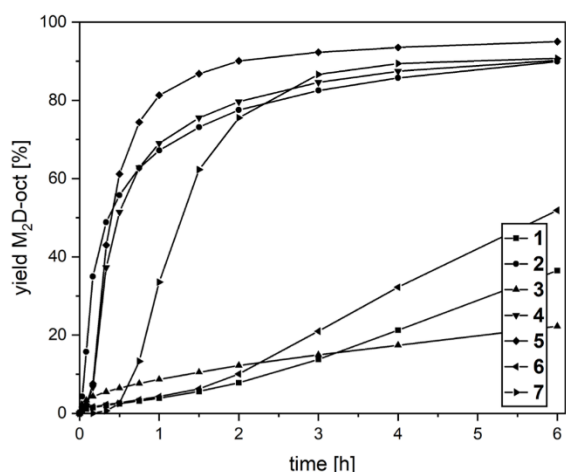


Fig. 4. Time dependent catalytic formation of product (M_2D -oct) by hydrosilylation of oct-1-ene (1.0 eq., 2.024 mmol, 0.5 M) with MD^{H^M} (1.0 eq., 2.024 mmol, 0.5 M) in *p*-xylene at 72 °C with 50 ppm [Pt] and *n*-decane (1.518 mmol) as internal standard. Analysis by GC-FID.

of the deactivation and transformation reactions are presented below. At this point a discrepancy of calculated selectivity ($S = Y \cdot X^{-1}$) and observed byproduct formation for 1, 3, and 6, which yield the least desired product is worth mentioning. This finding was however confirmed by a fourfold determination for each complex. The cause of this might be the minimal evaporation of oct-1-ene, which has the lowest boiling point in the catalysis mixture, and the resulting error propagation since no additional byproduct was identified by GC-FID. Addressing the difference of 4 and 7 again, not only does initiation occur faster for 4, but also the turnover frequency (TOF) of 38,000 h^{-1} more than doubles the TOF of 17,000 h^{-1} for 7. The highest TOF in this study is observed for 2 at 48,000 h^{-1} with no distinct induction period, just as for the monometallic $Im^{Me}Pt(dvtms)$, where a TOF of 31,000 h^{-1} was achieved [45]. The monometallic relative of 2, $Im^{Ph}Pt(dvtms)$, falls short at a TOF of 39,000 h^{-1} and a selectivity of 96% compared to 98% for 2, but forms more M_2D -oct at a yield of 94% (2: $Y = 90\%$) [45]. Contradicting our expectations, 4 and 5 exhibit virtually the same induction period, while in the case of the monometallic relatives $Im^{Mes}Pt(dvtms)$ and $Im^{DIPP}Pt(dvtms)$, the steric bulk of the later prolongs the induction period by 1/3 [41]. With the highest yield of 95% and a TOF of 43,000 h^{-1} at $S = 96\%$, 5 emerges with the best performance in the investigated series.

3.2.2. Catalytic reaction of vinylsiloxane MM^{VI} with MD^{H^M}

The hydrosilylation of MM^{VI} with MD^{H^M} is selected to simulate industrial-relevant three-dimensional silicone network formation by addition-cure crosslinking using a platinum catalyst ($\equiv B$) [82,83]. Experiments were carried out at 100 °C with a loading of 100 ppm [Pt] for direct comparison to the performance of the monometallic relatives of 1–6 [45]. The results are summarized in Table 4, showing excellent performance of the bimetallic complexes (reaction kinetics are provided in the ESI).

The highest yield of the target product $MM(C_2H_4)DM_2$ is achieved by 1, namely 75%, contradicting the results in A (*vide supra*), where poor performance was realized, due to deactivation. This is attributed to the raised reaction temperature of 100 °C compared to 72 °C in A, which supports the presumed transformation in A that is accompanied by an increase in activity. A TOF of 51,000 h^{-1} is calculated for 1, slightly exceeding 50,000 h^{-1} of $Im^{Me}Pt(dvtms)$ under equal conditions, which signals that the reaction is not limited by diffusion, even though two platinum atoms are linked in close proximity. Complex 2 is by far the most active with a TOF of 78,000 h^{-1} , outperforming the monometallic relatives by over 50%. Substitution of the phenyl wingtips in 2 with pyridine in 3 impairs catalytic performance significantly to a TOF of 34,000 h^{-1} . This detrimental effect of *N*-donors was previously reported for monometallic Markó-type (NHC)Pt(*dvtms*) complexes and is attributed to excessive stabilization of the Pt(II) state as mentioned above [45]. Lowering the catalyst loading and the temperature might prove beneficial in more clearly distinguishing the kinetics of 1–6 but was not pursued in the work presented here.

3.2.3. Comparison of a monometallic (7) and bimetallic (4) complex

In the following, a detailed comparison of the homobimetallic platinum system with the classical monometallic system is presented, with the mesityl-containing complexes 4 and 7 serving as representatives of their respective classes and A as benchmark reaction (Table 5). The temperature is fixed at $T = 72$ °C, while the [Pt] loading is set to 100, 50, 25, and 10 ppm and even as low as 5 ppm for 7. At a loading of 100 ppm, 4 yields 91% of the main product with a TOF of 42,000 h^{-1} which is calculated based on the recorded reaction kinetics (see ESI). Lowering the catalyst concentration to 50 and subsequently to 25 ppm yields 90 and 89% product while maintaining catalyst activity at TOFs of 38,000 and 42,000 h^{-1} , respectively. The difference in TOFs is negligible in terms of uncertainty and indicates that catalytic activity is decoupled from the catalyst loading. This is however contradicting experiments at 10 ppm of 4, where the TOF is reduced to half to 20,000 h^{-1} . Complex 7 on the other hand increases activity while catalyst loading is reduced. At 100 ppm a TOF of 11,000 h^{-1} is calculated that continuously improves and peaks at 33,000 h^{-1} at the lowest investigated loading of 5 ppm. This finding is attributed to catalytic overloading at higher catalyst

Table 4

Model reaction B: Catalytic formation of product ($MM(C_2H_4)DM_2$) by hydrosilylation of MM^{VI} (1.0 eq., 2.024 mmol, 0.5 M) with MD^{H^M} (1.0 eq., 2.024 mmol, 0.5 M) in *p*-xylene at 100 °C with 100 ppm [Pt] and *n*-decane (1.518 mmol) as internal standard. Analysis by GC-FID. Evaluation of selected byproducts is included in the ESI.

Catalyst	Y($MM(C_2H_4)DM_2$) [%]	X(MM^{VI}) [%]	X(MD^{H^M}) [%]	S(MM^{VI}) [%]	S(MD^{H^M}) [%]	TOF [h^{-1}] ^j
1	75	97	97	77	77	51,000
2	71	97	98	72	72	78,000
3	72	92	91	79	80	34,000
4	71	98	99	73	72	46,000
5	73	97	99	75	73	52,000
6	72	91	89	80	82	51,000
7	68	94	94	72	72	9000

Y = yield. X = conversion. S = selectivity. All data given at $t = 6$ h.

^j TOF of MM^{VI} calculated at the steepest slope.

Table 5

Catalytic hydrosilylation of oct-1-ene with MD^HM at varying temperature and catalyst loading. The corresponding reaction kinetics are included in the ESI.

Catalyst	T [°C]	Catalyst loading [ppm] ^k	Y(MM(C ₂ H ₄)DM ₂) [%]	TOF [h ⁻¹] ^l
4	72	100	91	42,000
4	72	50	90	38,000
4	72	25	89	42,000
4	72	10	59	20,000
4	62	50	86	29,000
4	52	50	84	12,000
7	72	100	94	11,000
7	72	50	91	17,000
7	72	25	91	26,000
7	72	10	82	31,000
7	72	5	62	33,000
7	62	50	78	6000
7	52	50	45	3000

Yields (Y) after 6 h.

^k denotes the loading of platinum.

^l TOF of oct-1-ene calculated at the steepest slope.

concentrations and emphasizes the inherently different nature of the investigated systems. To examine the thermal dependence of the catalysts, the temperature is lowered in steps of 10 K to 62 and 52 °C, while the platinum loading is fixed at 50 ppm. The bimetallic complex **4** achieves yields of 86 and 84% at TOFs of 29,000 and 12,000 h⁻¹ at 62 and 52 °C, respectively. This preserves 76 and 35% of the activity at standard conditions as the temperature is lowered. This retained activity to original activity ratio is significantly lower for **7**, where TOFs of 6000 and 3000 h⁻¹ reveal that merely 32 and 18% of the activity at standard conditions are preserved. This is rationalized in terms of the initiation process, which was determined as the rate-determining step for monometallic Markó-type complexes [42]. The induction period of **7** is considerably longer compared to **4** (Fig. 4) and is consequently more strongly affected as temperature is decreased. To summarize, the performance of **7** exceeds **4** at low catalyst loadings, while **4** is superior at low temperatures.

3.2.4. Addition of fresh reactants

The initiation behavior is further investigated by the addition of fresh reactants (equimolar ratio of oct-1-ene and MD^HM) after completion of a standard experiment (see ESI for kinetics and detailed experimental). Conversion of the second batch of reactants starts immediately without an induction period, demonstrating that **4** and **7** are still catalytically active. TOFs of 20,000 and 14,000 h⁻¹ are calculated (3 to 10 min) for **4** and **7**, respectively. The decrease in activity is – at least in part – attributable to the dilution of educts from 0.5 to 0.4 M due to their repeated addition. However, **4** only retains 53% activity, while **7** performs at 82%. This may be due to the continuous activation of **7** upon the addition of fresh reactants, due to the inherently slow initiation behavior of the monometallic complex. Previously, Im^{Cy}Pt(dvtms) was repeatedly subjected to fresh reactants under similar conditions [84]. The absence of the initiation period in follow-up runs was here also observed, but the TOF increased ninefold, while a third addition raised the activity 16 times compared to the first experiment. The disagreement with the herein presented results might be attributable to the different characteristics of the catalysts and applied methods.

3.2.5. Pre-catalytic reaction of complexes and MD^HM

Since it is assumed that the initiation process of Markó-type complexes proceeds by partial dissociation of the dvtms chelate and subsequent hydrosilylation of the latter by two SiH entities [42], model reaction A was modified with the objective of comparing “true” TOFs of **4** and **7**. The respective complex is reacted with MD^HM for defined durations t_{SiH} in the presence of solvent (*p*-xylene) and internal standard (*n*-decane) prior to the addition of oct-1-ene that launches catalysis (≡

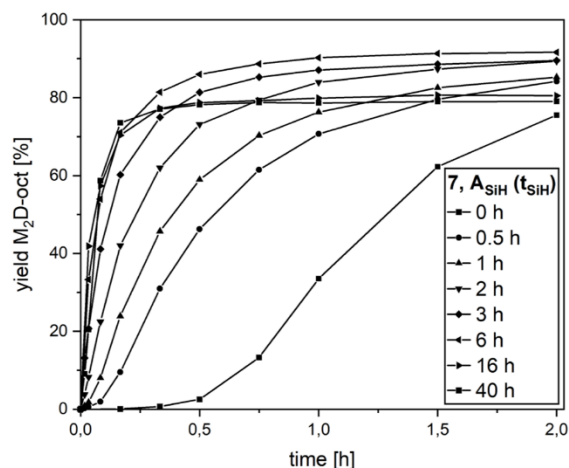


Fig. 5. A_{SiH} – Preceding reaction of **7** with MD^HM for defined durations t_{SiH}. Catalysis is launched upon addition of oct-1-ene. Reaction conditions: oct-1-ene (1.0 eq., 2.024 mmol, 0.5 M) and MD^HM (1.0 eq., 2.024 mmol, 0.5 M) in *p*-xylene at 72 °C with 50 ppm [Pt] and *n*-decane (1.518 mmol) as internal standard. Analysis by GC-FID.

A_{SiH}). As expected, the induction period is significantly shortened after exposing **7** to MD^HM for 0.5 h (Fig. 5), but disappears completely at t_{SiH} = 3 h, transforming the sigmoidal shape to a logarithmic curve. Activity accumulates to a TOF = 220,000 h⁻¹ at t_{SiH} = 6 h, a 13 times increase compared to the performance of **7** in A (Table 6). The selectivity and yield remain virtually unchanged at 91 and 92%, respectively, compared to 92 and 91% in A. At t_{SiH} = 16 and 40 h a notable decrease in yield to 81 and 79%, respectively, can be observed, accompanied by S = 82 and 81%. This indicates a transformation of the catalytically active species and is supported by TOFs of 296,000 h⁻¹ and a decline to 174,000 h⁻¹ after exposure of **7** to MD^HM for 16 and 40 h, respectively. The drop in activity at t_{SiH} = 40 h also transforms the kinetic curve back into a sigmoidal shape, reintroducing an initiation phase. Potential loss of the NHC moiety and platinum agglomeration might form colloids where reactivation due to the “oxygen effect” occurs [85,86]. This is further investigated by mercury poisoning experiments that are presented below.

Contrary to our expectations **4** shows inverse behavior to **7** in A_{SiH} (Fig. 6). Exposure of **4** to MD^HM before catalysis results in a prolonged induction period and activity loss, which is most pronounced at t_{SiH} = 6 h. The selectivity is slightly reduced to 92% and activity is cut down to 7000 h⁻¹, compared to 96% and 38,000 h⁻¹ in A, respectively. This indicates deactivation by transformation into another species. However, at longer t_{SiH} higher activities are observed again with TOFs of 25,000 and 79,000 h⁻¹ after 16 and 40 h, respectively, which is only a fraction of the activity of **7**. Interestingly, the selectivity remains at 92% and is even slightly enhanced to 95% at t_{SiH} = 40 h, which matches – within the

Table 6

Catalyst	t _{SiH} [h]	Y(M ₂ D-oct) [%]	S [%] ^m	TOF [h ⁻¹] ⁿ
7	6	92	91	220,000
7	16	81	82	296,000
7	40	79	81	174,000
4	6	48	92	7000
4	16	85	92	25,000
4	40	90	95	79,000

Y = yield. S = selectivity.

^m Selectivity regarding oct-1-ene at t = 2 h.

ⁿ TOF of oct-1-ene calculated at the steepest slope.

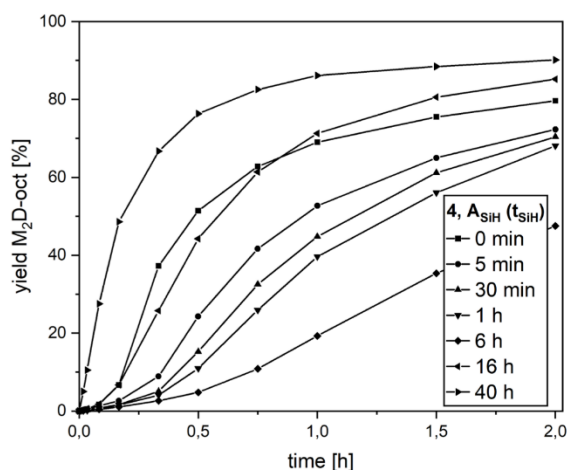


Fig. 6. A_{SiH} – Preceding reaction of **4** with MD^{HM} for defined durations t_{SiH} . Catalysis is launched upon addition of oct-1-ene. Reaction conditions: oct-1-ene (1.0 eq., 2.024 mmol, 0.5 M) and MD^{HM} (1.0 eq., 2.024 mmol, 0.5 M) in *p*-xylene at 72 °C with 50 ppm [Pt] and *n*-decane (1.518 mmol) as internal standard. Analysis by GC-FID.

margin of error – $S = 96\%$ under standard conditions. This indicates, that the Pt–C bond remains undamaged and an interim species is formed upon exposure of **4** to MD^{HM} . In this context, di- μ -hydrido platinum dimers **D** and **E** (Fig. 7) were reported to form in the presence of silanes [84,87]. The structures of both species were unequivocally resolved by SC-XRD. Catalytic evaluation of **D** revealed a longer initiation period and lower activity compared to $Im^{Cy}Pt(dvtms)$, which matches the behavior of **4** in the A_{SiH} method. To investigate this issue, **1** (1.0 eq.) is reacted with MD^{HM} (7.0 eq.) at 72 °C for 7 min. Analysis by 1H NMR reveals four major hydride resonances with ^{195}Pt satellites at $\delta = -4.25$ ($^1J_{Pt,H} = 640$ Hz), -5.16 , -7.18 ($^1J_{Pt,H} = 632$ Hz) and -9.46 ppm ($^1J_{Pt,H} = 652$ Hz). Chemical shifts and coupling constants are consistent with platinum hydride complexes, among them μ -hydrido platinum dimers [88–96]. Attempts to isolate or crystallize the formed species remained unsuccessful. Based on this, di- μ -hydrido-bridged species **C** is postulated, whose formation is favored due to the proximity of two platinum atoms in the bimetallic complex. This also serves as an explanation of the inferior performance of **1** in A_{SiH} , which indicates that the sterically least occupying methyl wingtips at the NHCs cannot prevent the formation of **C** even under standard catalytic conditions. In this context and also relevant for **7** in A_{SiH} , the di- μ -hydrido-bridged $Im^{Cy}Pt$ species of Markó *et al.* was obtained under relatively mild conditions with five equivalents silane at 80 °C for 10 h. Harsher conditions of 20 equivalents silane and

100 °C for 15 h however facilitate conversion of $Im^{Dipp}Pt(dvtms)$ into tricoordinate *bis*-(silyl)platinum(II)-NHC complex **F** that remains stable in the presence of excess silane even under ambient conditions [97]. Especially in the hydrosilylation of alkynes, **F** proves significantly more active and selective than the parent $Im^{Dipp}Pt(dvtms)$ complex [98]. Following this model, further conversion of **C** into a silyl species appears reasonable and explains the increase in activity [99,100]. In addition, the initial activation of *dvtms* is of particular interest as it was reported that the catalyst activation pathway for mono- and bimetallic complexes might be fundamentally different. Investigation of monometallic (NHC) Rh(COD) and bimetallic *bis*-NHC(RhCOD)₂ complexes revealed hydrogen transfer from one to another COD moiety that forms cycloocta-1,3,5-triene and opens up a free coordination site at the site with reduced cyclooctene [34]. This pathway is significantly faster than the dissociation of COD for the monometallic complex and increases catalytic performance. Work is currently in progress to unveil the origin of the synergistic effect and to elucidate the transformations of bimetallic *bis*-NHC($Pt(dvtms)$)₂ complexes, especially their induction period.

3.2.6. Mercury(0) poisoning experiments

The pre-catalytic reaction of **7** with MD^{HM} (*vide supra*) raised the question of (NHC)Pt stability and clearly demanded a more in-depth examination, as colloid formation for similar complexes has been assumed in previous reports [81,101]. The catalyst poisoning experiment with elemental mercury is commonly used to distinguish homogeneous molecular catalysis from heterogeneous catalysis [102,103] and is applied to the monometallic (**7**) and bimetallic (**4**) systems. The method is based on the assumption that Hg(0) will amalgamate Pt(0) clusters/colloids and nanoparticles and render them inactive. However, wrong conclusions might be drawn as it was shown that there are molecular complexes that are reactive to Hg(0) and a proper methodology is crucial to obtain meaningful results [102–106]. To overcome these issues 1500 equivalents of Hg(0) with regards to platinum are used and intimate contact of Hg(0) with the reaction mixture is ensured by raising the stirring frequency from 500 to 1400 rpm. Also, mercury is only added to the reactor, after educt conversion is higher than 10%, which results in a bending of the kinetic curve if Hg(0) influences the catalyst. On top of this, the mercury poisoning experiment is conducted under standard conditions (**A**) and after 40 h of pre-reaction of **4** and **7** with MD^{HM} . In this study, no visual discoloration of the reaction mixtures was observed, which would indicate the formation of colloidal platinum

Table 7

Results of mercury poisoning experiments (1500 eq. Hg/Pt) and observed final yields in parentheses.

Catalyst	A	A_{SiH} (40 h)
4	Negative (90%)	Negative (88%)
7	Negative (94%)	Positive (56%)

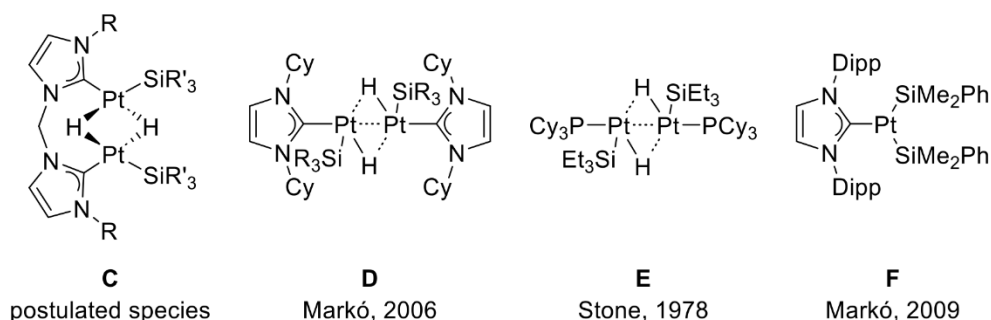


Fig. 7. Postulated di- μ -hydrido complex **C**. Platinum dimer **D** of Markó *et al.* with $SiR_3 = MDM$ [84]. Platinum dimer **E** of Stone *et al.* [87]. *Bis*-(silyl)platinum(II)-NHC complex **F** of Markó *et al.* [97].

species but does not necessarily rule out their existence. There is no abnormality in the kinetics of the mercury test of **4** in either **A** or A_{SiH} (40 h) as is expected from the maintained selectivities (Table 7, kinetics in ESI). While no poisoning is observed for **7** under standard conditions (**A**), $\text{Hg}(0)$ completely deactivates the catalyst in A_{SiH} (40 h). This matches with the behavior of **7** in A_{SiH} (40 h), without mercury addition, where a decrease in selectivity and activity was recorded, which even leads to the formation of an induction period. These independent results indicate the formation of colloidal platinum from **7** in the presence of $\text{MD}^{\text{H}}\text{M}$ after 40 h, while **4** is intermediately stabilized as di- μ -hydrido complex.

4. Conclusion

A series of six homobimetallic *bis*-NHC(Ptdvtms)₂ complexes **1–6** was prepared with the anticipation of cooperative effects. Characterization by NMR spectroscopy (¹H, ¹³C, ²⁹Si, and ¹⁹⁵Pt) and SC-XRD revealed the strong similarity of this new complex class to the parent monometallic Markó-type (NHC)Pt(dvtms) complexes. Hindered rotation of the Pt–C bond generates conformational isomers for **1–3** and **6** at room temperature. ¹H VT-NMR experiments with **5** disclose coalescence at 233 K, which gives $\Delta G^{\ddagger} = 52.5 \text{ kJ mol}^{-1}$ as a rotational barrier, using the Eyring equation. The bimetallic complexes prove to be potent catalyst precursors for the hydrosilylation of alkenes and are characterized by minuscule initiation periods compared to $\text{Im}^{\text{Mes}}\text{Pt}(\text{dvtms})$ (**7**) which is used as a reference to Markó-type complexes. Inverse behavior was observed for **4** and **7** in the pre-catalytic reaction of the complexes with $\text{MD}^{\text{H}}\text{M}$. Activation of **7** results in a TOF of 296,000 h⁻¹, with selectivity decreasing under harsh conditions, while **4** is first deactivated and then reactivated under harsh conditions, with selectivity being maintained. These findings are explained by the decomposition of **7** to platinum colloids after extended exposure to $\text{MD}^{\text{H}}\text{M}$ as revealed by mercury poisoning experiments and intermediate stabilization of **4** as the postulated di- μ -hydrido complex **C** under the same conditions. Relevant for the application is the performance of **7** at low catalyst loadings, while **4** is superior at low temperatures due to easier activation.

CRedit authorship contribution statement

Michael J. Sauer: Writing – review & editing, Writing – original draft, Visualization, Validation, Methodology, Investigation, Formal analysis, Conceptualization. **Jeff Offorjindu:** Methodology, Investigation. **Greta G. Zámbo:** Methodology, Investigation. **Robert M. Reich:** Supervision, Project administration. **Fritz E. Kühn:** Supervision, Project administration.

Declaration of competing interest

The authors declare that they have no known competing financial interests or personal relationships that could have appeared to influence the work reported in this paper.

Data availability

Data will be made available on request.

Acknowledgments

M.J.S. and G.G.Z. thank the TUM Graduate School and WACKER Chemie AG for financial support. J.O. gratefully acknowledges the support of AuTUM (Ausbildungszentrum der Technischen Universität München) and all authors thank AuTUM for the cooperation during J. O.'s apprenticeship.

Supplementary materials

Supplementary material associated with this article can be found, in the online version, at doi:10.1016/j.jorgchem.2024.123030.

References

- [1] R.H. Holm, P. Kennepohl, E.I. Solomon, Structural and functional aspects of metal sites in biology, *Chem. Rev.* 96 (1996) 2239–2314, <https://doi.org/10.1021/cr9500390>.
- [2] R.E. Stenkamp, Dioxygen and hemerythrin, *Chem. Rev.* 94 (1994) 715–726, <https://doi.org/10.1021/cr00027a008>.
- [3] E.I. Solomon, D.E. Heppner, E.M. Johnston, J.W. Ginsbach, J. Cirera, M. Qayyum, M.T. Kieber-Emmons, C.H. Kjaergaard, R.G. Hadt, L. Tian, Copper active sites in biology, *Chem. Rev.* 114 (2014) 3659–3853, <https://doi.org/10.1021/cr400327t>.
- [4] T. Guchhait, S. Sasmal, F.S.T. Khan, S.P. Rath, Oxo- and hydroxo-bridged diiron (II) porphyrin dimers: inorganic and bio-inorganic perspectives and effects of intermacrocylic interactions, *Coord. Chem. Rev.* 337 (2017) 112–144, <https://doi.org/10.1016/j.ccr.2017.02.008>.
- [5] A.L. Gavrilova, B. Bosnich, Principles of mononucleating and binucleating ligand design, *Chem. Rev.* 104 (2004) 349–384, <https://doi.org/10.1021/cr020604g>.
- [6] R. Boulatov, Understanding the reaction that powers this world: biomimetic studies of respiratory O₂ reduction by cytochrome oxidase, *Pure Appl. Chem.* 76 (2004) 303–319, <https://doi.org/10.1351/pac200476020303>.
- [7] E.Y. Tshuva, S.J. Lippard, Synthetic models for non-heme carboxylate-bridged diiron metalloproteins: strategies and tactics, *Chem. Rev.* 104 (2004) 987–1012, <https://doi.org/10.1021/cr020622y>.
- [8] J. Weston, Mode of action of Bi- and trinuclear zinc hydrolases and their synthetic analogues, *Chem. Rev.* 105 (2005) 2151–2174, <https://doi.org/10.1021/cr020057z>.
- [9] A. Magnuson, M. Anderlund, O. Johansson, P. Lindblad, R. Lomoth, T. Polivka, S. Ott, K. Stensjö, S. Styring, V. Sundström, L. Hammarström, Biomimetic and microbial approaches to solar fuel generation, *Acc. Chem. Res.* 42 (2009) 1899–1909, <https://doi.org/10.1021/ar900127h>.
- [10] S. Friedle, E. Reisner, S.J. Lippard, Current challenges of modeling diiron enzyme active sites for dioxygen activation by biomimetic synthetic complexes, *Chem. Soc. Rev.* 39 (2010) 2768–2779, <https://doi.org/10.1039/C003079C>.
- [11] M.M. Najafpour, G. Renger, M. Holyńska, A.N. Moghaddam, E.M. Aro, R. Carpentier, H. Nishihara, J.J. Eaton-Rye, J.R. Shen, S.I. Allakhverdiev, Manganese compounds as water-oxidizing catalysts: from the natural water-oxidizing complex to nanosized manganese oxide structures, *Chem. Rev.* 116 (2016) 2886–2936, <https://doi.org/10.1021/acs.chemrev.5b00340>.
- [12] V.C.C. Wang, S. Maji, P.P.Y. Chen, H.K. Lee, S.S.F. Yu, S.I. Chan, Alkane oxidation: methane monooxygenases, related enzymes, and their biomimetics, *Chem. Rev.* 117 (2017) 8574–8621, <https://doi.org/10.1021/acs.chemrev.6b00624>.
- [13] P. Buchwalter, J. Rosé, P. Braunstein, Multimetallic catalysis based on heterometallic complexes and clusters, *Chem. Rev.* 115 (2015) 28–126, <https://doi.org/10.1021/cr500208k>.
- [14] N.P. Mankad, Selectivity effects in bimetallic catalysis, *Chem. Eur. J.* 22 (2016) 5822–5829, <https://doi.org/10.1002/chem.201505002>.
- [15] J. Campos, Bimetallic cooperation across the periodic table, *Nat. Rev. Chem.* 4 (2020) 696–702, <https://doi.org/10.1038/s41570-020-00226-5>.
- [16] B. Chatterjee, W.C. Chang, S. Jena, C. Werlé, Implementation of cooperative designs in polarized transition metal systems—significance for bond activation and catalysis, *ACS Catal.* 10 (2020) 14024–14055, <https://doi.org/10.1021/acscatal.0c03794>.
- [17] R. Maity, B.S. Birenheide, F. Breher, B. Sarkar, Cooperative effects in multimetallic complexes applied in catalysis, *ChemCatChem* 13 (2021) 2337–2370, <https://doi.org/10.1002/cctc.202001951>.
- [18] A. Dey, Bimetallic cooperativity and hydrogen bonding allow efficient reduction of CO₂, *Angew. Chem. Int. Ed.* 62 (2023) e202301760, <https://doi.org/10.1002/anie.202301760>.
- [19] E.K. van den Beuken, B.L. Feringa, Bimetallic catalysis by late transition metal complexes, *Tetrahedron* 54 (1998) 12985–13011, [https://doi.org/10.1016/S0040-4020\(98\)00319-6](https://doi.org/10.1016/S0040-4020(98)00319-6).
- [20] J.M. Gil-Negrete, E. Hevia, Main group bimetallic partnerships for cooperative catalysis, *Chem. Sci.* 12 (2021) 1982–1992, <https://doi.org/10.1039/D0SC05116K>.
- [21] J. Park, S. Hong, Cooperative bimetallic catalysis in asymmetric transformations, *Chem. Soc. Rev.* 41 (2012) 6931–6943, <https://doi.org/10.1039/C2CS35129C>.
- [22] D.R. Pye, N.P. Mankad, Bimetallic catalysis for C–C and C–X coupling reactions, *Chem. Sci.* 8 (2017) 1705–1718, <https://doi.org/10.1039/C6SC05566G>.
- [23] K.J. Evans, S.M. Mansell, Functionalised N-Heterocyclic carbene ligands in bimetallic architectures, *Chem. Eur. J.* 26 (2020) 5927–5941, <https://doi.org/10.1002/chem.201905510>.
- [24] S. Klaus, M.W. Lehenmeier, C.E. Anderson, B. Rieger, Recent advances in CO₂/epoxide copolymerization—new strategies and cooperative mechanisms, *Coord. Chem. Rev.* 255 (2011) 1460–1479, <https://doi.org/10.1016/j.ccr.2010.12.002>.
- [25] J.I. van der Vlugt, Cooperative catalysis with first-row late transition metals, *Eur. J. Inorg. Chem.* (2012) 363–375, <https://doi.org/10.1002/ejic.201100752>, 2012.

- [26] N. Xiong, G. Zhang, X. Sun, R. Zeng, Metal-metal cooperation in dinuclear complexes involving late transition metals directed towards organic catalysis, *Chin. J. Chem* 38 (2020) 185–201, <https://doi.org/10.1002/cjoc.201900371>.
- [27] C. Adams, P. Riviere, M. Riviere-Baudet, C. Morales-Verdejo, M. Dahrouch, V. Morales, A. Castel, F. Delpech, J.M. Manriquez, I. Chávez, Catalytic study of heterobimetallic rhodium complexes derived from partially alkylated s-indacene in dehydrogenative silylation of olefins, *J. Organomet. Chem.* 749 (2014) 266–274, <https://doi.org/10.1016/j.jorganchem.2013.10.017>.
- [28] V. Comte, P. Le Gendre, P. Richard, C. Moise, [TiPHOS(Rh)]⁺: a fortuitous coordination mode and an effective Hydrosilylation bimetallic catalyst, *Organometallics* 24 (2005) 1439–1444, <https://doi.org/10.1021/om040058c>.
- [29] A.J. Huckaba, T.K. Hollis, T.O. Howell, H.U. Valle, Y. Wu, Synthesis and characterization of a 1,3-Phenylene-Bridged *N*-Alkyl Bis(benzimidazole) CCC-NHC pincer ligand precursor: homobimetallic silver and rhodium complexes and the catalytic Hydrosilylation of Phenylacetylene, *Organometallics* 32 (2013) 63–69, <https://doi.org/10.1021/om3008037>.
- [30] V. Diachenko, M.J. Page, M.R.D. Gatus, M. Bhadbhade, B.A. Messerle, Bimetallic *N*-Heterocyclic Carbene Rh(I) complexes: probing the cooperative effect for the Catalyzed Hydroreduction of Alkynes, *Organometallics* 34 (2015) 4543–4552, <https://doi.org/10.1021/acs.organomet.5b00594>.
- [31] M.R.D. Gatus, I. Pernik, J.A. Tompsett, S.C. Binding, M.B. Peterson, B.A. Messerle, Simple and reactive Ir(I) *N*-heterocyclic carbene complexes for alkyne activation, *Dalton Trans* 48 (2019) 4333–4340, <https://doi.org/10.1039/C9DT00313D>.
- [32] S. Leelasubcharoen, P.A. Zhizhko, L.G. Kuzmina, A.V. Churakov, J.A.K. Howard, G.I. Nikonov, Niobium/Rhodium Bimetallic complexes: synthesis, structure, and catalytic hydrosilylation of acetophenone and benzaldehyde, *Organometallics* 28 (2009) 4500–4506, <https://doi.org/10.1021/om900363r>.
- [33] A.E. Findlay, S. Leelasubcharoen, L.G. Kuzmina, J.A.K. Howard, G.I. Nikonov, Phosphido-bridged Ta/Rh bimetallic complex: synthesis, structure, and catalytic hydrosilylation of acetophenone, *Dalton Trans* 39 (2010) 9264–9269, <https://doi.org/10.1039/C0DT00141D>.
- [34] R.H. Lam, S.T. Keaveney, B.A. Messerle, I. Pernik, Bimetallic rhodium complexes: precatalyst activation-triggered bimetallic enhancement for the hydrosilylation transformation, *ACS Catal* 13 (2023) 1999–2010, <https://doi.org/10.1021/acscatal.2c04388>.
- [35] W. Zhou, S.L. Marquard, M.W. Bezpalko, B.M. Foxman, C.M. Thomas, Catalytic hydrosilylation of ketones using a Co/Zr heterobimetallic complex: evidence for an unusual mechanism involving Ketyl Radicals, *Organometallics* 32 (2013) 1766–1772, <https://doi.org/10.1021/om301194g>.
- [36] J.L. Speier, D.E. Hook, *Process for the Production of Organosilicon Compounds*, 1958 US2823218, February 11.
- [37] B.D. Karstedt, *Platinum Complexes of Unsaturated Siloxanes and Platinum Containing Organopolysiloxanes*, 1973 US3775452, November 27.
- [38] D. Troegel, J. Stohrer, Recent advances and actual challenges in late transition metal catalyzed hydrosilylation of olefins from an industrial point of view, *Coord. Chem. Rev.* 255 (2011) 1440–1459, <https://doi.org/10.1016/j.ccr.2010.12.025>.
- [39] N. Nakata, M. Sakashita, C. Komatsubara, A. Ishii, Synthesis, structure, and catalytic activity of bimetallic Pt(II)–Ir(III) complexes Bridged by Cyclooctane-1,2-dithiolato ligands, *Eur. J. Inorg. Chem.* (2010) 447–453, <https://doi.org/10.1002/ejic.200900958>, 2010.
- [40] I.E. Markó, S. Stérin, O. Buisine, G. Mignani, P. Branlard, B. Tinant, J.P. Declercq, Selective and efficient Platinum(0)-Carbene complexes as hydrosilylation catalysts, *Science* 298 (2002) 204–206, <https://doi.org/10.1126/science.1073338>.
- [41] I.E. Markó, S. Stérin, O. Buisine, G. Berthon, G. Michaud, B. Tinant, J.P. Declercq, Highly active and selective Platinum(0)-Carbene complexes. Efficient, catalytic hydrosilylation of functionalised olefins, *Adv. Synth. Catal.* 346 (2004) 1429–1434, <https://doi.org/10.1002/adsc.200404048>.
- [42] G. Berthon-Gelloz, O. Buisine, J.F. Brière, G. Michaud, S. Stérin, G. Mignani, B. Tinant, J.P. Declercq, D. Chapon, I.E. Markó, Synthetic and structural studies of NHC–Pt(dvtms) complexes and their application as alkene hydrosilylation catalysts (NHC = *N*-heterocyclic carbene, dvtms = divinyltetramethylsiloxane), *J. Organomet. Chem.* 690 (2005) 6156–6168, <https://doi.org/10.1016/j.jorganchem.2005.08.020>.
- [43] O. Buisine, G. Berthon-Gelloz, J.F. Brière, S. Stérin, G. Mignani, P. Branlard, B. Tinant, J.P. Declercq, I.E. Markó, Second generation *N*-heterocyclic carbene–Pt(0) complexes as efficient catalysts for the hydrosilylation of alkenes, *Chem. Commun.* (2005) 3856–3858, <https://doi.org/10.1039/B506369H>.
- [44] D. Brissy, M. Skander, P. Retailleau, G. Frison, A. Marinetti, Platinum(II) complexes featuring chiral diphosphines and *N*-heterocyclic carbene ligands: synthesis and evaluation as cycloisomerization catalysts, *Organometallics* 28 (2009) 140–151, <https://doi.org/10.1021/om800743r>.
- [45] M.J. Sauer, L.F. Richter, J. Offorjindu, R.M. Reich, F.E. Kühn, Synthesis and characterization of Markó-type (NHC)Pt(dvtms) complexes and their evaluation in the hydrosilylation reaction of alkenes, *J. Organomet. Chem.* 1005 (2024) 122995–123005, <https://doi.org/10.1016/j.jorganchem.2023.122995>.
- [46] T.K. Meister, J.W. Kück, K. Riener, A. Pöthig, W.A. Herrmann, F.E. Kühn, Decoding catalytic activity of platinum carbene hydrosilylation catalysts, *J. Catal.* 337 (2016) 157–166, <https://doi.org/10.1016/j.jcat.2016.01.032>.
- [47] T. Strassner, M. Muehlhofer, A. Zeller, E. Herdtweck, W.A. Herrmann, The counterion influence on the CH-activation of methane by palladium(II) biscarbene complexes – structures, reactivity and DFT calculations, *J. Organomet. Chem.* 689 (2004) 1418–1424, <https://doi.org/10.1016/j.jorganchem.2004.02.013>.
- [48] M. Micksch, T. Strassner, Palladium(II) Complexes with chelating biscarbene ligands in the catalytic suzuki–miyaura cross-coupling reaction, *Eur. J. Inorg. Chem.* (2012) 5872–5880, <https://doi.org/10.1002/ejic.201200940>, 2012.
- [49] T. Wagner, A. Pöthig, H.M.S. Augenstein, T.D. Schmidt, M. Kaposi, E. Herdtweck, W. Brütting, W.A. Herrmann, F.E. Kühn, From simple ligands to complex structures: structural diversity of Silver(I) complexes bearing Tetradentate (alkylenebimpy) NHC ligands, *Organometallics* 34 (2015) 1522–1529, <https://doi.org/10.1021/om5013067>.
- [50] J.F. Schlagintweit, L. Nguyen, F. Dyckhoff, F. Kaiser, R.M. Reich, F.E. Kühn, Exploring different coordination modes of the first tetradentate NHC/1,2,3-triazole hybrid ligand for group 10 complexes, in: *Dalton Trans.*, 48, 2019, pp. 14820–14828, <https://doi.org/10.1039/C9DT03430G>.
- [51] H. Richter, H. Schwertfeger, P.R. Schreiner, R. Fröhlich, F. Glorius, Thieme chemistry journal awardes - where are they now? synthesis of diamantane-Derived *N*-heterocyclic carbenes and applications in catalysis, *Synlett* (2009) 193–197, <https://doi.org/10.1055/s-0028-1087676>, 2009.
- [52] APEX Suite of Crystallographic Software (Version APEX4), Bruker AXS Inc., 2021.
- [53] SAINT (Version 8.38A), Bruker AXS Inc., 2017.
- [54] SADABS (Version 2016/2), Bruker AXS Inc., 2016.
- [55] C.B. Hübschle, G.M. Sheldrick, B. Dittrich, ShelXle: a Qt graphical user interface for SHELXL, *J. Appl. Crystallogr.* 44 (2011) 1281–1284, <https://doi.org/10.1107/S0021889111043202>.
- [56] G.M. Sheldrick, Crystal structure refinement with SHELXL, *Acta Crystallogr. Sect. C* 71 (2015) 3–8, <https://doi.org/10.1107/S2053229614024218>.
- [57] G.M. Sheldrick, SHELXT - Integrated space-group and crystal-structure determination, *Acta Crystallogr. Sect. A* 71 (2015) 3–8, <https://doi.org/10.1107/S2053273314026370>.
- [58] A.J. Wilson, *International Tables for Crystallography*, Kluwer Academic Publishers, Dordrecht, 1992.
- [59] A. Spek, Structure validation in chemical crystallography, *Acta Crystallogr. Sect. D* 65 (2009) 148–155, <https://doi.org/10.1107/S090744490804362X>.
- [60] G. Chandra, P.Y. Lo, P.B. Hitchcock, M.F. Lappert, A Complex and Novel Route to Bis(η -alkyne)platinum(0) and other Platinum(0) Conventions from Speier's Hydrosilylation Catalyst H₂[PtCl₂·xH₂O. X-ray Structure of [Pt{(η -CH₂=CHSiMe₂)₂O}(P-*t*-Bu₃)], *Organometallics* 6 (1987) 191–192, <https://doi.org/10.1021/om00144a036>.
- [61] P.B. Hitchcock, M.F. Lappert, N.J.W. Warhurst, Synthesis and structure of a rac-Tris(divinylsiloxane)diplatinum(0) complex and its reaction with maleic anhydride, *Angew. Chem. Int. Ed.* 30 (1991) 438–440, <https://doi.org/10.1002/anie.199104381>.
- [62] B. Schulze, U.S. Schubert, Beyond click chemistry – supramolecular interactions of 1,2,3-triazoles, *Chem. Soc. Rev.* 43 (2014) 2522–2571, <https://doi.org/10.1039/C3CS60386E>.
- [63] S. Sinn, B. Schulze, C. Friebe, D.G. Brown, M. Jäger, E. Altuntas, J. Kübel, O. Guntner, C.P. Berlinguette, B. Dietzek, U.S. Schubert, Physicochemical analysis of Ruthenium(II) sensitizers of 1,2,3-Triazole-derived mesoionic carbene and cyclometalating ligands, *Inorg. Chem.* 53 (2014) 2083–2095, <https://doi.org/10.1021/ic402702z>.
- [64] B.P. Maliszewski, N.V. Tzouras, S.G. Guillet, M. Saab, M. Beliš, K. Van Hecke, F. Nagra, S.P. Nolan, A general protocol for the synthesis of Pt-NHC (NHC = *N*-heterocyclic carbene) hydrosilylation catalysts, *Dalton Trans.* 49 (2020) 14673–14679, <https://doi.org/10.1039/D0DT03480K>.
- [65] B.P. Maliszewski, I. Ritacco, M. Beliš, I.I. Hashim, N.V. Tzouras, L. Caporaso, L. Cavallo, K. Van Hecke, F. Nagra, C.S.J. Cazin, S.P. Nolan, A green route to platinum *N*-heterocyclic carbene complexes: mechanism and expanded scope, *Dalton Trans* 51 (2022) 6204–6211, <https://doi.org/10.1039/D2DT00504B>.
- [66] J.J. Dunsford, K.J. Cavell, B. Kariuki, Expanded ring *N*-heterocyclic carbene complexes of zero valent platinum dvtms (divinyltetramethylsiloxane): highly efficient hydrosilylation catalysts, *J. Organomet. Chem.* 696 (2011) 188–194, <https://doi.org/10.1016/j.jorganchem.2010.08.045>.
- [67] A.M. Ruiz-Varilla, E.A. Baquero, G.F. Silvestri, C. Gonzalez-Arellano, E. de Jesús, J.C. Flores, Synthesis and behavior of novel sulfonated water-soluble *N*-heterocyclic carbene (η^4 -diene) platinum(0) complexes, *Dalton Trans.* 44 (2015) 18360–18369, <https://doi.org/10.1039/C5DT02622A>.
- [68] N. Schneider, S. Bellemine-Laponnaz, H. Wadeppel, L.H. Gade, A new class of modular Oxazoline-NHC ligands and their coordination chemistry with platinum metals, *Eur. J. Inorg. Chem.* (2008) 5587–5598, <https://doi.org/10.1002/ejic.200800908>, 2008.
- [69] J.R.L. Priqueler, I.S. Butler, F.D. Rochon, An overview of ¹⁹⁵Pt nuclear magnetic resonance spectroscopy, *Appl. Spectrosc. Rev.* 41 (2006) 185–226, <https://doi.org/10.1080/05704920600620311>.
- [70] B.M. Still, P.G.A. Kumar, J.R. Aldrich-Wright, W.S. Price, ¹⁹⁵Pt NMR—theory and application, *Chem. Soc. Rev.* 36 (2007) 665–686, <https://doi.org/10.1039/B606190G>.
- [71] T. Troadec, A. Prades, R. Rodriguez, R. Mirgalet, A. Bacedero, N. Saffon-Merceron, V. Branchadell, T. Kato, Silacyclopropylideneplatinum(0) Complex as a robust and efficient hydrosilylation catalyst, *Inorg. Chem.* 55 (2016) 8234–8240, <https://doi.org/10.1021/acs.inorgchem.6b01505>.
- [72] T. Iimura, N. Akasaka, T. Kosai, T. Iwamoto, A Pt(0) complex with cyclic (alkyl) (amino)silylene and 1,3-divinyl-1,1,3,3-tetramethylsiloxane ligands: synthesis, molecular structure, and catalytic hydrosilylation activity, *Dalton Trans.* 46 (2017) 8868–8874, <https://doi.org/10.1039/C7DT01113J>.
- [73] H. Gunther, The influence of dynamic effects on ¹H nuclear magnetic resonance spectra, in: H. Gunther (Ed.), *NMR Spectroscopy*, Wiley, New York, 1995, pp. 335–390.

- [74] M.T. Huggins, T. Kesharwani, J. Buttrick, C. Nicholson, Variable temperature NMR experiment studying restricted bond rotation, *J. Chem. Educ.* 97 (2020) 1425–1429, <https://doi.org/10.1021/acs.jchemed.0c00057>.
- [75] L.N. Appelhans, C.D. Incarvito, R.H. Crabtree, Synthesis of monodentate bis(*N*-heterocyclic carbene) complexes of iridium: mixed complexes of abnormal NHCs, normal NHCs, and triazole NHCs, *J. Organomet. Chem.* 693 (2008) 2761–2766, <https://doi.org/10.1016/j.jorganchem.2008.05.024>.
- [76] M. Dangelov, M. Stoyanova, P. Petrov, M. Putala, N.G. Vassilev, Fluxional Pd(II) NHC complexes – synthesis, structure elucidation and catalytic studies, *J. Organomet. Chem.* 817 (2016) 1–14, <https://doi.org/10.1016/j.jorganchem.2016.05.002>.
- [77] C.P. Newman, R.J. Deeth, G.J. Clarkson, J.P. Rourke, Synthesis of mixed NHC/L Platinum(II) complexes: restricted rotation of the NHC group, *Organometallics* 26 (2007) 6225–6233, <https://doi.org/10.1021/om700671y>.
- [78] P. Zak, M. Bolt, B. Dudzic, M. Kubicki, Synthesis of (E)-1,4-disiloxylquinoxylsubstituted but-1-en-3-yne via platinum-catalyzed dimerization of ethynylsiloxylquinoxanes, *Dalton Trans* 48 (2019) 2657–2663, <https://doi.org/10.1039/C8DT05142A>.
- [79] P. Zak, M. Bolt, J. Lorkowski, M. Kubicki, C. Pietraszuk, Platinum complexes bearing Bulky *N*-Heterocyclic carbene ligands as efficient catalysts for the fully selective dimerization of terminal alkynes, *ChemCatChem* 9 (2017) 3627–3631, <https://doi.org/10.1002/cctc.201700580>.
- [80] S.A. Rzhavskiy, M.A. Topchiy, K.A. Lyssenko, A.N. Philippova, M.A. Belaya, A. A. Agheshina, M.V. Bermeshev, M.S. Nechaev, A.F. Asachenko, New expanded-ring NHC platinum(0) complexes: synthesis, structure and highly efficient dimerization of terminal alkenes, *J. Organomet. Chem.* 912 (2020) 121140–121162, <https://doi.org/10.1016/j.jorganchem.2020.121140>.
- [81] P. Zak, M. Bolt, M. Kubicki, C. Pietraszuk, Highly selective hydrosilylation of olefins and acetylenes by platinum(0) complexes bearing bulky *N*-heterocyclic carbene ligands, *Dalton Trans* 47 (2018) 1903–1910, <https://doi.org/10.1039/C7DT04392A>.
- [82] R.J. Hofmann, M. Vlatković, F. Wiesbrock, Fifty years of Hydrosilylation in polymer science: a review of current trends of low-cost transition-metal and metal-free catalysts, non-thermally triggered hydrosilylation reactions, and industrial applications, *Polymers (Basel)* 9 (2017) 534–570, <https://doi.org/10.3390/polym9100534>.
- [83] J.M. Lambert, The nature of platinum in silicones for biomedical and healthcare use, *J. Biomed. Mater. Res. Part B Appl. Biomater.* 78B (2006) 167–180, <https://doi.org/10.1002/jbm.b.30471>.
- [84] G. Berthon-Gelloz, I.E. Markó, Efficient and selective Hydrosilylation of Alkenes and Alkynes Catalyzed by Novel *N*-Heterocyclic Carbene Pt(0) Complexes. *N-Heterocyclic Carbenes in Synthesis*, WILEY-VCH, Weinheim, 2006, pp. 119–161.
- [85] J. Stein, L.N. Lewis, Y. Gao, R.A. Scott, *In Situ* determination of the active catalyst in hydrosilylation reactions using highly reactive Pt(0) catalyst precursors, *J. Am. Chem. Soc.* 121 (1999) 3693–3703, <https://doi.org/10.1021/ja9825377>.
- [86] L.N. Lewis, On the mechanism of metal colloid catalyzed hydrosilylation: proposed explanations for electronic effects and oxygen cocatalysis, *J. Am. Chem. Soc.* 112 (1990) 5998–6004, <https://doi.org/10.1021/ja00172a014>.
- [87] M. Ciriano, M. Green, J.A.K. Howard, J. Proud, J.L. Spencer, F.G.A. Stone, C. A. Tsipis, Synthesis of *trans*-di- μ -hydrido-bis(silyl)bis(trialkylphosphine)di-platinum complexes: crystal and molecular structure of di- μ -hydrido-bis(tricyclohexylphosphine)bis(triethylsilyl)diplatinum, *J. Chem. Soc., Dalton Trans.* (1978) 801–808, <https://doi.org/10.1039/DT9780000801>.
- [88] S. Ouis, D.A. Rouag, L. Bendjeddou, C. Bailly, Crystal structure of homodinuclear platinum complex containing a metal-metal bond bridged by hydride and phosphide ligands, *Acta Crystallogr. Sect. E* 74 (2018) 977–980, <https://doi.org/10.1107/S205698901800868X>.
- [89] J. Chang, F. Fang, J. Zhang, X. Chen, Hydrosilylation of aldehydes and ketones catalysed by Bis(phosphinite) pincer platinum hydride complexes, *Adv. Synth. Catal.* 362 (2020) 2709–2715, <https://doi.org/10.1002/adsc.202000166>.
- [90] H.C. Clark, M.J.H. Smith, Chemistry of platinum hydrides: a platinum(II) *cis*-dihydride or a platinum(0) η^2 -dihydrogen complex? *J. Am. Chem. Soc.* 108 (1986) 3829–3830, <https://doi.org/10.1021/ja00273a047>.
- [91] S.P. Millar, M. Jang, R.J. Lachicotte, R. Eisenberg, Hydride complexes of platinum (II) containing unsymmetrical di(phosphine) ligands: synthesis, characterization and evidence for pairwise addition of hydrogen based on parahydrogen induced polarization, *Inorg. Chim. Acta* 270 (1998) 363–375, [https://doi.org/10.1016/S0020-1693\(97\)05870-2](https://doi.org/10.1016/S0020-1693(97)05870-2).
- [92] M. Brendel, R. Engelke, V.G. Desai, F. Rominger, P. Hofmann, Synthesis and reactivity of Platinum(II) *cis*-Dialkyl, *cis*-Alkyl Chloro, and *cis*-Alkyl Hydrido Bis-*N*-heterocyclic Carbene Chelate Complexes, *Organometallics* 34 (2015) 2870–2878, <https://doi.org/10.1021/acs.organomet.5b00204>.
- [93] J. Real, E. Prat-Gil, M. Pagès-Barenys, A. Polo, J.F. Piniella, A. Álvarez-Larena, Platinum phosphinothiolato hydride complexes: synthesis, structure and evaluation as tin-free hydroformylation catalysts, *Dalton Trans.* 45 (2016) 3964–3973, <https://doi.org/10.1039/C5DT04107D>.
- [94] M.P. Brown, R.J. Puddephatt, M. Rashidi, K.R. Seddon, Some binuclear hydrides of platinum, *J. Chem. Soc., Dalton Trans.* (1978) 516–522, <https://doi.org/10.1039/DT9780000516>.
- [95] N. Hidalgo, F. de la Cruz-Martínez, M.T. Martín, M.C. Nicasio, J. Campos, A highly constrained *cis*-dihydride platinum complex trapped by cooperative gold/platinum dihydrogen activation, *Chem. Commun.* 58 (2022) 9144–9147, <https://doi.org/10.1039/D2CC03089F>.
- [96] A.L. Bandini, G. Banditelli, G. Minghetti, Binuclear hydrido platinum(II) complexes: syntheses of [(Pt(P-P))₂(μ -CHCH₂R)(μ -H)] [BF₄] (R=C₆H₅, H) and easy cleavage of a P-C bond in a chelating 1,4-bis(diphenyl)phosphinobutane (P-P), *J. Organomet. Chem.* 595 (2000) 224–231, [https://doi.org/10.1016/S0022-328X\(99\)00628-2](https://doi.org/10.1016/S0022-328X(99)00628-2).
- [97] G. Berthon-Gelloz, B. deBruin, B. Tinant, I.E. Markó, Structure and reactivity of a unique Y-Shaped Tricoordinate Bis(silyl)platinum(II)-NHC complex, *Angew. Chem. Int. Ed.* 48 (2009) 3161–3164, <https://doi.org/10.1002/anie.200900435>.
- [98] S. Dierick, E. Vercruyse, G. Berthon-Gelloz, I.E. Markó, User-friendly platinum catalysts for the highly stereoselective hydrosilylation of alkynes and alkenes, *Chem. Eur. J.* 21 (2015) 17073–17078, <https://doi.org/10.1002/chem.201502643>.
- [99] M.J. Michalczyk, J.C. Calabrese, C.A. Recatto, M.J. Fink, Reaction of disilanes with a *cis*-platinum dihydride: novel platinum complexes with terminal disilanyl groups and bridging disilene ligands, *J. Am. Chem. Soc.* 114 (1992) 7955–7957, <https://doi.org/10.1021/ja00046a077>.
- [100] A.K. Roy, R.B. Taylor, The First Alkene–platinum–silyl complexes: lifting the hydrosilylation mechanism shroud with long-lived precatalytic intermediates and true Pt catalysts, *J. Am. Chem. Soc.* 124 (2002) 9510–9524, <https://doi.org/10.1021/ja0127335>.
- [101] B.P. Maliszewski, T.A.C.A. Bayrakdar, P. Lambert, L. Hamdouna, X. Trivelli, L. Cavallo, A. Poater, M. Belis, O. Lafon, K. Van Hecke, D. Ormerod, C.S.J. Cazin, F. Nahra, S.P. Nolan, Pt(II)–*N*-heterocyclic carbene complexes in solvent-free Alkene Hydrosilylation, *Chem. Eur. J.* 29 (2023) e202301259, <https://doi.org/10.1002/chem.202301259>.
- [102] V.M. Chernyshev, A.V. Astakhov, I.E. Chikunov, R.V. Tyurin, D.B. Eremin, G. S. Ranny, V.N. Khrustalev, V.P. Ananikov, Pd and Pt catalyst poisoning in the study of reaction mechanisms: what does the mercury test mean for catalysis? *ACS Catal.* 9 (2019) 2984–2995, <https://doi.org/10.1021/acscatal.8b03683>.
- [103] O.N. Gorunova, I.M. Novitskiy, Y.K. Grishin, I.P. Glorizov, V.A. Roznyatovsky, V. N. Khrustalev, K.A. Kochetkov, V.V. Dunina, When applying the mercury poisoning test to palladacycle-catalyzed reactions, one should not consider the common misconception of Mercury(0) selectivity, *Organometallics* 37 (2018) 2842–2858, <https://doi.org/10.1021/acs.organomet.8b00363>.
- [104] J.A. Widegren, R.G. Finke, A review of the problem of distinguishing true homogeneous catalysis from soluble or other metal-particle heterogeneous catalysis under reducing conditions, *J. Mol. Catal. A: Chem.* 198 (2003) 317–341, [https://doi.org/10.1016/S1381-1169\(02\)00728-8](https://doi.org/10.1016/S1381-1169(02)00728-8).
- [105] J.A. Widegren, M.A. Bennett, R.G. Finke, Is it homogeneous or heterogeneous catalysis? Identification of bulk ruthenium metal as the true catalyst in benzene hydrogenations starting with the monometallic precursor, Ru(II)(η^5 -C₆Me₆)(OAc)₂, plus kinetic characterization of the heterogeneous nucleation, then autocatalytic surface-growth mechanism of metal film formation, *J. Am. Chem. Soc.* 125 (2003) 10301–10310, <https://doi.org/10.1021/ja021436c>.
- [106] G.M. Whitesides, M. Hackett, R.L. Brainard, J.P.P.M. Lavalleye, A.F. Sowinski, A. N. Izumi, S.S. Moore, D.W. Brown, E.M. Staudt, Suppression of unwanted heterogeneous platinum(0)-catalyzed reactions by poisoning with mercury(0) in systems involving competing homogeneous reactions of soluble organoplatinum compounds: thermal decomposition of bis(triethylphosphine)-3,3,4,4-tetramethylplatinacyclopentane, *Organometallics* 4 (1985) 1819–1830, <https://doi.org/10.1021/om00129a023>.

4 Conclusion and Outlook

In this thesis, two distinct strategies to overcome the limitations of Markó-type hydrosilylation catalysts are described, consisting of the preparation and characterization of mono- and bimetallic platinum complexes and their evaluation in the hydrosilylation of alkenes.

The first section focuses on classical, monometallic Markó-type complexes of the general formula (NHC)Pt(dvtms) where selected alkyl and aromatic NHC wingtips were employed, that were not investigated hitherto and also allow determination of the effect of the lone pair of nitrogen (e.g. Ph vs. Py). ^{195}Pt NMR data reveal that the $-I$ effect for the pyridine and 1,2,3-triazole wingtips outweigh the potential intra- or intermolecular interaction of nitrogen with platinum, rendering the respective compounds electron-poor compared to complexes with phenyl or methyl wingtips, respectively. The first ever described abnormal 1,2,3-triazole-5-ylidene Pt(0) complex is presented, confirming the enhanced σ -donor strength of the ligand with an upfield shifted resonance of $\delta = 168.4$ ppm for the carbene shift, with respect to the imidazole-2-ylidene compounds that exhibit carbene shifts in the range of $\delta = 179.9$ – 186.5 ppm. However, the alkylated backbone of the triazole limits the flexibility of the mesityl wingtips, leading to a distortion of $\theta = 59^\circ$ for the dvtms ligand to reduce the steric strain, an elongated Pt–NHC bond of $2.054(3)$ Å, and in consequence to a downfield shifted platinum resonance ($\delta = -5306$ ppm), compared to the imidazole-2-ylidene congener ($\delta = -5392$ ppm). This trait is also reflected by the performance in the hydrosilylation of oct-1-ene with MD^HM, with a TOF of $12,000\text{ h}^{-1}$ for the 1,2,3-triazole-5-ylidene, while the imidazole-2-ylidene achieves $17,000\text{ h}^{-1}$. The presumed hemilabile *N*-donors impede the catalytic process, which is attributed to the durability of a Pt(II) species by excessive stabilization, disclosing the promoting effect of *N*-donors as an erroneous assumption. Overall, phenyl wingtips at the NHC give the most potent catalyst precursor, that achieves a TOF of $39,000\text{ h}^{-1}$ in combination with excellent yield and selectivity after a minor induction period, using oct-1-ene as substrate.

The concept of bimetallic catalysts is applied to Markó-type complexes in the second part, revealing synergistic interaction of two platinum centers, that is not yet fully understood. Multinuclear NMR spectroscopy and SC-XRD data demonstrate electronic and structural analogy of the mono- and bimetallic system, which is a prerequisite for meaningful deduction of the implication of the bimetallic nature. Depending on their NHC wingtips, these complexes are present as rotamers. Investigation of the rotational barrier by ^1H VT-NMR disclosed coalescence at 233 K in the case of Dipp as wingtip gives $\Delta G^\ddagger = 52.5\text{ kJ}\cdot\text{mol}^{-1}$, using the Eyring equation. *N*-donors (pyridine, triazole) as NHC wingtips were examined once more, however, the bimetallic complexes also proved incapable of overcoming the Pt(II) stabilization issue, which was evident for monometallic complexes. Generally, the bimetallic class

of complexes proves to be superior to monometallic complexes, achieving higher TOFs (up to $48,000 \text{ h}^{-1}$) and exhibiting shorter induction periods. An in-depth comparison of the mono- and bimetallic complexes is presented using mesityl wingtip compounds in both cases. The bimetallic catalyst is less dependent on temperature than the monometallic relative, implicating a lower activation barrier. Also, the reactivity of the catalyst classes is fundamentally different, as the TOF of the investigated bimetallic complex is independent of the catalyst concentration, while the TOF of the monometallic complex increases as the concentration is lowered. Further experiments, especially substrate screening, and calculations are required to fully elucidate the origin of the synergistic effect and understand the mechanism with regard to activation and the catalytic cycle. Preceding reaction of the selected representatives of the complex classes with silane initially leads to activation in the case of the monometallic complex and inverse behavior for the bimetallic catalyst. Coupling of this experiment with mercury poisoning studies highlights the stability of the bimetallic system compared to the monometallic one and is attributed to intermediate stabilization thereof as a di- μ -hydrido complex. Stoichiometric reaction of silane with the bimetallic complex and analysis by ^1H NMR exposes hydridic reflexes with reasonable Pt–H coupling as additional evidence.

The herein-disclosed results demonstrate the impressive performance of platinum-based catalysts in the hydrosilylation of alkenes. To the best of my knowledge, the alkenyl complexes of Markó (gen. 2.2) were not yet tested in the hydrosilylation of alkenes, which is demanded by the outstanding results when alkynes are employed as substrates. Generally, exploring unsaturated compounds, which are frequently used as inhibitors for thermally activated catalysts, as leaving groups appears promising. Investigation of *N*-heterocyclic heavier tetrylenes, especially silylenes, as strong donors with balanced acceptor properties is currently in progress in other groups, but suffers from insufficient stability, which might be tackled by kinetic or thermodynamic protection. Cyclic(alkyl)(amino)carbenes (CAACs) are also exceptionally strong donors that might be worth examining in this context. Concerning the bimetallic complexes of this thesis, the best combination of activity and product yield is achieved by Dipp, which is the most sterically demanding NHC wingtip in this study. Therefore, increasing the steric bulk even further might be beneficial and would also prevent formation of the inactive di- μ -hydrido complex. One could also employ benzimidazole-2-ylidenes for the bimetallic complexes, incorporating the knowledge gained during the studies of the second-generation Markó catalysts.

5 Reprint Permissions

First Major Publication:

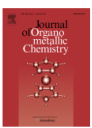
“Synthesis and Characterization of Markó-type (NHC)Pt(dvtms) Complexes and their Evaluation in the Hydrosilylation Reaction of Alkenes”

Michael J. Sauer, Leon F. Richter, Jeff Offorjindu, Robert M. Reich, Fritz E. Kühn*

J. Organomet. Chem. **2024**, *1005*, 122995-123005.

<https://doi.org/10.1016/j.jorganchem.2023.122995>

*Corresponding author



Synthesis and Characterization of Markó-type (NHC)Pt(dvtms) Complexes and their Evaluation in the Hydrosilylation Reaction of Alkenes
 Author: Michael J. Sauer, Leon F. Richter, Jeff Offorjindu, Robert M. Reich, Fritz E. Kühn
 Publication: Journal of Organometallic Chemistry
 Publisher: Elsevier
 Date: 1 February 2024
© 2023 Elsevier B.V. All rights reserved.

Journal Author Rights
 Please note that, as the author of this Elsevier article, you retain the right to include it in a thesis or dissertation, provided it is not published commercially. Permission is not required, but please ensure that you reference the journal as the original source. For more information on this and on your other retained rights, please visit: <https://www.elsevier.com/about/our-business/policies/copyright#Author-rights>

BACK
CLOSE WINDOW

Second Major Publication:


“Homobimetallic bis-NHC(Ptdvtms)₂ Complexes for the Hydrosilylation of Alkenes”

Michael J. Sauer, Jeff Offorjindu, Greta G. Zámbo, Robert M. Reich, Fritz E. Kühn*

J. Organomet. Chem. **2024**, *1007*, 123030-123044.

<https://doi.org/10.1016/j.jorganchem.2024.123030>

*Corresponding author



Homobimetallic bis-NHC(Ptdvtms)₂ Complexes for the Hydrosilylation of Alkenes
 Author: Michael J. Sauer, Jeff Offorjindu, Greta G. Zámbo, Robert M. Reich, Fritz E. Kühn
 Publication: Journal of Organometallic Chemistry
 Publisher: Elsevier
 Date: 1 March 2024
© 2024 The Author(s). Published by Elsevier B.V.

Journal Author Rights
 Please note that, as the author of this Elsevier article, you retain the right to include it in a thesis or dissertation, provided it is not published commercially. Permission is not required, but please ensure that you reference the journal as the original source. For more information on this and on your other retained rights, please visit: <https://www.elsevier.com/about/our-business/policies/copyright#Author-rights>

BACK
CLOSE WINDOW

6 Complete List of Publications

“Acetate Acetylacetonate Ampy Ruthenium(II) Complexes as Efficient Catalysts for Ketone Transfer Hydrogenation”

Daniela A. Hey, **Michael J. Sauer**, Pauline J. Fischer, Eva-Maria H. J. Esslinger, Fritz. E. Kühn*, Walter Baratta*

ChemCatChem **2020**, *12*, 3537-3544.

<https://doi.org/10.1002/cctc.202000542>

“Ruthenium and Osmium Complexes containing NHC and π -Acid Ligands”

Alexander D. Böth[§], **Michael J. Sauer**[§], Robert M. Reich, Fritz E. Kühn*

Book chapter in *Comprehensive Organometallic Chemistry IV* **2022**, *7*, 444-527.

<https://doi.org/10.1016/B978-0-12-820206-7.00142-6>

“Abnormal NHC Ruthenium Catalysts: Mechanistic Investigations of their Preparation and Steric Influence on Catalytic Performance”

Alexander D. Böth, **Michael J. Sauer**, Walter Baratta*, Fritz E. Kühn*

Cat. Sci. Tech. **2022**, *12*, 5597-5603.

<https://doi.org/10.1039/D2CY01036D>

“Synthesis and Characterisation of a Heterobimetallic N-heterocyclic Carbene Rhodium Ruthenium Complex as Catalyst for Transfer Hydrogenation”

Mohammad Kaikhosravi[§], Alexander D. Böth[§], **Michael J. Sauer**, Robert M. Reich and Fritz E. Kühn*

J. Organometall. Chem. **2022**, *979*, 122498-122502.

<https://doi.org/10.1016/j.jorganchem.2022.122498>

“The first macrocyclic abnormally coordinating tetra-1,2,3-triazole-5-ylidene iron complex: a promising candidate for olefin epoxidation”

Greta G. Zámbo, Johannes Mayr, **Michael J. Sauer**, Tim P. Schlachta, Robert M. Reich, Fritz E. Kühn

Dalton. Trans. **2022**, *51*, 13591-13595.

<https://doi.org/10.1039/D2DT02561B>

“Tailoring activity and stability: Effects of electronic variations on iron-NHC epoxidation catalysts”

Tim P. Schlachta, Greta G. Zámbo, **Michael J. Sauer**, Isabelle Rüter, Carla A. Hofer, Serhiy Demeshko, Franc Meyer, Fritz E. Kühn*

J. Catal. **2023**, *426*, 234-246.

<https://doi.org/10.1016/j.jcat.2023.07.018>

“Synthesis and characterization of Markó-type (NHC)Pt(dvtms) complexes and their evaluation in the hydrosilylation reaction of alkenes”

Michael J. Sauer, Leon F. Richter, Jeff Offorjindu, Robert M. Reich, Fritz E. Kühn*

J. Organomet. Chem. **2024**, *1005*, 122995-123005.

<https://doi.org/10.1016/j.jorganchem.2023.122995>

“Homobimetallic bis-NHC(Ptdvtms)₂ Complexes for the Hydrosilylation of Alkenes”

Michael J. Sauer, Jeff Offorjindu, Greta G. Zámbo, Robert M. Reich, Fritz E. Kühn*

J. Organomet. Chem. **2024**, *1007*, 123030-123044.

<https://doi.org/10.1016/j.jorganchem.2024.123030>

Annotations

[§]These authors contributed equally.

*Corresponding author(s).

7 References

- [1] a) B. Lindström, L.J. Pettersson, *CATTECH* **2003**, *7*, 130-138. <https://doi.org/10.1023/A:1025001809516>; b) W. Reschetilowski, Einführung in die Heterogene Katalyse, Springer-Verlag, Berlin, Heidelberg, **2015**.
- [2] C.D. Leake, *Isis* **1925**, *7*, 14-24. <https://doi.org/10.1086/358296>.
- [3] A. Mittasch, *Naturwissenschaften* **1936**, *50*, 785-790.
- [4] a) D. Steinborn, Grundlagen der Metallorganischen Komplexkatalyse, Springer-Verlag, Berlin, **2019**; b) A. Mittasch, Kurze Geschichte der Katalyse in Praxis und Theorie, Julius Springer, Berlin, **1939**; c) J.J. Berzelius, Årsberättelse om Framstegen i Fysik och Kemi, P. A. Norstedt & Söner, Stockholm, **1835**; d) J.J. Berzelius, F. Wöhler, Jahres-Bericht über die Fortschritte der physischen Wissenschaften, Heinrich Laupp, Tübingen, **1836**.
- [5] E. Vedejs, S.E. Denmark, Lewis Base Catalysis in Organic Synthesis, Wiley-VCH, Weinheim, **2016**.
- [6] The Nobel Prize, accessed 21.02.2024, <https://www.nobelprize.org/>.
- [7] R.A.v. Santen, Modern Heterogeneous Catalysis: An Introduction, Wiley-VCH, Weinheim, **2017**.
- [8] a) S. Bagheri, Catalysis for Green Energy and Technology, Springer International, Cham, **2017**; b) A.J. Kirby, From enzyme models to model enzymes, Royal Society of Chemistry, Cambridge, **2009**; c) G. Emig, *Chem. unserer Zeit* **1987**, *21*, 128-137. <https://doi.org/10.1002/ciuz.19870210405>; d) U. Hanefeld, L. Lefferts, Catalysis - An Integrated Textbook for Students, Wiley-VCH, Weinheim, **2018**; e) P.A. Dub, T. Ikariya, *J. Am. Chem. Soc.* **2013**, *135*, 2604-2619. <https://doi.org/10.1021/ja3097674>; f) S. Bhaduri, D. Mukesh, Homogeneous Catalysis, John Wiley & Sons, Inc., Hoboken, **2014**; g) J.M. Thomas, R.J.P. Williams, *Philosophical Transactions of the Royal Society A: Mathematical, Physical and Engineering Sciences* **2005**, *363*, 765-791. <https://doi.org/10.1098/rsta.2004.1534>; h) A. Behr, A.J. Vorholt, Homogeneous Catalysis with renewables, Springer International, Cham, **2012**; i) E. Riedel, Allgemeine und Anorganische Chemie, Walter de Gruyter, Berlin, New York, **2010**; j) G. Rothenberg, Catalysis - Concepts and Green Applications, Wiley-VCH, Weinheim, **2008**.
- [9] T. Taseska, W. Yu, M.K. Wilsey, C.P. Cox, Z. Meng, S.S. Ngarnim, A.M. Müller, *Top. Catal.* **2023**, *66*, 338-374. <https://doi.org/10.1007/s11244-023-01799-3>.
- [10] K.P.d. Jong, Synthesis of Solid Catalysts, Wiley-VCH, Weinheim, **2009**.
- [11] P.J. Fischer, F.E. Kühn, *Chem. unserer Zeit* **2019**, *53*, 112-124. <https://doi.org/10.1002/ciuz.201800848>.
- [12] G. Duca, Homogeneous Catalysis with Metal Complexes - Fundamentals and Applications, Springer-Verlag, Berlin, Heidelberg, **2012**.
- [13] S. Kozuch, J.M.L. Martin, *ACS Catal.* **2012**, *2*, 2787-2794. <https://doi.org/10.1021/cs3005264>.
- [14] a) J.M. Lambert, *J. Biomed. Mater. Res. Part B Appl. Biomater.* **2006**, *78B*, 167-180. <https://doi.org/10.1002/jbm.b.30471>; b) E. Yilgör, I. Yilgör, *Prog. Polym. Sci.* **2014**, *39*, 1165-1195. <https://doi.org/10.1016/j.progpolymsci.2013.11.003>; c) A.S. Palsule, S.J. Clarson, C.W. Widenhouse, *Journal of Inorganic and Organometallic Polymers and Materials* **2008**, *18*, 207-221. <https://doi.org/10.1007/s10904-008-9205-0>.
- [15] a) K. Mojsiewicz-Pieńkowska, M. Jamrógiwicz, K. Szymkowska, D. Krenczkowska, *Front. Pharmacol.* **2016**, *7*, <https://doi.org/10.3389/fphar.2016.00132>; b) W. Heilen, S. Herrwerth, Silicone Resins and their Combinations, 2nd, Quensen Druck + Verlag GmbH & Co. KG, Hildesheim, Germany, **2015**.
- [16] a) R.R. LeVier, M.C. Harrison, R.R. Cook, T.H. Lane, *Journal of Clinical Epidemiology* **1995**, *48*, 513-517. [https://doi.org/10.1016/0895-4356\(94\)00207-7](https://doi.org/10.1016/0895-4356(94)00207-7); b) D. Wang, J. Klein, E. Mejía, *Chem. Asian J.* **2017**, *12*, 1180-1197. <https://doi.org/10.1002/asia.201700304>.
- [17] a) L.N. Lewis, J. Stein, Y. Gao, R.E. Colborn, G. Hutchins, *Platinum Met. Rev.* **1997**, *41*, 66-75. <https://doi.org/10.1595/003214097X4126675>; b) H.-H. Moretto, M. Schulze, G. Wagner, Silicones, in: Ullmann's Encyclopedia of Industrial Chemistry, Wiley-VCH, Weinheim, **2005**; c) J. Stein, L.N. Lewis, Y. Gao, R.A. Scott, *J. Am. Chem. Soc.* **1999**, *121*, 3693-3703. <https://doi.org/10.1021/ja9825377>.

- [18] M.J. Owen, *Macromol. Rapid Commun.* **2021**, *42*, 2000360. <https://doi.org/10.1002/marc.202000360>.
- [19] a) R. Schliebs, J. Ackermann, *Chem. unserer Zeit* **1987**, *21*, 121-127. <https://doi.org/10.1002/ciuz.19870210404>; b) F. de Buyl, *Int. J. Adhes. Adhes.* **2001**, *21*, 411-422. [https://doi.org/10.1016/S0143-7496\(01\)00018-5](https://doi.org/10.1016/S0143-7496(01)00018-5).
- [20] S.C. Shit, P. Shah, *National Academy Science Letters* **2013**, *36*, 355-365. <https://doi.org/10.1007/s40009-013-0150-2>.
- [21] A.J. O'Lenick, *Journal of Surfactants and Detergents* **2000**, *3*, 229-236. <https://doi.org/10.1007/s11743-000-0130-3>.
- [22] J. Sołoducho, D. Zając, K. Spychalska, S. Baluta, J. Cabaj, *Molecules* **2021**, *26*, 2012. <https://doi.org/10.3390/molecules26072012>.
- [23] F. Liravi, E. Toyserkani, *Additive Manufacturing* **2018**, *24*, 232-242. <https://doi.org/10.1016/j.addma.2018.10.002>.
- [24] a) S. Hamdani, C. Longuet, D. Perrin, J.-M. Lopez-cuesta, F. Ganachaud, *Polym. Degrad. Stab.* **2009**, *94*, 465-495. <https://doi.org/10.1016/j.polymdegradstab.2008.11.019>; b) M. Zare, E.R. Ghomi, P.D. Venkatraman, S. Ramakrishna, *J. Appl. Polym. Sci.* **2021**, *138*, 50969. <https://doi.org/10.1002/app.50969>; c) R. Schierl, A. Lemmer, A. Böhlandt, L. Friedl, S. Haneder, D. Nowak, *Environ. Res.* **2014**, *132*, 269-272. <https://doi.org/10.1016/j.envres.2014.04.017>; d) M.B. Schear, M. Laskoski, *J. Polym. Sci., Part A: Polym. Chem.* **2014**, *52*, 523-526. <https://doi.org/10.1002/pola.27027>.
- [25] N.D. Vu, A. Boulègue-Mondière, N. Durand, J. Raynaud, V. Monteil, *Green Chem.* **2023**, *25*, 3869-3877. <https://doi.org/10.1039/D3GC00293D>.
- [26] a) E.G. Rochow, Preparation of organosilicon halides, US2380995A, August 7, **1945**; b) E.G. Rochow, *J. Am. Chem. Soc.* **1945**, *67*, 963-965. <https://doi.org/10.1021/ja01222a026>; c) R. Müller, *J. Chem. Educ.* **1965**, *42*, 41. <https://doi.org/10.1021/ed042p41>.
- [27] a) D. Troegel, J. Stohrer, *Coord. Chem. Rev.* **2011**, *255*, 1440-1459. <https://doi.org/10.1016/j.ccr.2010.12.025>; b) Y. Naganawa, K. Inomata, K. Sato, Y. Nakajima, *Tetrahedron Lett.* **2020**, *61*, 151513. <https://doi.org/10.1016/j.tetlet.2019.151513>.
- [28] a) L. Rösch, P. John, R. Reitmeier, Silicon Compounds, Organic, in: Ullmann's Encyclopedia of Industrial Chemistry, **2012**; b) A. Mitra, D.A. Atwood, Polysiloxanes & Polysilanes Based in part on the article Polysiloxanes & Polysilanes by Robert West which appeared in the Encyclopedia of Inorganic Chemistry, First Edition, in: Encyclopedia of Inorganic Chemistry, **2005**; c) J. Ackermann, V. Damrath, *Chem. unserer Zeit* **1989**, *23*, 86-99. <https://doi.org/10.1002/ciuz.19890230304>.
- [29] a) B. Marciniak, H. Maciejewski, C. Pietraszuk, P. Pawluć, Hydrosilylation and Related Reactions of Silicon Compounds, in: B. Cornils, W.A. Herrmann, M. Beller and R. Paciello, Applied Homogeneous Catalysis with Organometallic Compounds, WILEY-VCH, **2017**; b) Y. Nakajima, S. Shimada, *RSC Adv.* **2015**, *5*, 20603-20616. <https://doi.org/10.1039/C4RA17281G>; c) R.J. Hofmann, M. Vlatković, F. Wiesbrock, *Polymers* **2017**, *9*, 534-570. <https://doi.org/10.3390/polym9100534>; d) R.Y. Lukin, A.M. Kuchkaev, A.V. Sukhov, G.E. Bekmukhamedov, D.G. Yakhvarov, *Polymers* **2020**, *12*, 2174. <https://doi.org/10.3390/polym12102174>.
- [30] B. Marciniak, Hydrosilylation of Alkenes and Their Derivatives, in: J. Matison, Hydrosilylation - A Comprehensive Review on Recent Advances, Springer, Poland, **2009**.
- [31] a) J.L. Speier, Homogeneous Catalysis of Hydrosilylation by Transition Metals, in: F.G.A. Stone and R. West, Adv. Organomet. Chem., Academic Press, **1979**; b) L.D. de Almeida, H. Wang, K. Junge, X. Cui, M. Beller, *Angew. Chem. Int. Ed.* **2021**, *60*, 550-565. <https://doi.org/10.1002/anie.202008729>; c) J.V. Obligacion, P.J. Chirik, *Nat. Rev. Chem.* **2018**, *2*, 15-34. <https://doi.org/10.1038/s41570-018-0001-2>.
- [32] a) G. Yang, Y. Wei, Z. Huang, J. Hu, G. Liu, M. Ou, S. Lin, Y. Tu, *ACS Appl. Mater. Interfaces* **2018**, *10*, 6778-6784. <https://doi.org/10.1021/acsami.7b19644>; b) D. Friedman, T. Masciangioli, S. Olson, The Role of the Chemical Sciences in Finding Alternatives to Critical Resources: A Workshop Summary, The National Academies Press, Washington, DC, **2012**; c) H.U. Sverdrup, K.V.

- Ragnarsdottir, *Resour. Conserv. Recycl.* **2016**, *114*, 130-152.
<https://doi.org/10.1016/j.resconrec.2016.07.011>.
- [33] A.E. Hughes, N. Haque, S.A. Northey, S. Giddey, *Resources* **2021**, *10*, 93.
<https://doi.org/10.3390/resources10090093>.
- [34] P. Sahu, M.S. Jena, N.R. Mandre, R. Venugopal, *Miner. Process. Extr. Metall. Rev.* **2021**, *42*, 521-534. <https://doi.org/10.1080/08827508.2020.1795848>.
- [35] F. Zereini, C.L.S. Wiseman, *Platinum Metals in the Environment*, Springer-Verlag, Berlin, Heidelberg, **2015**.
- [36] T. Feix, A.A. Fadhil, D. Troegel, *Hydrometallurgy* **2024**, 106283.
<https://doi.org/10.1016/j.hydromet.2024.106283>.
- [37] A. Elshkaki, *Resources Policy* **2013**, *38*, 241-251.
<https://doi.org/10.1016/j.resourpol.2013.04.002>.
- [38] a) B. Marciniak, *Appl. Organomet. Chem.* **2000**, *14*, 527-538. [https://doi.org/10.1002/1099-0739\(200010\)14:10<527::AID-AOC35>3.0.CO;2-X](https://doi.org/10.1002/1099-0739(200010)14:10<527::AID-AOC35>3.0.CO;2-X); b) K. Maeda, K. Motokura, *Journal of the Japan Petroleum Institute* **2020**, *63*, 1-9. <https://doi.org/10.1627/jpi.63.1>.
- [39] F. Seitz, M.S. Wrighton, *Angew. Chem. Int. Ed.* **1988**, *27*, 289-291.
<https://doi.org/10.1002/anie.198802891>.
- [40] C.L. Reichel, M.S. Wrighton, *Inorg. Chem.* **1980**, *19*, 3858-3860.
<https://doi.org/10.1021/ic50214a058>.
- [41] C.L. Randolph, M.S. Wrighton, *J. Am. Chem. Soc.* **1986**, *108*, 3366-3374.
<https://doi.org/10.1021/ja00272a035>.
- [42] F.R. Anderson, M.S. Wrighton, *J. Am. Chem. Soc.* **1984**, *106*, 995-999.
<https://doi.org/10.1021/ja00316a030>.
- [43] A.J. Chalk, J.F. Harrod, *J. Am. Chem. Soc.* **1965**, *87*, 16-21. <https://doi.org/10.1021/ja01079a004>.
- [44] Y. Gao, L. Wang, L. Deng, *ACS Catal.* **2018**, *8*, 9637-9646.
<https://doi.org/10.1021/acscatal.8b02513>.
- [45] S.B. Duckett, R.N. Perutz, *Organometallics* **1992**, *11*, 90-98.
<https://doi.org/10.1021/om00037a022>.
- [46] a) J.A. Reichl, D.H. Berry, Recent Progress in Transition Metal-Catalyzed Reactions of Silicon, Germanium, and Tin, in: R. West and A.F. Hill, *Adv. Organomet. Chem.*, Academic Press, **1999**; b) M.A. Brook, *Silicon in Organic, Organometallic and Polymer Chemistry*, Wiley, New York, **2000**.
- [47] D.M. Haddleton, R.N. Perutz, *J. Chem. Soc., Chem. Commun.* **1985**, 1372-1374.
<https://doi.org/10.1039/C39850001372>.
- [48] S.B. Duckett, D.M. Haddleton, S.A. Jackson, R.N. Perutz, M. Poliakov, R.K. Upmacis, *Organometallics* **1988**, *7*, 1526-1532. <https://doi.org/10.1021/om00097a013>.
- [49] S.B. Duckett, R.N. Perutz, *J. Chem. Soc., Chem. Commun.* **1991**, 28-31.
<https://doi.org/10.1039/C3991000028>.
- [50] a) P.O. Bentz, J. Ruiz, B.E. Mann, C.M. Spencer, P.M. Maitlis, *J. Chem. Soc., Chem. Commun.* **1985**, 1374-1375. <https://doi.org/10.1039/C39850001374>; b) J. Ruiz, P.O. Bentz, B.E. Mann, C.M. Spencer, B.F. Taylor, P.M. Maitlis, *J. Chem. Soc., Dalton Trans.* **1987**, 2709-2713.
<https://doi.org/10.1039/DT9870002709>; c) M. Paneque, P.M. Maitlis, *J. Chem. Soc., Chem. Commun.* **1989**, 105-106. <https://doi.org/10.1039/C39890000105>.
- [51] M. Brookhart, B.E. Grant, *J. Am. Chem. Soc.* **1993**, *115*, 2151-2156.
<https://doi.org/10.1021/ja00059a008>.
- [52] a) G.F. Schmidt, M. Brookhart, *J. Am. Chem. Soc.* **1985**, *107*, 1443-1444.
<https://doi.org/10.1021/ja00291a073>; b) M. Brookhart, A.F. Volpe, Jr., D.M. Lincoln, I.T. Horvath, J.M. Millar, *J. Am. Chem. Soc.* **1990**, *112*, 5634-5636. <https://doi.org/10.1021/ja00170a035>.
- [53] P.B. Glaser, T.D. Tilley, *J. Am. Chem. Soc.* **2003**, *125*, 13640-13641.
<https://doi.org/10.1021/ja037620v>.
- [54] a) P.G. Hayes, R. Waterman, P.B. Glaser, T.D. Tilley, *Organometallics* **2009**, *28*, 5082-5089.
<https://doi.org/10.1021/om900348m>; b) A.D. Böth, M.J. Sauer, R.M. Reich, F.E. Kühn, 7.08 -

- Ruthenium and Osmium Complexes Containing NHC and π -Acid Ligands, in: G. Parkin, K. Meyer and D. O'hare, *Comprehensive Organometallic Chemistry IV*, Elsevier, Oxford, **2022**.
- [55] L.H. Sommer, E.W. Pietrusza, F.C. Whitmore, *J. Am. Chem. Soc.* **1947**, *69*, 188-188. <https://doi.org/10.1021/ja01193a508>.
- [56] a) J.L. Speier, J.A. Webster, G.H. Barnes, *J. Am. Chem. Soc.* **1957**, *79*, 974-979. <https://doi.org/10.1021/ja01561a054>; b) J.L. Speier, D.E. Hook, Process for the Production of Organosilicon Compounds, US2823218, February 11, **1958**; c) R.A. Benkeser, J. Kang, *J. Organomet. Chem.* **1980**, *185*, C9-C12. [https://doi.org/10.1016/S0022-328X\(00\)94412-7](https://doi.org/10.1016/S0022-328X(00)94412-7).
- [57] A. Shaver, *Can. J. Chem.* **1978**, *56*, 2281-2285. <https://doi.org/10.1139/v78-376>.
- [58] a) S.D. Robinson, B.L. Shaw, *Z. Naturforsch.* **1963**, *B18*, 507-507. ; b) S.D. Robinson, B.L. Shaw, *J. Chem. Soc.* **1965**, 1529-1530.
- [59] a) K.W. Egger, *J. Organomet. Chem.* **1970**, *24*, 501-506. [https://doi.org/10.1016/S0022-328X\(00\)80295-8](https://doi.org/10.1016/S0022-328X(00)80295-8); b) I.S. Kolomnikov, V.P. Kukolev, E.V.p. Mark, *Russian Chemical Reviews* **1974**, *43*, 399. <https://doi.org/10.1070/RC1974v043n05ABEH001812>.
- [60] a) T.J. Drahnak, Radiation Activated Hydrosilylation, EP0146307A2, June 26, **1985**; b) T.J. Drahnak, Hydrosilylation process using a (eta 5-cyclopentadienyl)tri(sigma-aliphatic) platinum complex as the catalyst, US4600484A, July 15, **1986**.
- [61] R.A. Faltynek, *Inorg. Chem.* **1981**, *20*, 1357-1362. <https://doi.org/10.1021/ic50219a004>.
- [62] a) R.S. Paonessa, A.L. Prignano, W.C. Trogler, *Organometallics* **1985**, *4*, 647-657. <https://doi.org/10.1021/om00123a006>; b) A.L. Prignano, W.C. Trogler, *J. Am. Chem. Soc.* **1987**, *109*, 3586-3595. <https://doi.org/10.1021/ja00246a015>.
- [63] R.P. Eckberg, Inhibited precious metal catalyzed organopolysiloxane compositions, US4670531A, June 2, **1987**.
- [64] L.D. Boardman, *Organometallics* **1992**, *11*, 4194-4201. <https://doi.org/10.1021/om00060a042>.
- [65] Z. Xue, H. Thridandam, H.D. KAESZ, R.F. Hicks, *Chem. Mater.* **1992**, *4*, 162-166. <https://doi.org/10.1021/cm00019a032>.
- [66] a) S. Rist, S. Bosshammer, M. Putzer, T. Naumann, U. Irmer, Use of Light-Activated Hardenable Silicon Compositions for the Production of Thick-Walled Moulded Articles or Thick-Walled Coatings, EP1817372B1, September 30, **2009**; b) M. Jandke, W. Brennenstuhl, Pt-Catalyzed, Addition-Crosslinking Silicone Compositions Self-Adhesive at Room Temperature, US2010256300A1, October 7, **2010**.
- [67] M.D. Butts, Irradiation-curable silicone compositions containing photo-active platinum (IV) compounds, EP1050538A2, November 8, **2000**.
- [68] J.D. Oxman, L.D. Boardman, P. Saint, Hydrosilylation Reaction, EP0561893A1, September 29, **1993**.
- [69] a) H.F. Lamoreaux, Organosilicon Process Using a Chloroplatinic Acid Reaction Product as the Catalyst, US3220972, November 30, **1965**; b) L.N. Lewis, C.A. Sumpster, *J. Mol. Catal. A: Chem.* **1996**, *104*, 293-297. [https://doi.org/10.1016/1381-1169\(95\)00147-6](https://doi.org/10.1016/1381-1169(95)00147-6).
- [70] D.N. Willing, Catalysts for the Reaction of SiH with Organic Compounds Containing Aliphatic Unsaturation, US3419593, December 31, **1968**.
- [71] a) B.D. Karstedt, Platinum Complexes of Unsaturated Siloxanes and Platinum Containing Organopolysiloxanes, US3775452, November 27, **1973**; b) P.B. Hitchcock, M.F. Lappert, N.J.W. Warhurst, *Angew. Chem. Int. Ed.* **1991**, *30*, 438-440. <https://doi.org/10.1002/anie.199104381>; c) G. Chandra, P.Y. Lo, P.B. Hitchcock, M.F. Lappert, *Organometallics* **1987**, *6*, 191-192. <https://doi.org/10.1021/om00144a036>.
- [72] H. Maciejewski, B. Marciniak, I. Kownacki, *J. Organomet. Chem.* **2000**, *597*, 175-181. [https://doi.org/10.1016/S0022-328X\(99\)00685-3](https://doi.org/10.1016/S0022-328X(99)00685-3).
- [73] B.A. Ashby, Platinum-Olefin Complex Catalyzed Addition of Hydrogen- and Alkenyl-substituted Siloxanes, US3159601, December 1, **1964**.
- [74] a) I.E. Markó, S. Stérin, O. Buisine, G. Mignani, P. Branlard, B. Tinant, J.-P. Declercq, *Science* **2002**, *298*, 204-206. <https://doi.org/10.1126/science.1073338>; b) I.E. Markó, S. Stérin, O. Buisine, G.

- Berthon, G. Michaud, B. Tinant, J.-P. Declercq, *Adv. Synth. Catal.* **2004**, *346*, 1429-1434. <https://doi.org/10.1002/adsc.200404048>.
- [75] a) J.J. Dunsford, K.J. Cavell, B. Kariuki, *J. Organomet. Chem.* **2011**, *696*, 188-194. <https://doi.org/10.1016/j.jorganchem.2010.08.045>; b) L. Chen, I.S. Ali, S.L. Tait, *ChemCatChem* **2020**, *12*, 3576-3584. <https://doi.org/10.1002/cctc.202000085>.
- [76] I. Alvarado-Beltran, A. Baceiredo, N. Saffon-Merceron, V. Branchadell, T. Kato, *Angew. Chem. Int. Ed.* **2016**, *55*, 16141-16144. <https://doi.org/10.1002/anie.201609899>.
- [77] T. Iimura, N. Akasaka, T. Kosai, T. Iwamoto, *Dalton Trans.* **2017**, *46*, 8868-8874. <https://doi.org/10.1039/C7DT01113J>.
- [78] G. Berthon-Gelloz, O. Buisine, J.-F. Brière, G. Michaud, S. Stérin, G. Mignani, B. Tinant, J.-P. Declercq, D. Chapon, I.E. Markó, *J. Organomet. Chem.* **2005**, *690*, 6156-6168. <https://doi.org/10.1016/j.jorganchem.2005.08.020>.
- [79] T.K. Meister, J.W. Kück, K. Riener, A. Pöthig, W.A. Herrmann, F.E. Kühn, *J. Catal.* **2016**, *337*, 157-166. <https://doi.org/10.1016/j.jcat.2016.01.032>.
- [80] a) O. Buisine, G. Berthon-Gelloz, J.-F. Brière, S. Stérin, G. Mignani, P. Branlard, B. Tinant, J.-P. Declercq, I.E. Markó, *Chem. Commun.* **2005**, 3856-3858. <https://doi.org/10.1039/B506369H>; b) G. De Bo, G. Berthon-Gelloz, B. Tinant, I.E. Markó, *Organometallics* **2006**, *25*, 1881-1890. <https://doi.org/10.1021/om050866j>; c) S. Dierick, D.F. Dewez, I.E. Markó, *Organometallics* **2014**, *33*, 677-683. <https://doi.org/10.1021/om4008955>.
- [81] a) V. Lillo, J. Mata, J. Ramírez, E. Peris, E. Fernandez, *Organometallics* **2006**, *25*, 5829-5831. <https://doi.org/10.1021/om060666n>; b) V. Lillo, J.A. Mata, A.M. Segarra, E. Peris, E. Fernandez, *Chem. Commun.* **2007**, 2184-2186. <https://doi.org/10.1039/B700800G>; c) N. Schneider, S. Bellemin-Laponnaz, H. Wadepohl, L.H. Gade, *Eur. J. Inorg. Chem.* **2008**, *2008*, 5587-5598. <https://doi.org/10.1002/ejic.200800908>; d) D. Brissy, M. Skander, P. Retailleau, G. Frison, A. Marinetti, *Organometallics* **2009**, *28*, 140-151. <https://doi.org/10.1021/om800743r>; e) G.F. Silbestri, J.C. Flores, E. de Jesús, *Organometallics* **2012**, *31*, 3355-3360. <https://doi.org/10.1021/om300148q>; f) A.M. Ruiz-Varilla, E.A. Baquero, G.F. Silbestri, C. Gonzalez-Arellano, E. de Jesús, J.C. Flores, *Dalton Trans.* **2015**, *44*, 18360-18369. <https://doi.org/10.1039/C5DT02622A>; g) P. Žak, M. Bołt, J. Lorkowski, M. Kubicki, C. Pietraszuk, *ChemCatChem* **2017**, *9*, 3627-3631. <https://doi.org/10.1002/cctc.201700580>; h) P. Žak, M. Bołt, M. Kubicki, C. Pietraszuk, *Dalton Trans.* **2018**, *47*, 1903-1910. <https://doi.org/10.1039/C7DT04392A>; i) P. Žak, M. Bołt, C. Pietraszuk, *Eur. J. Inorg. Chem.* **2019**, *2019*, 2455-2461. <https://doi.org/10.1002/ejic.201900217>; j) P. Žak, M. Bołt, B. Dudziec, M. Kubicki, *Dalton Trans.* **2019**, *48*, 2657-2663. <https://doi.org/10.1039/C8DT05142A>; k) S.A. Rzhavskiy, M.A. Topchiy, K.A. Lyssenko, A.N. Philippova, M.A. Belaya, A.A. Ageshina, M.V. Bermeshev, M.S. Nechaev, A.F. Asachenko, *J. Organomet. Chem.* **2020**, *912*, 121140-121162. <https://doi.org/10.1016/j.jorganchem.2020.121140>.
- [82] B.P. Maliszewski, T.A.C.A. Bayrakdar, P. Lambert, L. Hamdouna, X. Trivelli, L. Cavallo, A. Poater, M. Beliš, O. Lafon, K. Van Hecke, D. Ormerod, C.S.J. Cazin, F. Nahra, S.P. Nolan, *Chem. Eur. J.* **2023**, *29*, e202301259. <https://doi.org/10.1002/chem.202301259>.
- [83] W.A. Herrmann, C. Köcher, L.J. Gooßen, G.R.J. Artus, *Chem. Eur. J.* **1996**, *2*, 1627-1636. <https://doi.org/10.1002/chem.1996002122>.
- [84] a) B.P. Maliszewski, N.V. Tzouras, S.G. Guillet, M. Saab, M. Beliš, K. Van Hecke, F. Nahra, S.P. Nolan, *Dalton Trans.* **2020**, *49*, 14673-14679. <https://doi.org/10.1039/D0DT03480K>; b) B.P. Maliszewski, I. Ritacco, M. Beliš, I.I. Hashim, N.V. Tzouras, L. Caporaso, L. Cavallo, K. Van Hecke, F. Nahra, C.S.J. Cazin, S.P. Nolan, *Dalton Trans.* **2022**, *51*, 6204-6211. <https://doi.org/10.1039/D2DT00504B>.
- [85] S. Fantasia, J.L. Petersen, H. Jacobsen, L. Cavallo, S.P. Nolan, *Organometallics* **2007**, *26*, 5880-5889. <https://doi.org/10.1021/om700857j>.
- [86] a) G. Berthon-Gelloz, J.-M. Schumers, F. Lucaccioni, B. Tinant, J. Wouters, I.E. Markó, *Organometallics* **2007**, *26*, 5731-5734. <https://doi.org/10.1021/om7007088>; b) G. Berthon-Gelloz, J.-M. Schumers, G. De Bo, I.E. Markó, *J. Org. Chem.* **2008**, *73*, 4190-4197. <https://doi.org/10.1021/jo800411e>.

- [87] a) P. Steffanut, J.A. Osborn, A. DeCian, J. Fisher, *Chem. Eur. J.* **1998**, *4*, 2008-2017. [https://doi.org/10.1002/\(SICI\)1521-3765\(19981002\)4:10<2008::AID-CHEM2008>3.0.CO;2-K](https://doi.org/10.1002/(SICI)1521-3765(19981002)4:10<2008::AID-CHEM2008>3.0.CO;2-K); b) J.W. Sprengers, M.J. Mars, M.A. Duin, K.J. Cavell, C.J. Elsevier, *J. Organomet. Chem.* **2003**, *679*, 149-152. [https://doi.org/10.1016/S0022-328X\(03\)00514-X](https://doi.org/10.1016/S0022-328X(03)00514-X); c) Jeroen W. Sprengers, M. de Greef, Marcel A. Duin, Cornelis J. Elsevier, *Eur. J. Inorg. Chem.* **2003**, *2003*, 3811-3819. <https://doi.org/10.1002/ejic.200300088>; d) J.W. Sprengers, M.J. Agerbeek, C.J. Elsevier, H. Kooijman, A.L. Spek, *Organometallics* **2004**, *23*, 3117-3125. <https://doi.org/10.1021/om049913i>; e) M.A. Duin, M. Lutz, A.L. Spek, C.J. Elsevier, *J. Organomet. Chem.* **2005**, *690*, 5804-5815. <https://doi.org/10.1016/j.jorganchem.2005.07.059>; f) J. Krause, G. Cestarić, K.-J. Haack, K. Seevogel, W. Storm, K.-R. Pörschke, *J. Am. Chem. Soc.* **1999**, *121*, 9807-9823. <https://doi.org/10.1021/ja983939h>.
- [88] S. Dierick, E. Vercruyse, G. Berthon-Gelloz, I.E. Markó, *Chem. Eur. J.* **2015**, *21*, 17073-17078. <https://doi.org/10.1002/chem.201502643>.
- [89] G. Berthon-Gelloz, B. de Bruin, B. Tinant, I.E. Markó, *Angew. Chem. Int. Ed.* **2009**, *48*, 3161-3164. <https://doi.org/10.1002/anie.200900435>.
- [90] a) J.R.L. Priqueler, I.S. Butler, F.D. Rochon, *Appl. Spectrosc. Rev.* **2006**, *41*, 185-226. <https://doi.org/10.1080/05704920600620311>; b) B.M. Still, P.G.A. Kumar, J.R. Aldrich-Wright, W.S. Price, *Chem. Soc. Rev.* **2007**, *36*, 665-686. <https://doi.org/10.1039/B606190G>.
- [91] a) T. Troadec, A. Prades, R. Rodriguez, R. Mirgalet, A. Baceiredo, N. Saffon-Merceron, V. Branchadell, T. Kato, *Inorg. Chem.* **2016**, *55*, 8234-8240. <https://doi.org/10.1021/acs.inorgchem.6b01505>; b) T. Iimura, N. Akasaka, T. Iwamoto, *Organometallics* **2016**, *35*, 4071-4076. <https://doi.org/10.1021/acs.organomet.6b00741>.
- [92] Y. Mizuhata, T. Sasamori, N. Tokitoh, *Chem. Rev.* **2009**, *109*, 3479-3511. <https://doi.org/10.1021/cr900093s>.
- [93] a) R.H. Holm, P. Kennepohl, E.I. Solomon, *Chem. Rev.* **1996**, *96*, 2239-2314. <https://doi.org/10.1021/cr9500390>; b) R.E. Stenkamp, *Chem. Rev.* **1994**, *94*, 715-726. <https://doi.org/10.1021/cr00027a008>; c) E.I. Solomon, D.E. Heppner, E.M. Johnston, J.W. Ginsbach, J. Cirera, M. Qayyum, M.T. Kieber-Emmons, C.H. Kjaergaard, R.G. Hadt, L. Tian, *Chem. Rev.* **2014**, *114*, 3659-3853. <https://doi.org/10.1021/cr400327t>; d) T. Guchhait, S. Sasmal, F.S.T. Khan, S.P. Rath, *Coord. Chem. Rev.* **2017**, *337*, 112-144. <https://doi.org/10.1016/j.ccr.2017.02.008>.
- [94] a) A.L. Gavrilova, B. Bosnich, *Chem. Rev.* **2004**, *104*, 349-384. <https://doi.org/10.1021/cr020604g>; b) V.V. Barynin, J.W. Whittaker, Manganese Catalase, in: *Encyclopedia of Inorganic and Bioinorganic Chemistry*, **2011**; c) V.C.C. Wang, S. Maji, P.P.Y. Chen, H.K. Lee, S.S.F. Yu, S.I. Chan, *Chem. Rev.* **2017**, *117*, 8574-8621. <https://doi.org/10.1021/acs.chemrev.6b00624>; d) S. Friedle, E. Reisner, S.J. Lippard, *Chem. Soc. Rev.* **2010**, *39*, 2768-2779. <https://doi.org/10.1039/C003079C>.
- [95] a) R. Boulatov, *Pure Appl. Chem.* **2004**, *76*, 303-319. <https://doi.org/10.1351/pac200476020303>; b) E.Y. Tshuva, S.J. Lippard, *Chem. Rev.* **2004**, *104*, 987-1012. <https://doi.org/10.1021/cr020622y>; c) J. Weston, *Chem. Rev.* **2005**, *105*, 2151-2174. <https://doi.org/10.1021/cr020057z>; d) A. Magnuson, M. Anderlund, O. Johansson, P. Lindblad, R. Lomoth, T. Polivka, S. Ott, K. Stensjö, S. Styring, V. Sundström, L. Hammarström, *Acc. Chem. Res.* **2009**, *42*, 1899-1909. <https://doi.org/10.1021/ar900127h>; e) M.M. Najafpour, G. Renger, M. Hołyńska, A.N. Moghaddam, E.-M. Aro, R. Carpentier, H. Nishihara, J.J. Eaton-Rye, J.-R. Shen, S.I. Allakhverdiev, *Chem. Rev.* **2016**, *116*, 2886-2936. <https://doi.org/10.1021/acs.chemrev.5b00340>.
- [96] a) P. Buchwalter, J. Rosé, P. Braunstein, *Chem. Rev.* **2015**, *115*, 28-126. <https://doi.org/10.1021/cr500208k>; b) N.P. Mankad, *Chem. Eur. J.* **2016**, *22*, 5822-5829. <https://doi.org/10.1002/chem.201505002>; c) J. Campos, *Nat. Rev. Chem.* **2020**, *4*, 696-702. <https://doi.org/10.1038/s41570-020-00226-5>; d) B. Chatterjee, W.-C. Chang, S. Jena, C. Werlé, *ACS Catal.* **2020**, *10*, 14024-14055. <https://doi.org/10.1021/acscatal.0c03794>; e) R. Maity, B.S. Birenheide, F. Breher, B. Sarkar, *ChemCatChem* **2021**, *13*, 2337-2370. <https://doi.org/10.1002/cctc.202001951>.

- [97] a) A. Dey, *Angew. Chem. Int. Ed.* **2023**, *62*, e202301760. <https://doi.org/10.1002/anie.202301760>; b) E.K. van den Beuken, B.L. Feringa, *Tetrahedron* **1998**, *54*, 12985-13011. [https://doi.org/10.1016/S0040-4020\(98\)00319-6](https://doi.org/10.1016/S0040-4020(98)00319-6); c) J.M. Gil-Negrete, E. Hevia, *Chem. Sci.* **2021**, *12*, 1982-1992. <https://doi.org/10.1039/D0SC05116K>; d) J. Park, S. Hong, *Chem. Soc. Rev.* **2012**, *41*, 6931-6943. <https://doi.org/10.1039/C2CS35129C>; e) D.R. Pye, N.P. Mankad, *Chem. Sci.* **2017**, *8*, 1705-1718. <https://doi.org/10.1039/C6SC05556G>; f) K.J. Evans, S.M. Mansell, *Chem. Eur. J.* **2020**, *26*, 5927-5941. <https://doi.org/10.1002/chem.201905510>; g) S. Klaus, M.W. Lehenmeier, C.E. Anderson, B. Rieger, *Coord. Chem. Rev.* **2011**, *255*, 1460-1479. <https://doi.org/10.1016/j.ccr.2010.12.002>; h) J.I. van der Vlugt, *Eur. J. Inorg. Chem.* **2012**, *2012*, 363-375. <https://doi.org/10.1002/ejic.201100752>; i) N. Xiong, G. Zhang, X. Sun, R. Zeng, *Chin. J. Chem.* **2020**, *38*, 185-201. <https://doi.org/10.1002/cjoc.201900371>.
- [98] a) C. Adams, P. Riviere, M. Riviere-Baudet, C. Morales-Verdejo, M. Dahrouch, V. Morales, A. Castel, F. Delpech, J.M. Manriquez, I. Chávez, *J. Organomet. Chem.* **2014**, *749*, 266-274. <https://doi.org/10.1016/j.jorganchem.2013.10.017>; b) V. Comte, P. Le Gendre, P. Richard, C. Moïse, *Organometallics* **2005**, *24*, 1439-1444. <https://doi.org/10.1021/om040058c>; c) A.J. Huckaba, T.K. Hollis, T.O. Howell, H.U. Valle, Y. Wu, *Organometallics* **2013**, *32*, 63-69. <https://doi.org/10.1021/om3008037>; d) V. Diachenko, M.J. Page, M.R.D. Gatus, M. Bhadbhade, B.A. Messerle, *Organometallics* **2015**, *34*, 4543-4552. <https://doi.org/10.1021/acs.organomet.5b00594>; e) M.R.D. Gatus, I. Pernik, J.A. Tompsett, S.C. Binding, M.B. Peterson, B.A. Messerle, *Dalton Trans.* **2019**, *48*, 4333-4340. <https://doi.org/10.1039/C9DT00313D>; f) S. Leelasubcharoen, P.A. Zhizhko, L.G. Kuzmina, A.V. Churakov, J.A.K. Howard, G.I. Nikonov, *Organometallics* **2009**, *28*, 4500-4506. <https://doi.org/10.1021/om900363r>; g) A.E. Findlay, S. Leelasubcharoen, L.G. Kuzmina, J.A.K. Howard, G.I. Nikonov, *Dalton Trans.* **2010**, *39*, 9264-9269. <https://doi.org/10.1039/C0DT00141D>; h) R.H. Lam, S.T. Keaveney, B.A. Messerle, I. Pernik, *ACS Catal.* **2023**, *13*, 1999-2010. <https://doi.org/10.1021/acscatal.2c04388>; i) W. Zhou, S.L. Marquard, M.W. Bezpalko, B.M. Foxman, C.M. Thomas, *Organometallics* **2013**, *32*, 1766-1772. <https://doi.org/10.1021/om301194g>; j) G.T.S. Andavan, E.B. Bauer, C.S. Letko, T.K. Hollis, F.S. Tham, *J. Organomet. Chem.* **2005**, *690*, 5938-5947. <https://doi.org/10.1016/j.jorganchem.2005.07.088>; k) A.J. Huckaba, T.K. Hollis, S.W. Reilly, *Organometallics* **2013**, *32*, 6248-6256. <https://doi.org/10.1021/om400452q>.
- [99] N. Nakata, M. Sakashita, C. Komatsubara, A. Ishii, *Eur. J. Inorg. Chem.* **2010**, *2010*, 447-453. <https://doi.org/10.1002/ejic.200900958>.
- [100] a) A.K. Roy, R.B. Taylor, *J. Am. Chem. Soc.* **2002**, *124*, 9510-9524. <https://doi.org/10.1021/ja0127335>; b) W. Caseri, P.S. Pregosin, *J. Organomet. Chem.* **1988**, *356*, 259-269. [https://doi.org/10.1016/0022-328X\(88\)83096-1](https://doi.org/10.1016/0022-328X(88)83096-1); c) W. Caseri, P.S. Pregosin, *Organometallics* **1988**, *7*, 1373-1380. <https://doi.org/10.1021/om00096a023>; d) X. Coqueret, G. Wegner, *Organometallics* **1991**, *10*, 3139-3145. <https://doi.org/10.1021/om00055a030>; e) D. Brand, H.-H. Moretto, M. Schulze, D. Wrobel, *Journal für Praktische Chemie/Chemiker-Zeitung* **1994**, *336*, 218-224. <https://doi.org/10.1002/prac.19943360306>; f) M.N. Jagadeesh, W. Thiel, J. Köhler, A. Fehn, *Organometallics* **2002**, *21*, 2076-2087. <https://doi.org/10.1021/om0200196>.
- [101] a) S. Sakaki, N. Mizoe, M. Sugimoto, *Organometallics* **1998**, *17*, 2510-2523. <https://doi.org/10.1021/om980190a>; b) S. Sakaki, N. Mizoe, M. Sugimoto, Y. Musashi, *Coord. Chem. Rev.* **1999**, *190-192*, 933-960. [https://doi.org/10.1016/S0010-8545\(99\)00130-7](https://doi.org/10.1016/S0010-8545(99)00130-7).
- [102] S. Sakaki, N. Mizoe, Y. Musashi, M. Sugimoto, *Journal of Molecular Structure: THEOCHEM* **1999**, *461-462*, 533-546. [https://doi.org/10.1016/S0166-1280\(98\)00432-1](https://doi.org/10.1016/S0166-1280(98)00432-1).
- [103] a) L.N. Lewis, *J. Am. Chem. Soc.* **1990**, *112*, 5998-6004. <https://doi.org/10.1021/ja00172a014>; b) L.N. Lewis, R.J. Uriarte, *Organometallics* **1990**, *9*, 621-625. <https://doi.org/10.1021/om00117a015>; c) J. Stein, L.N. Lewis, K.A. Smith, K.X. Lettko, *J. Inorg. Organomet. Polym.* **1991**, *1*, 325-334. <https://doi.org/10.1007/BF00702496>.
- [104] M. A. Schroeder, M. S. Wrighton, *J. Organomet. Chem.* **1977**, *128*, 345-358. [https://doi.org/10.1016/S0022-328X\(00\)92207-1](https://doi.org/10.1016/S0022-328X(00)92207-1).

- [105] a) L.N. Lewis, N. Lewis, *J. Am. Chem. Soc.* **1986**, *108*, 7228-7231. <https://doi.org/10.1021/ja00283a016>; b) L.N. Lewis, R.J. Uriarte, N. Lewis, *J. Catal.* **1991**, *127*, 67-74. [https://doi.org/10.1016/0021-9517\(91\)90209-M](https://doi.org/10.1016/0021-9517(91)90209-M).
- [106] L.N. Lewis, N. Lewis, *Chem. Mater.* **1989**, *1*, 106-114. <https://doi.org/10.1021/cm00001a021>.
- [107] M. Gómez-Gallego, M.A. Sierra, *Chem. Rev.* **2011**, *111*, 4857-4963. <https://doi.org/10.1021/cr100436k>.
- [108] a) A. Onopchenko, E.T. Sabourin, *J. Org. Chem.* **1987**, *52*, 4118-4121. <https://doi.org/10.1021/jo00227a033>; b) D.L. Kleyer, Method for Controlling Hydrosilylation in a Reaction Mixture, US5359111, October 25, **1994**.
- [109] A.K. Roy, A Review of Recent Progress in Catalyzed Homogeneous Hydrosilylation (Hydrosilylation), in: R. West, A.F. Hill and M.J. Fink, *Adv. Organomet. Chem.*, Academic Press, **2007**.
- [110] T.K. Meister, K. Riener, P. Gigler, J. Stohrer, W.A. Herrmann, F.E. Kühn, *ACS Catal.* **2016**, *6*, 1274-1284. <https://doi.org/10.1021/acscatal.5b02624>.
- [111] a) S. Dierick, I.E. Markó, NHC Platinum(0) Complexes: Unique Catalysts for the Hydrosilylation of Alkenes and Alkynes, in: S.P. Nolan, *N-Heterocyclic Carbenes*, WILEY-VCH, Weinheim, **2014**; b) G. Berthon-Gelloz, I.E. Markó, Efficient and Selective Hydrosilylation of Alkenes and Alkynes Catalyzed by Novel N-Heterocyclic Carbene Pt(0) Complexes, in: *N-Heterocyclic Carbenes in Synthesis*, WILEY-VCH, Weinheim, **2006**.
- [112] J.C. Bernhammer, H.V. Huynh, *Organometallics* **2014**, *33*, 172-180. <https://doi.org/10.1021/om400929t>.
- [113] M.J. Sauer, L.F. Richter, J. Offorjindu, R.M. Reich, F.E. Kühn, *J. Organomet. Chem.* **2024**, *1005*, 122995-123005. <https://doi.org/10.1016/j.jorganchem.2023.122995>.
- [114] a) O. Schuster, L. Yang, H.G. Raubenheimer, M. Albrecht, *Chem. Rev.* **2009**, *109*, 3445-3478. <https://doi.org/10.1021/cr8005087>; b) J.D. Crowley, A.-L. Lee, K.J. Kilpin, *Aust. J. Chem.* **2011**, *64*, 1118-1132. <https://doi.org/10.1071/CH11185>; c) D. Schweinfurth, L. Hettmanczyk, L. Suntrup, B. Sarkar, *Z. Anorg. Allg. Chem.* **2017**, *643*, 554-584. <https://doi.org/10.1002/zaac.201700030>.
- [115] M.J. Sauer, J. Offorjindu, G.G. Zámbo, R.M. Reich, F.E. Kühn, *J. Organomet. Chem.* **2024**, *1007*, 123030-123044. <https://doi.org/10.1016/j.jorganchem.2024.123030>.